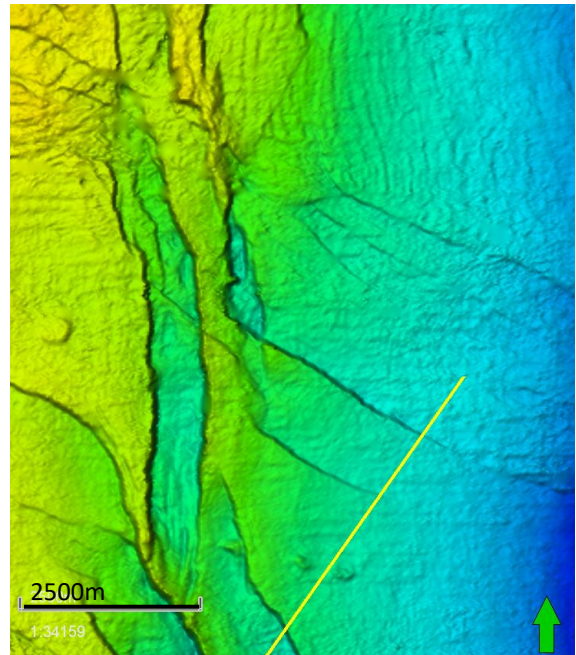
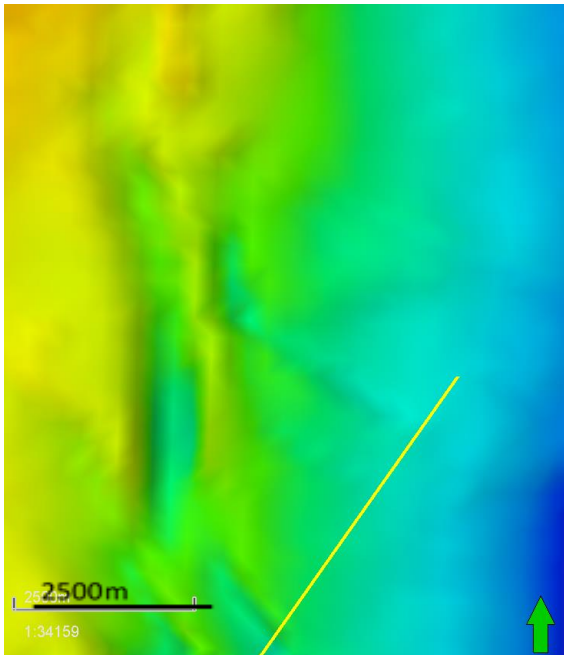


Quantifying the Minimum Fault Throw Resolution using Ant Tracking and High Resolution Mega Mapping



AUTHOR YOEL BEAUCAIRE

STUDENT NR. 2562955

DATE 23-09-2019

DAILY SUPERVISOR Guido Hoetz (EBN)

FIRST SUPERVISOR Klaudia F. Kuiper (Vrije Universiteit Amsterdam)

SECOND ASSESSOR: Wim van Westrenen (Vrije Universiteit Amsterdam)

Master thesis for the degree of Master of Science: Earth Sciences, track Geology & Geochemistry, Vrije Universiteit Amsterdam

Title page: comparison of the DGM v5 (left) and the result of this study (right) for the same area.

Table of Content

Abstract	4
1. Introduction	5
1.1 Geothermal Energy in the Netherlands	6
1.2 TNO DGM-Deep v5	6
1.3 Quantifying Minimum Fault Throw Resolution Using HIRES MEMA and Ant Tracking	8
2. Geological Background.....	10
3. Methods and Data.....	13
3.1 Seismic Data.....	13
3.2 High Resolution Interpretations	14
3.3 Seismic Interpretation	14
3.4 Available Horizons by TNO.....	15
3.5 Quality Check of Seismic-to-Well Ties.....	16
3.6 Ant Tracking Approach	17
3.7 Seismic Preconditioning for Ant Tracking	17
3.8 Quantifying the Minimum Fault Throw Resolution using HIRES MEMA and Ant Tracking	18
4. Results	19
4.1 Seismic interpretation	19
4.1.1 Base Upper North Sea	19
4.1.2 Base North Sea Supergroup.....	20
4.1.3 Base Chalk Group	25
4.2 Ant Tracking Results	25
4.3 Minimum Fault Throw Resolution	29
5. Discussion.....	31
5.1 Fault Spacing.....	31
5.2 Seismic Interference	33
5.3 Angle of the Horizon	34
5.4 Dip Direction Relative to the Inline and Crossline	34
5.5 Ant Tracking Settings	36
6. Conclusion	37
Acknowledgements.....	38
References.....	39
Appendix A - Fault Measurement Images	41
Appendix B - Mapping Workflow	48
Appendix C – Ant Tracking Workflow.....	51

Abstract

With the Masterplan Aardwarmte, the Dutch government has set goals to increase the role of geothermal energy in the Dutch energy mix. Currently, geothermal energy (2-4 km deep) is still relatively unexplored in the Netherlands, with only 22 geothermal doublets in the Dutch onshore subsurface. Smaller companies and operators are trying to participate in this new and upcoming market, but do not have the same facilities as larger operators. Therefore, most of their analyses are based on the freely available digital ground model (DGM-Deep) published by the Dutch geological survey, part of TNO. The grid resolution of these key geological maps is 250x250m. Because the resolution of the available seismic data on which these horizons are typically interpreted is 25m, many detailed structural features might not be seen on these horizons which can have crucial consequences when planning the well site or trajectory. As faults could pose a drilling hazard, as they have might constitute pressure barriers, missing faults when planning a new well location can potentially lead to blowouts.

During this study, as part of a 5 month internship at EBN B.V. (Energie Beheer Nederland), detailed seismic interpretations were conducted for three key stratigraphic intervals for the West Netherlands Basin: the base Upper North Sea Group, the base North Sea Group, and the base Chalk Group. This interpretation makes use of the full grid resolution of 25x25m, which is defined by the 3D seismic data available. In addition, Schlumberger's Ant Tracking software (advanced Petrel functionality to automatically detect faults) was used for fault analysis, building on the results of Kortekaas and Jaarsma (2017). After careful manual interpretation, 50 representative faults were selected and measured in detail to quantify what the minimum fault throw detection limit is for the different mapping methods. This analysis shows that when viewing horizons with a 25x25m resolution, using optimized display settings, faults with a vertical fault throw of just 1 ms (~ 1 m in depth) can already be detected at a depth ~1 km. On the coarse DGM grids, the fault detection threshold is 10 ms at best. Ant tracking delivers fault maps quickly and results are similar to the high resolution interpretation, with faults showing up starting from 1.5 ms fault throw. The consequences are that many faults, most notably when there is a second set of (conjugate) faults, are not visible on the DGM horizons. It is therefore strongly recommended that well planning makes use of high resolution surfaces, rather than the DGM surfaces.

1. Introduction

The Dutch subsurface is one of the most studied in the world and known for the production of large amounts of hydrocarbon (HC), both oil and gas. Due to a combination of active (induced) seismicity in Groningen, a decline in HC production, and climate agreements on the reducing role of fossil fuels in the energy mix, the Netherlands are preparing for an energy transition from fossil fuels towards greener options. One candidate is geothermal energy (> 500 m), which makes use of the natural heat produced by the Earth's interior. While the Netherlands have a large amount of information of the subsurface through the production of hydrocarbons, these targets are often situated in the structural highs of a porous lithology, whereas geothermal energy is more often applied in the warmer structural lows. Unlike gas & oil production, geothermal energy is not expected to be profitable soon and governmental subsidies are required for (early) developments. To obtain accurate depth estimates of these structures, accurate seismic interpretations in time at high resolution are required.

TNO, the Dutch Organization for applied scientific research, creates maps of different horizons on a national-regional scale, but these maps are restricted to a modest resolution of 250 by 250 meters due to historical and practical reasons. While sufficient in providing an insight to the general structure of certain horizons, as well as for general time-depth conversions, they often lack the resolution required for prospects/plays. The resolution of the seismic data used by most operators is 20 by 20 to 25 by 25 meters, implying a factor of 100 more datapoints per surface area than the horizons provided by TNO. The first feature to suffer as a result of the reduced resolution of a horizon are fault lineations. Faults are important for operators to determine the placement of a well or, as often the case with geothermal energy, a doublet. Faults can have either sealing or conductive properties, and can therefore pose a hazard during drilling, e.g. a blowout (Yanez-Banda *et al.*, 2017). The questions therefore are:

What is the minimum fault throw we can observe in the lower resolution maps? How many more faults can we see when using maps at the full resolution as defined by the underlying (3D) seismic datasets?

The HIRES MEMA project, short for High Resolution Mega Mapping project, is a project by EBN (Energie Beheer Nederland) to merge high resolution interpretations (25x25m), where available, into the low resolution regional maps (250x250m) available from TNO. The results are new, national-scale maps of key horizons in the Dutch subsurface, both offshore and onshore, combining the benefits of full resolution (HiRes) with large coverage (Mega) maps. The onshore map HIRES MEMA is certainly of great value to the currently growing Dutch geothermal energy market, whereas offshore maps are expected to be of use to contribute to various exploration studies. Subsequent merging On and Offshore HIRES MEMA maps introduces further challenges due to datum and time shifts. For correct and continuous maps, it is important that the proper loops are chosen, picked correctly and bulkshifted where required. More information about seismic interpretation can be found in Chapter 3. Replacing the low resolution DGM v5 horizons by the high resolution horizons is automated as much as possible using workflows in Petrel by Schlumberger. The workflow itself is a project deliverable for EBN and is also discussed to some extent in this thesis.

In addition to creating new maps with high resolution of the Dutch subsurface, ant tracking will be used to detect faults pseudo-automatically in the West Netherlands Basin (WNB). The specifics of fault detection through ant tracking are discussed in Appendix C. The WNB is known for its numerous and complex structures, mainly due to inversion tectonics. An interactive regional overview at different depths of these faults can therefore be of value to geothermal energy related projects, as faults play an important role in geothermal energy. Quantifying the minimum fault throw resolution of these faults will be the main purpose of this research. The final products delivered to EBN are:

1. Detailed time maps of the base Upper North Sea Group, base North Sea Group and base Chalk (25x25m) in the subsurface of the West Netherlands Basin and East Netherlands;
2. A workflow in Petrel that allows any user to add new, high-resolution data of a certain area to the existing model, automatically replacing the previous lower resolution model;
3. A map of automatically detected and extracted faults for the WNB using ant tracking for each horizon level, which will be the focus of this research.

1.1 Geothermal Energy in the Netherlands

With the ‘Masterplan Aardwarmte Nederland’, the Dutch government has set certain goals to reduce the role of gas in the energy mix and cut CO₂ emissions by 49% by 2030, and increase the role of Geothermal energy from the current 3 Petajoule (PJ) to 50 PJ by 2030, and even 200 PJ by 2050. There are currently around 35 000 geothermal energy systems in the Netherlands, of which 99.6% are located in the top 500 meters depth. These are classified by the Dutch government as ‘bodemenergie’, making use of low temperature (< 30 C°) aquifers for storage of heat, and fall under the Groundwater Act (Dutch: Grondwaterwet). Every geothermal project below 500 meters requires a permit by the Dutch Mining Act (Mijnbouwwet) and is considered ‘geothermische energie’, or geothermal energy. To further differentiate:

- From 500 – 1000 m is referred to as shallow geothermal energy;
- From 1000 – 4000 m is considered deep geothermal energy;
- Below 4000 meters is considered Ultra Deep Geothermal energy (UDG), with a potential for industrial applications, which is currently investigated (*Platform Geothermie 2019*).

As of 2019, there are 21 active geothermal doublets, of which 12 are located in the West Netherlands Basin. Fig.1 shows the relatively high amount of permits for geothermal energy in the WNB, indicating the interest in the area for geothermal energy. Geothermal plays are located in the Rijnland & Schieland Groups, with a possibly for the Germanic Trias Group.

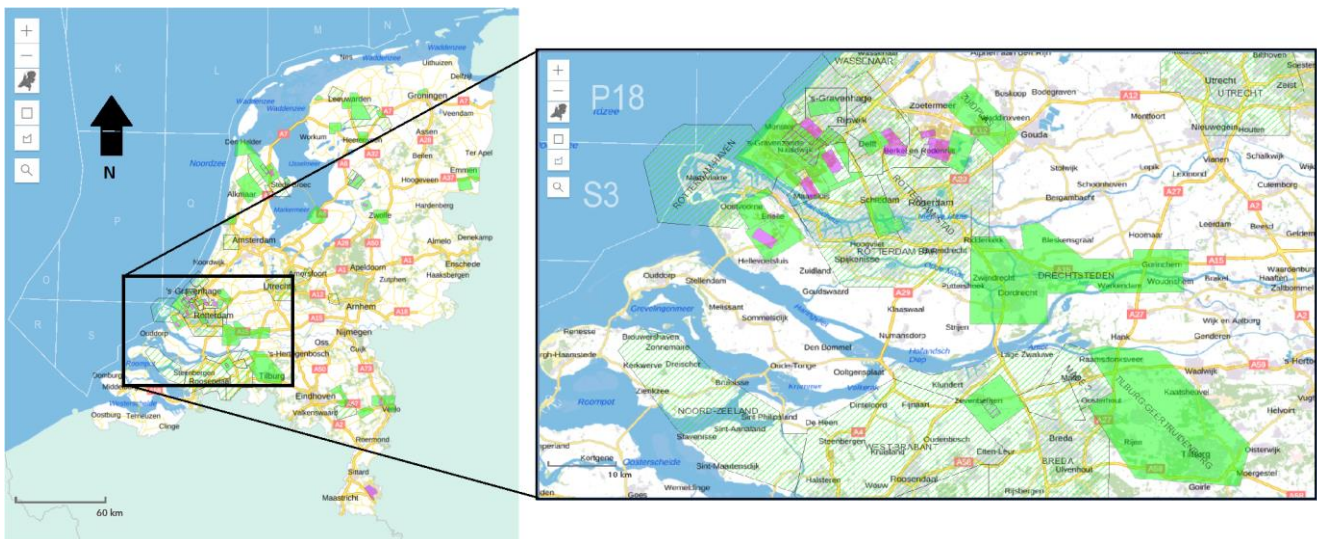


Fig. 1 - Overview of permits for Geothermal energy in the Netherlands as of 27-5-2019. Note the relatively higher number of permits in the Rotterdam area/West Netherlands basin. Green = exploration permit (granted), striped green = exploration permit (applied for), purple = production permit (granted), striped purple = production permit (applied for).

1.2 TNO DGM-Deep v5

Since 1985, the Geological Survey of the Netherlands is commissioned to compile a consistent, regional-scale petroleum geological framework for the deep subsurface of the Netherlands, both offshore and onshore. This model consists of the key horizons in the subsurface and is based on a combination of available non-confidential 3D and 2D seismic data, well data of approximately 5800 wells, and geological maps previously published on paper. The model contains its own velocity model (VelMod-1 to the current VelMod-3) to create a regional depth model of the Dutch subsurface for HC and geothermal applications. The first model was released in 2002 which covered only onshore Netherlands. This was then followed by v2 in 2006 (on- and offshore), v3 in 2010 (offshore), and v4 in 2014 (onshore). In April '19, TNO has released their latest DGM v5, which consists of both on- and offshore data. Onshore, the differences with the previous v3 model are mainly noticeable in the areas that lack 3D seismic coverage: central and south-east Netherlands (Fig. 2). According to TNO, the differences are due to the use of 2D data in the DGM v5 model in areas where 3D seismic data lack. 2D is not used in DGM v3. The resolution of these horizons are published in is 250 x 250 m. Fig. 3 gives an example of the lower resolution of the base North Sea Group, provided by TNO, which clearly indicates the 250x250m grid size. An important detail to note is that the surfaces are not only displayed at 250x250m, but also picked/auto-tracked on a 250x250m grid.

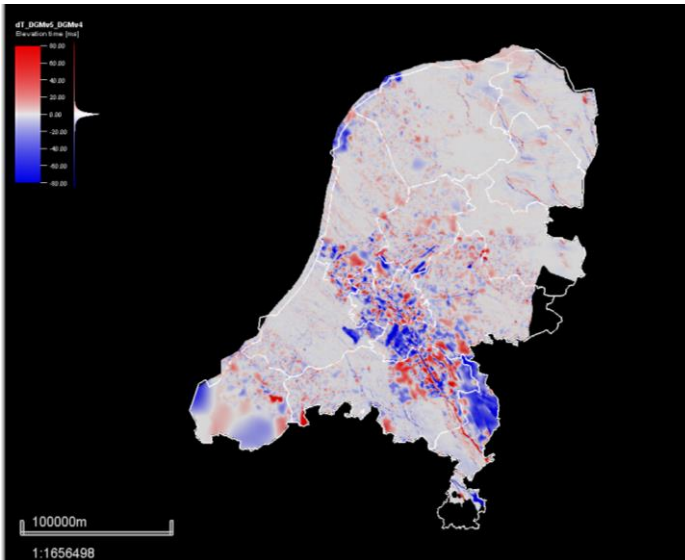


Fig. 2 – Time differences in ms between TNO's DGM v5 and DGM v4 for the base North Sea Group. Positive values indicate a decrease in time of the new model. The differences are largest in areas that have no 3D seismic coverage (in blue, right image).

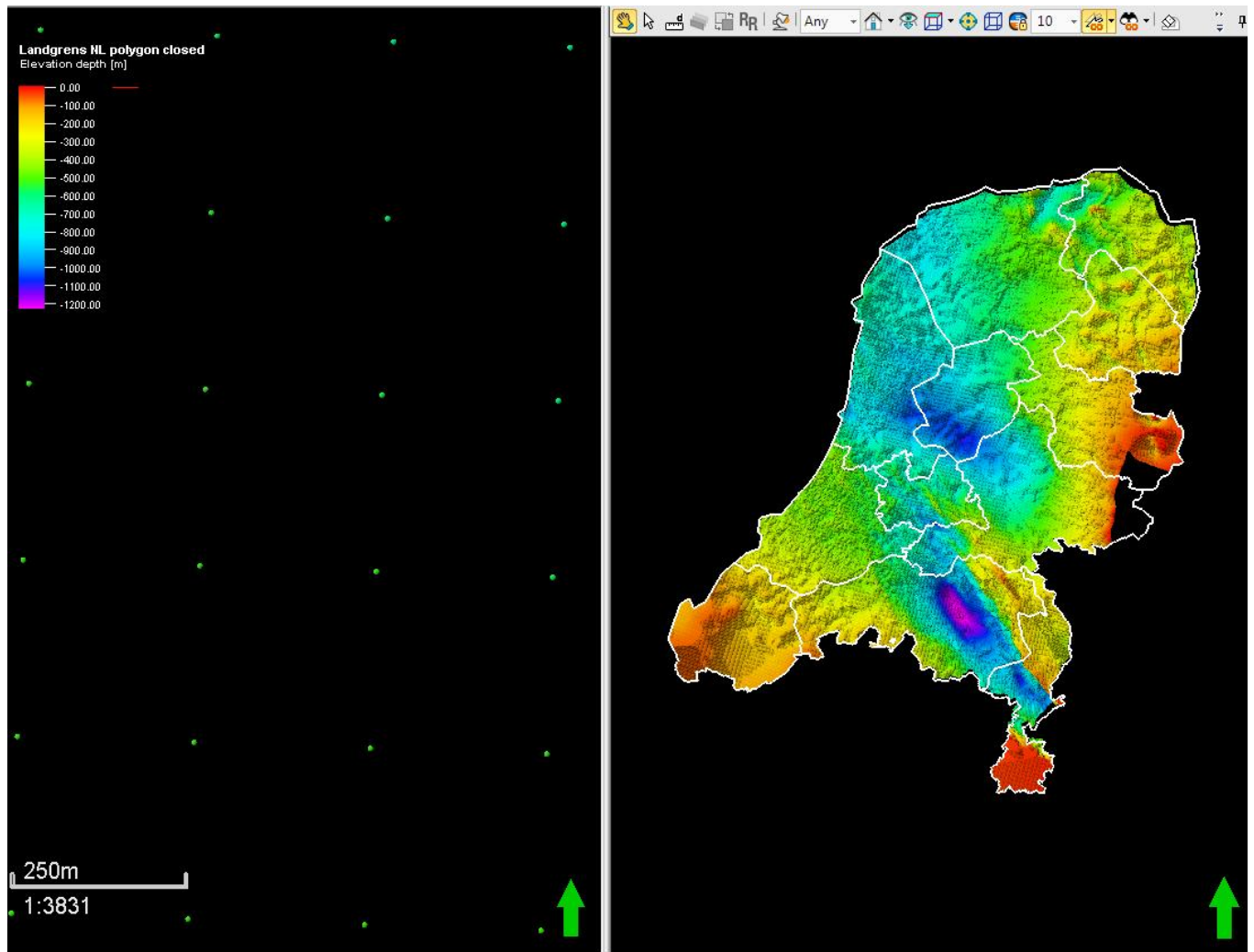


Fig. 3 - Right: a point set of the DGM v5 base North Sea Group.. The left image is zoomed in to illustrate the 250 x 250 meter resolution used by TNO

1.3 Quantifying Minimum Fault Throw Resolution Using HIRES MEMA and Ant Tracking

How does a higher lateral resolution contribute to the imaging of faults? What is the minimum fault throw required to accurately distinguish faults on a time surface? What is the minimum fault throw required to detect faults using ant tracking? Are the publicly available DGM v5 maps sufficient in imaging faults? To be able to answer these questions, a comparison is made between the DGM v5 maps of the three upper key horizons and high resolution interpretations made for this study in terms of fault imaging. The common approach, if resources allow for it, is to manually interpret the faults, usually with some help from the different volume attributes in Petrel which enhance discontinuity in the seismic data. For an area the size of the West Netherlands Basin this is very time exhaustive, even though it is still the preferred method for small target areas (< 4 km km²) where accurate fault interpretation is crucial to forecast the viability of a geothermal (or HC) play.

For this study, the minimum fault throw resolution is based on a map view of both the TNO maps and HIRES MEMA maps. Fault lineations are first observed on the TNO surface on a map view, and the corresponding fault throw is then measured on a seismic interpretation window (sub)perpendicular to the structure. As mentioned before, the TNO maps are gridded every 250 meters, with faults appearing more flexural, with no clear view of the position of the fault itself. Especially below a certain fault throw, faults become indistinguishable with such a low resolution (Fig. 4). As known from previously existing high resolution surfaces, we know that faults require a much lower throw to be interpreted manually on a seismic intersection. After the HIRES MEMA maps have been completed, an indexation is made to indicate the threshold fault throw that can be distinguished on both the HIRES MEMA and TNO DGM v5 maps. Finally, we can quantify how much better the fault resolution is when using HIRES MEMA compared to DGM v5.

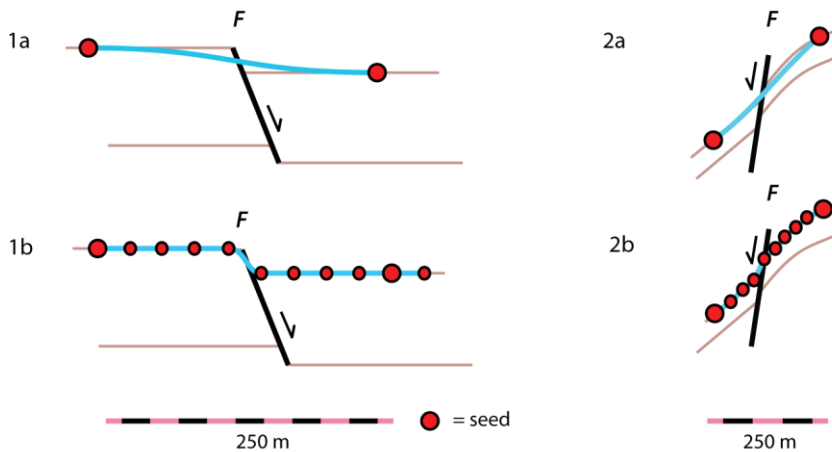


Fig. 4 – Simplified example of fault imaging with (a) a resolution of 250m and (b) a resolution of 25m. 2 shows a scenario in which the strata is at high angle relative to the fault. In this case, a fault can only be distinguished using high resolution. Both types of examples of fault are numerous in the West Netherlands Basin.

Another aim in this research is to design a Petrel workflow that allows major fault systems to be automatically detected and extracted from a seismic survey. Manual picking of faults is most often time and labor costly, especially for large surveys. Ant tracking can save a lot of time if performed properly. It does require some preconditioning of the data to improve the results of the ant tracking later on in the process. The ant tracking attribute itself requires discontinuity or edge cube (variance, chaos, etc.) and connects those discontinuities based on settings that can be determined by the user. The process is similar to an ant track made in the forest, where ants leave a trail of pheromones for other ants to follow who on their turn enforce the existing trail of pheromones by following it. Finally, the trails that are travelled the most have the strongest signal. Ant tracking in Petrel is used for either larger (faults) or smaller discontinuities (e.g. fractures). Because of this, it comes with three settings for the parameters: passive, aggressive, and custom. Passive has more conservative parameter settings, intended to outline larger structures, with the aggressive setting intended for fractures. Because ant tracking is sensitive to the scale of the structures, it requires the user to determine the scale of the discontinuities that

needs to be outlined. As EBN currently does not have fault maps for the WNB, it was therefore chosen to outline the regional scale faults that can be distinguished on a seismic intersection and on a 3D surface.

Ant tracking itself only results in a seismic cube that indicates the connected discontinuities (e.g. faults), but requires fault extraction to convert the ant tracking results into 3D geometries. Fault extraction is process in Petrel that has two settings: normal confidence and high confidence. Normal confidence generally gives a higher number of objects and takes a longer time to complete and vice versa. After these 3D geometries have been extracted, the user can filter out objects based on dip angle, dip azimuth, surface area, etc., to most accurately approximate the larger faults in the area. In summary, to get a fault map that best approximates the larger fault structures, we need to:

1. Determine the best approach to precondition the seismic cube for ant tracking;
2. Determine the parameters for ant tracking in the WNB;
3. Determine the parameters for fault extraction of the ant tracking results;
4. Filter the extracted faults to closely resemble the faults observed in the seismic section/on the horizon surface.

2. Geological Background

This chapter will provide mainly background on the geological development of the horizons that are of interest for geothermal applications in the study area, which are down to the base Schieland Group (Jurassic). This research focusses mainly on the West Netherlands Basin, abbreviated as the WNB, located in the west of the Netherlands, spanning from The Hague in its northwestern extent to the southeast, where it transitions into the Roer valley Graben (Fig. 5). Although ant tracking was only applied in the West Netherlands Basin interpretation of the Base NU, NLNM, and CK Groups has also been performed in Drenthe, East Netherlands.

The West Netherlands Basin has been targeted for oil and gas since 1955, initially with oil, later with gas as well. While production is ongoing, the current production values are a small fraction of the Groningen gas field's. Due to the horst-and-graben structure of the WNB, nearly all HC plays in the WNB are located in the horsts (structural highs). Geothermal energy explores the grabens (structural lows) of the same area, and therefore the lithological properties of the formations at larger depths are hardly known (De Jager, 2007).

Categorized as a Kimmerian rift basin, the WNB formed during the Kimmerian tectonic phase (Triassic – Jurassic in age), at the onset of the break-up of Pangea (De Jager, 2007). The break-up of the Pangea supercontinent resulted in crustal extension in the North Sea area, with the degree of extension decreasing southwards (Ziegler, 1988; De Jager, 2007). This extension was mainly in E-W in the current northern Dutch offshore, and NE-SW in the Dutch onshore, and resulted in the Dutch Central Graben in the north, and the Broad Fourteen Basin and West Netherlands Basin in the west. From the Late Jurassic to the Early Cretaceous, strong rifting resulted in the segmentation of the WNB along with oblique-slip effects in the extension basin. Some blocks remained more quiescent, which other blocks subsiding fast, resulting in strong erosion of the highs, and the infill of syn-rift sediments packages in the basin. As a result, the distribution patterns are very complex (Van Adrichem Boogaert & Kouwe, 1993). Towards the Early Cretaceous, rifting only continued in the north, e.g. Norwegian and Greenland seas, and effectively ceased in the Netherlands.

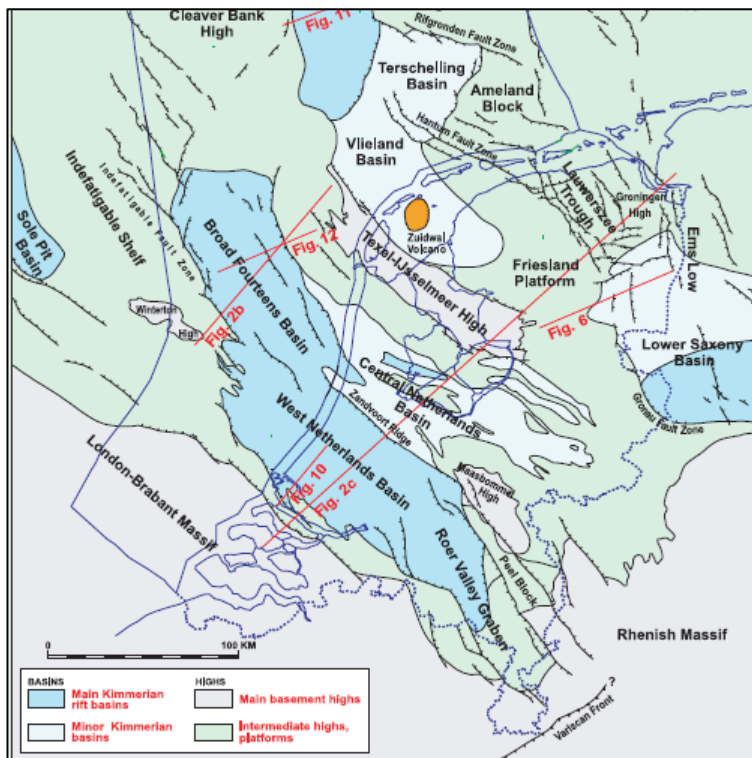
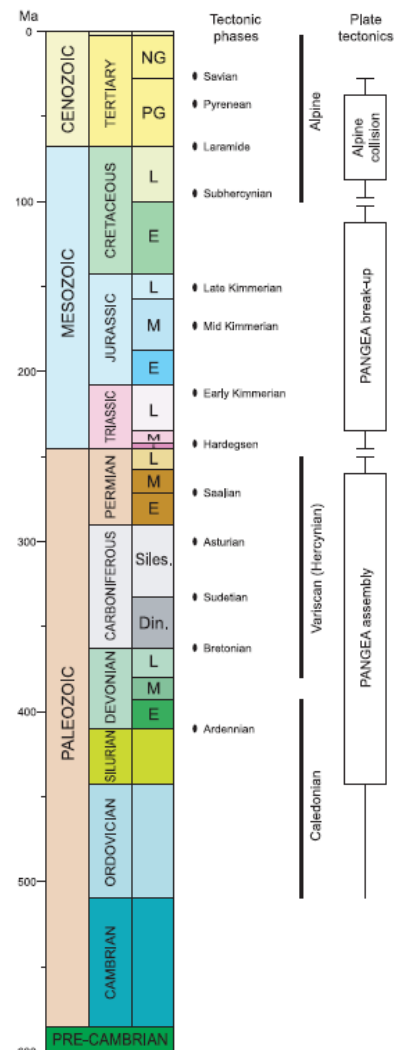


Fig. 5 – Left: Map of the important structural elements in the Dutch subsurface. A cross section of Fig. 10 can be found on the next page. From *Geology of the Netherlands* (2007). Right: Geologic time scale, along with the tectonic phases and association with plate tectonics, e.g. the break-up of Pangea.



NE-SW extension of the crust during the Kimmerian tectonic phase resulted in a NW-SE block-faulted transtensional rift system with volcanic activity, as is evidenced by the occurrence of volcanic rocks and intrusive sills (De Jager, 2007). From the Late Tertiary to the Middle Jurassic, the long-lived London-Brabant Massif formed a structural high to the south of the WNB, with the East Netherlands High to the north and east, with a uniform deposition of marine and pelagic sediment of up to 1800 m (Fig. 6). The Middle Jurassic to Early Cretaceous is characterized by syn-rift sediments, with largely varying thicknesses, accompanied by erosion of the higher blocks.

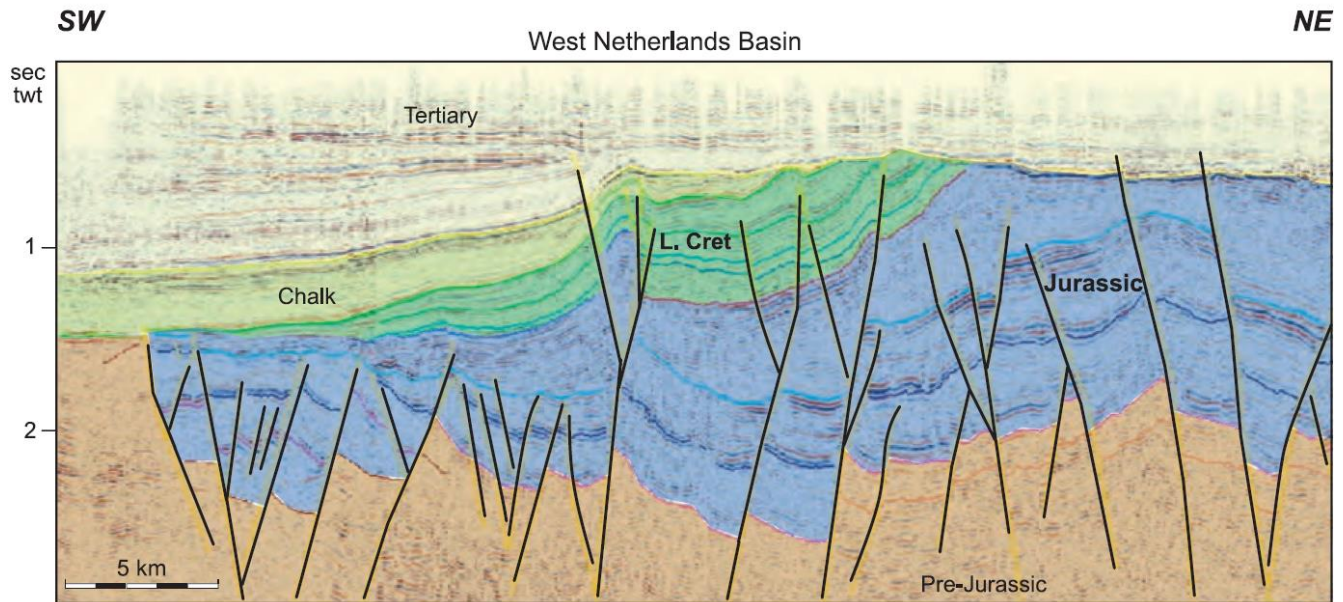


Fig. 6 – Cross section of the West Netherlands Basin with color overlay, indicating Pre-Jurassic (orange), Jurassic (blue), Lower Cretaceous (green), Chalk (dark yellow) and Tertiary (light yellow) groups. Note the number of normal faults in the Jurassic and the unconformity of the Tertiary and the underlying groups. From *Geology of the Netherlands* (2007).

The Altena Group forms the first group of mainly argillaceous sediments from the Triassic-Jurassic boundary up until the Oxfordian (Late Jurassic), after the classification by Van Adrichem Boogert & Kouwe (1993-1997). The Altena Group consists of sediments deposited mainly pre-rift with some syn-rift sedimentation towards the Late Jurassic. Due to the absence of evaporitic deposits in the WNB during the Jurassic or the Permian (Zechstein salts), the WNB is characterized at this moment by tilted half-grabens, unlike other basins of similar age and origin, e.g. the Broad Fourteens Basin and the Dutch Central Graben. The base of the Altena Group (B_AT) is one of the key horizons provided in the DGM-Deep model.

The Schieland Group forms the second group of mainly continental sediments from the Late Jurassic to Lower Cretaceous, containing the Delfland Subgroup and the Central Graben Subgroup. The base of the Schieland Group (B_S) is also one of the key horizons provided in the DGM-Deep model. It is in these Early Cretaceous deposits that most members of interest for geothermal energy are located, e.g. the Delft Sandstone member and the Alblasterdam formation (Worum & Van Wees, 2017). The Delft Sandstone Member (DSSM) of Valangian age (Early Cretaceous) is part of the Delfland Subgroup that is deposited in the West Netherlands Basin and is currently exploited for geothermal projects, e.g. the Delft Aardwarmte Project, at a depth of 2.2 km, with a locally varying thickness of 0 - 130 m and temperatures of 68-78 C° at the top of the reservoir (Donselaar *et al.* 2015).

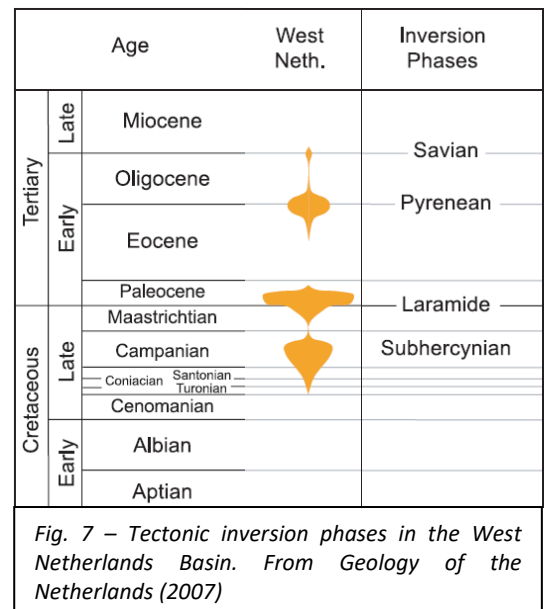
The Alblasterdam Member, also part of the Delfland Subgroup, overlies the DSSM as clay- and siltstones from a fluvial-plain forming a seal on top of the DSSM. The thickness of the member varies from less than 100 m to more than 1300 m, controlled by the syn-rift deposition and a rapid pinch-out in SW direction towards the London-Brabant Massif (Fig. 6). Both the Alblasterdam and Delft Sandstone members are thought to be part of fluvial channels, with variable lateral sediment distribution.

The Rijnland Group forms the third lithostratigraphic group, from the Late Jurassic up to the Late Cretaceous and is also a key horizon provided in the DGM-Deep model as the base Rijnland Group (B_KN). It comprises mainly argillaceous (and some marly) formations which may contain sandstone beds at the base and, locally, similar coarse clastic intercalations at higher levels contiguous with the basin margin.

It is during the Late Cretaceous that the first tectonic pulse emanating from the collision of the Eurasian and African plates resulted in N-S oriented compression in the crust, causing tectonic inversion of the large faults in the WNB (Fig. 7). The first inversion pulse, the Subhercynian, is associated with chalk deposits of the Chalk Group in a shallow marine setting, thinning towards the axis of highest uplift in the NE (Fig. 6). Uplift is estimated to have been no higher than 1 – 1.5 km (Herngreen & Wong, 2007). The second inversion pulse, the Laramide, resulted in a renewal of inversion tectonics and thought to have a stronger impact, lasting into the Paleocene, Tertiary, with complete termination of chalk deposition, erosion of said chalk, the Lower Cretaceous, and the Jurassic deposits, and onset of siliciclastic deposition of the North Sea Group (Fig. 6). The third pulse, the Pyrenean, was the final inversion pulse that can be detected in the Dutch subsurface, which caused broad basin uplift without fault reactivation. Due to the lack of Zechstein salts in the WNB, the fault blocks remain tilted.

During deposition of the North Sea Supergroup siliciclastic sediments, tectonic activity remained relatively limited, resulting in horizontal beds reaching up to 1200 m in the WNB, increasing in thickness towards the SW. The North Sea Supergroup is divided into the Lower, Middle and Upper North Sea Group, with each of the bases unconformable. Due to the variable presence of the Lower North Sea Group in the Dutch subsurface, the bases of the Middle (B_NM) and Lower North Sea Group (B_NL) are combined to one in TNO's DGM-Deep model (B_NLNM). The Lower North Sea Group reaches up to 650 m in thickness in the northern offshore, thinning towards the south. The Upper North Sea Group reaches its maximum depth of 1400 m in the Roer Valley Graben (Wong *et al.*, 2007).

As most of the plays in the WNB that are of interest to the geothermal energy sector are located in the Lower Cretaceous, it is important to have high resolution maps of the WNB for the overlying bases of the Rijnland Group, Chalk Group, Lower and Middle North Sea Group, and the Upper North Sea Group. Of these horizons, only the base Rijnland Group (B_KN) has not been interpreted. Of these four interpreted horizons, most faults are expected in the base North Sea Group, due to the geological history of the area.



3. Methods and Data

3.1 Seismic Data

3D seismic covers 56% of the Dutch on- and offshore subsurface (De Jager & Geluk 2007). This number is lower for the onshore by its own - around 35% - and can be categorized into three areas: northeast (Groningen), northwest (Alkmaar), and southwest (Rotterdam). The seismic coverage for the WNB spans from the Monster seismic cube at the coast, to Waalwijk in the province of Brabant (Fig. 8). This data is available as separate surveys, or merged (Table 1). The NAM has merged three seismic cubes into one, and reprocessed it to increase the resolution at larger depths (> 2 ms). The quality of the data varies between the surveys, with Monster having the lowest quality relatively (Table 1). This means that the Monster cube has large and/or many data gaps, and the processing performed is therefore not optimal, resulting in a weak continuation of the loops, a low signal-to-noise ratio, and an overall more chaotic distribution of the loops. The effect of such quality seismic is seen in the interpreted surfaces, as well as the ant tracking results.

Table 1 – Seismic Surveys Used in this Study

Name	Quality	Operator	Year	Merged
L3NAM	Very good	NAM	1985, 1989, 1990	Yes
Waalwijk	Very good	CLYDE	1997 (2006 Repr.)	No
Monster	Poor to good	NAM	1990	No
Andel	Good	NAM	2007	No



Fig. 8 – Extent of the seismic used in this study, with the names added. These names will be consistently referred to as such in this thesis.

3.2 High Resolution Interpretations

The seismic interpretations of the key horizons used for this project are both supplied by EBN and self-generated (see 3.3 – Seismic Interpretation). EBN is involved in multiple onshore projects, with some interpreted horizons for e.g. the base Chalk, that can be implemented in this project. While these other available interpretations are not used for this research, they can be used in the mapping workflow (see Appendix B). Future interpretations for onshore projects can also be implemented in the mapping workflow. An example are the interpretations for the Groningen gas field, with the local interpretations for the top Rotliegend, which can be added for the final onshore geological map of the base Zechstein.

3.3 Seismic Interpretation

Seismic interpretation for this research is limited to the base Upper North Sea (NU), the base North Sea Group (NLNM) and the base Chalk (CK) in the West Netherlands Basin and Drenthe (East Netherlands) and is performed in Petrel, both manually and using the auto-tracking feature. Manual interpretation is time-costly, but precise, whereas auto-tracking can be time-saving, but prone to errors. To make use of the auto-tracking function whilst minimizing erroneously picked loops, seeds are interpreted every 16th in- or crossline, going down to every 2nd or 4th inline near structural features (mainly faults). The remainder is either auto-tracked or interpolated. Interpolation is used most often where seismic data is not continuous but the strata is, due to e.g. a shallow gas event, or around the area where a single reflector splits into two, also known as a doublet (Fig. 9).

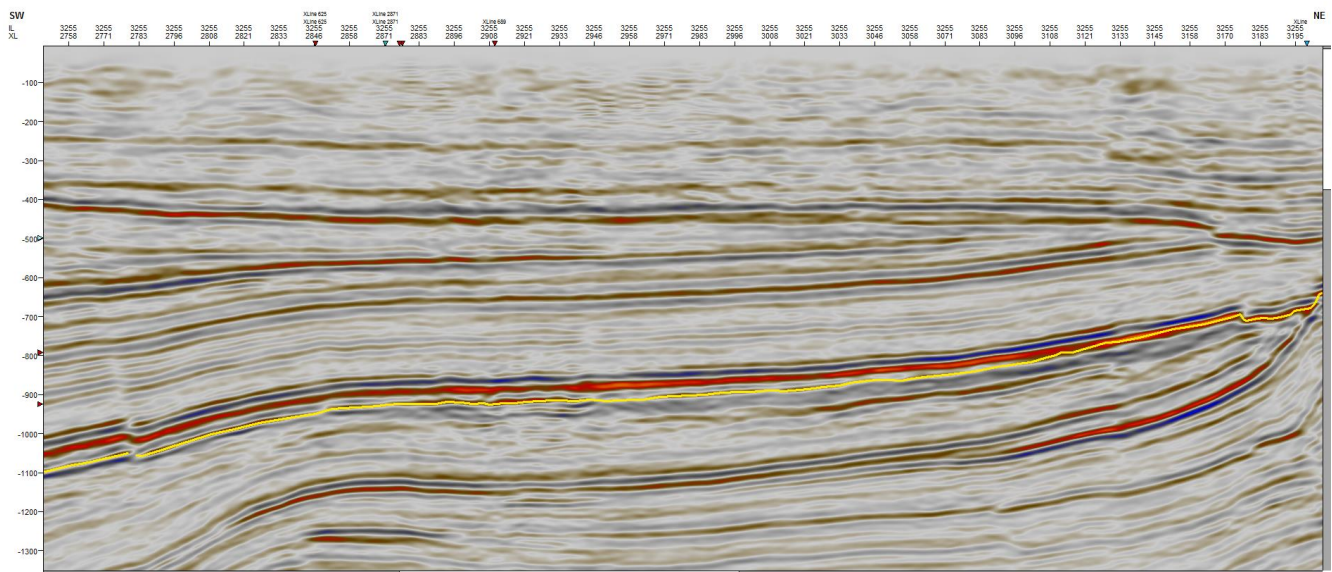


Fig. 9 – Example of a doublet in the seismic interpretation window for the base North Sea Group. The reflector splits into two reflectors in southwestern direction at crossline 3121, of which the lower, weaker reflector (yellow) is the true base verified by well top data further to the southwest.

The base NU, NLNM, and CK horizons are relatively continuous with a weak (NU) to strong (NLNM & CK) amplitude. For anything below the base Chalk, e.g. the Rijnland group, auto-tracking will most likely be problematic. Using auto-tracking automatically results in multiple QC attributes: amplitude, confidence level, distance. By removing auto-tracked areas with a low confidence, and performing auto-tracking multiple times, it should be possible to retrieve an auto-tracked interpretation with a high level of confidence. The only way auto-tracking can work optimally, is if enough effort is spent in quality checking (QC'ing) the data for errors (loop skips) after each run. A summary of the workflow can be seen on the right (Fig. 10). In most cases there are areas, like the aforementioned doublets, where auto-tracking will generate loop skips, as it jumps from the shallower, stronger reflector to the weaker reflector. 'Wedge effects' make it difficult to indicate the emergence of the lower loop, and therefore this area must be interpolated (Fig. 17).

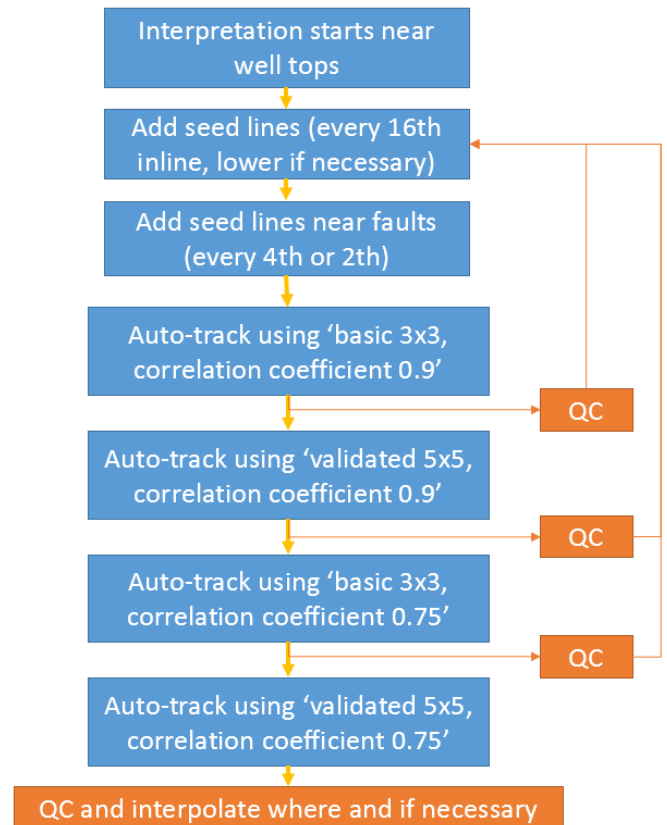


Fig. 10 – Interpretation workflow. After each step, a Quality Check (QC) was performed to prevent seismic artifacts, e.g. loop jumps, as much as possible.

3.4 Available Horizons by TNO

TNO provides nine key horizons in time and depth for the Dutch subsurface that will be used as a basis for the HIRE MEMA project (Table 2). These contain the most important transitions in lithologically similar and seismically recognizable units, such as the transition from the base North Sea Group, a sedimentary, siliciclastic member, to the Chalk group, a carbonate deposit that is seen as a hard kick in the seismic, and is easily recognizable by its wedge shape. Another important transition in the Dutch subsurface is the base Zechstein, which for offshore Netherlands and Groningen correlate to the top Rotliegend, although it is absent in the West Netherlands Basin. The base Upper North Sea Group (Fig. 11) is also provided, but because it is both difficult to recognize in the subsurface, and it does not impact the velocity model significantly, TNO released a velocity model in which the base North Sea Supergroup is calculated as one lithological unit, rather than two (personal communications, Walter Eikelenboom). As mentioned before, all nine key horizons will be able to work with the mapping workflow, although only the upper three horizons will be used for the comparison of fault imaging.

Table 2 – Key Horizons in the Dutch Subsurface	
TNO's Reference Name	Full Name
B_NU	Base of Upper North Sea Group
B_NLNM	Base of Middle & Lower North Sea Group/ Base of North Sea Group
B_CK	Base of Chalk Group
B_KN	Base of Rijnland/Vlieland Group
B_S	Base of Upper Jurassic
B_AT	Base of Altona Group
B_RN	Base of Upper Germanic Trias Group
B_RB	Base of Lower Germanic Trias Group
B_ZE	Base of Zechstein

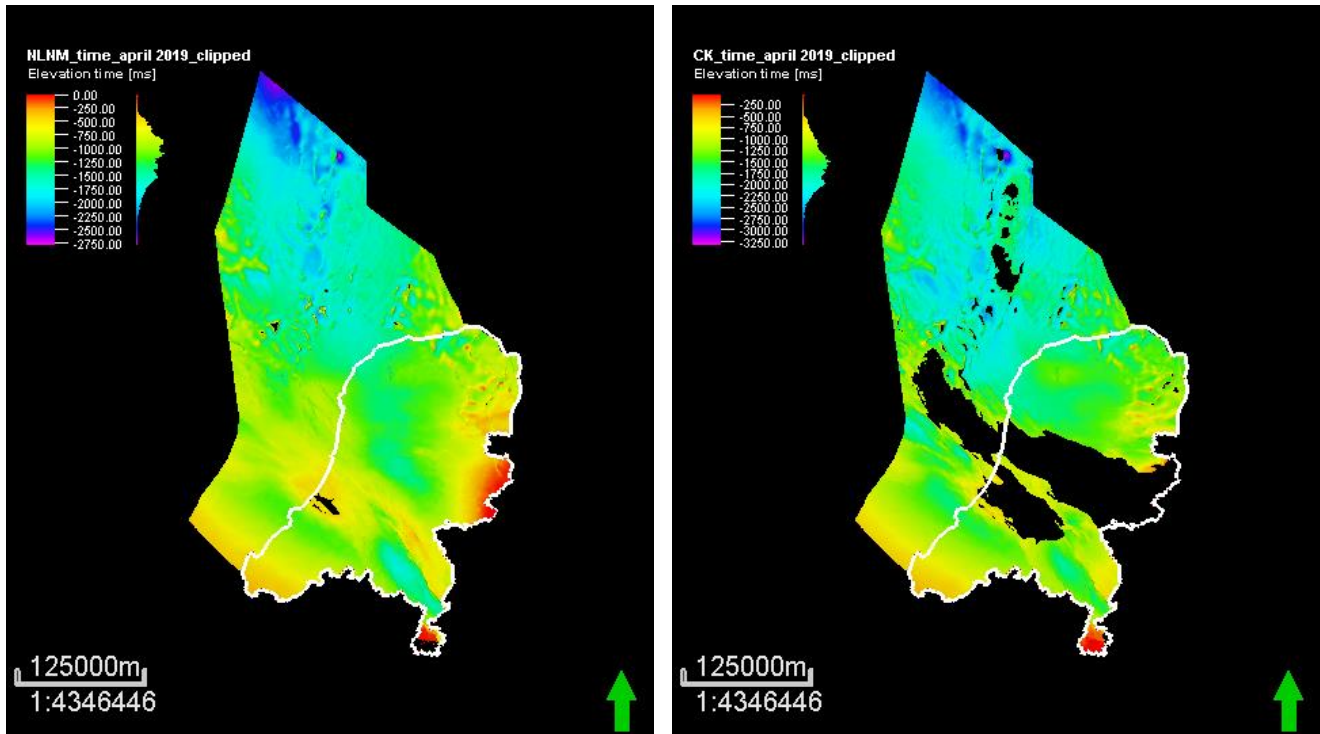


Fig. 11 – Examples of both the base NLNM (North Sea Supergroup) and the base Chalk Group. Note that difference in coverage between the base NLNM and the base CK, mainly in the center of the Netherlands.

3.5 Quality Check of Seismic-to-Well Ties

Time differences often occur between reflectors in the seismic and the pseudo well pick. A pseudo well pick is an artificially generated time for a certain point or reflector, e.g. base Chalk, that is not directly measured at the well, but results from a time-depth relation based on a check shot. At some wells, check shot data is gathered by generating a sound and measuring interval velocities for each 100 meters it propagates through the subsurface at the well. This results in a time-depth relation, or T-Z relation. Dividing the depth (in m) of a well marker, e.g. the top Chalk, by the velocities measured in the subsurface gives an artificial depth in time, a pseudo-pick. This can be relatively accurate for a well that contains check-shot data. For other wells, the T-Z relation of the nearest well is used. The seismic data (in ms) can then be correlated in time to the well data (in meters), although this process does not always work for every well in a seismic survey. Picking a certain reflector (B_CK) can therefore produce a time difference with the pseudo-pick, and result in a depth residual after time-depth conversion of the time surface.

It is important therefore to check the seismic to well ties between different wells in different seismic cubes. An example of a seismic to well match can be seen below, the seismic-well tie matches quite closely, with a large increase in porosity (log on the left of borehole) and a large decrease in Gamma Ray (log on the right side) at 947 ms, correlating with the strong red reflector with a negative amplitude (Fig. 12). There is a difference of 3 ms between center of the strong red reflector and the transition seen in the well data. This translates to around ~ 3 m difference in depth, which can be considered negligible.

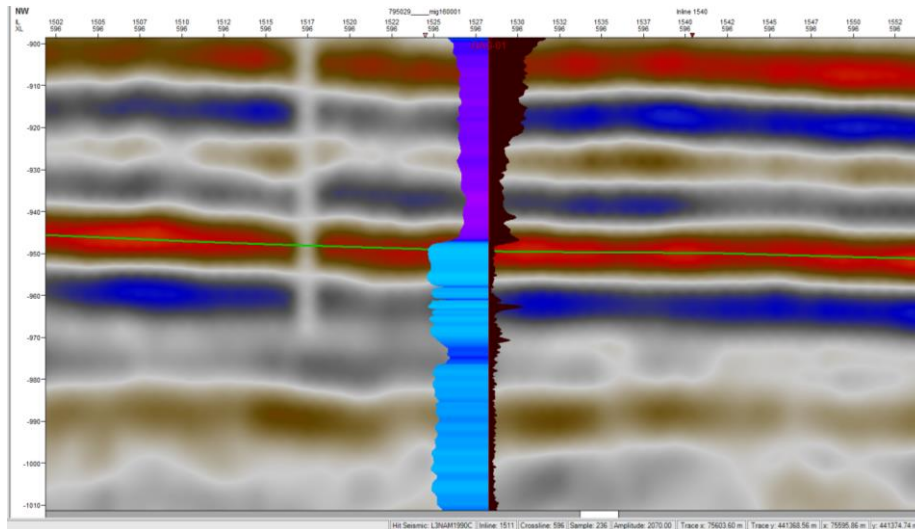


Fig. 12 – Example of a seismic to well match at the base of the Upper North Sea Group. The change in gamma ray (GR) values (right, in black) and the increase in porosity indicate a sharp transition that fits well with the red reflector (3 ms).

3.6 Ant Tracking Approach

Ant tracking is a CPU and time-intensive process, and therefore needs to be tested on a smaller volume before processing the whole seismic cube. Different cropped volumes of seismic cube are therefore made that are within 100 – 200 Mb in size. This is either achieved by cropping only the vertical extent, e.g. from 400-1200 ms, capturing all the faults in the base North Sea Group, or creating a small cube with a high vertical extent.

Ant tracking itself is performed on the main four seismic cubes (Monster, L3NAM, Andel, and Waalwijk) as to observe the influence of the data and signal quality on the results. Eventually, the results of the ant tracking are extracted as a surface attribute for e.g. the base NLNM in Petrel. This calculates where the ant tracking results intersect the surface, making it easier to compare the faults picked up by ant tracking and the faults we can distinguish on the surface.

To optimize the final result of ant tracking, preconditioning of the seismic data is required. Petrel harbors many different plug-ins to optimize or enhance certain seismic attributes, which will be discussed below. A systematic approach was chosen to process a cropped seismic volume multiple runs with the same volume attribute and only one varying parameter. Finally, a workflow is made that best captures the dominant fault structures in a given seismic survey.

3.7 Seismic Preconditioning for Ant Tracking

Seismic preconditioning is required for successful ant tracking. The following order of seismic attributes is based mostly on papers by Bahorich & Farmer (1995), Randen *et al.* (2001) and Silve *et al.* (2005). To ensure a good continuation of the loops, *Structural Smoothing* can be applied to remove noise from the seismic signal and allows for better continuity of the data in either X, Y, or Z direction. Additionally, the user can opt for either planar or directional smoothing (dip guided), and even edge enhancement. Plain is used most often to smooth (sub)parallel reflectors, whereas dip guided smoothing anticipates the continuation of a certain reflector and smooths in that direction. The relative direction in which smoothing occurs can be manipulated by the sigma X, sigma Y, and sigma Z. Before enhancing discontinuity, we want to decrease lateral and vertical variations in amplitude due to weakening of the seismic signal with depth. We use the *Graphic Equalizer* (Graphic EQ) to enhance the weaker amplitudes at depth relative to the stronger amplitudes in the shallow part (< 2 s TWT).

The next step is to apply another volume attribute that enhances discontinuity in the seismic signal, which is how faults are often recognized on seismic data. There are multiple attributes that can be used, with mainly two fault-enhancing attributes commonly used: the *Variance* and *Chaos* Attribute. The *Variance* attribute is used to extract a reflection continuity, where it measures a similarity between waveforms and extracts strong lateral changes in both waveform character and amplitude. Faults are a main cause of large variations in the dip estimate of the strata, which are enhanced by the Variance attribute.

The *Chaos* attribute enhances discontinuity or ‘chaos’ in the seismic signal. The *Edge Evidence* attribute can also be used to outline the ‘edges’ found in seismic and even set a preferred orientation and dip for outlining these edges. Apart from determining the best use of the parameters for each volume attribute, it is important to determine the order in which the volume attributes are linked to each other (Fig. 13).

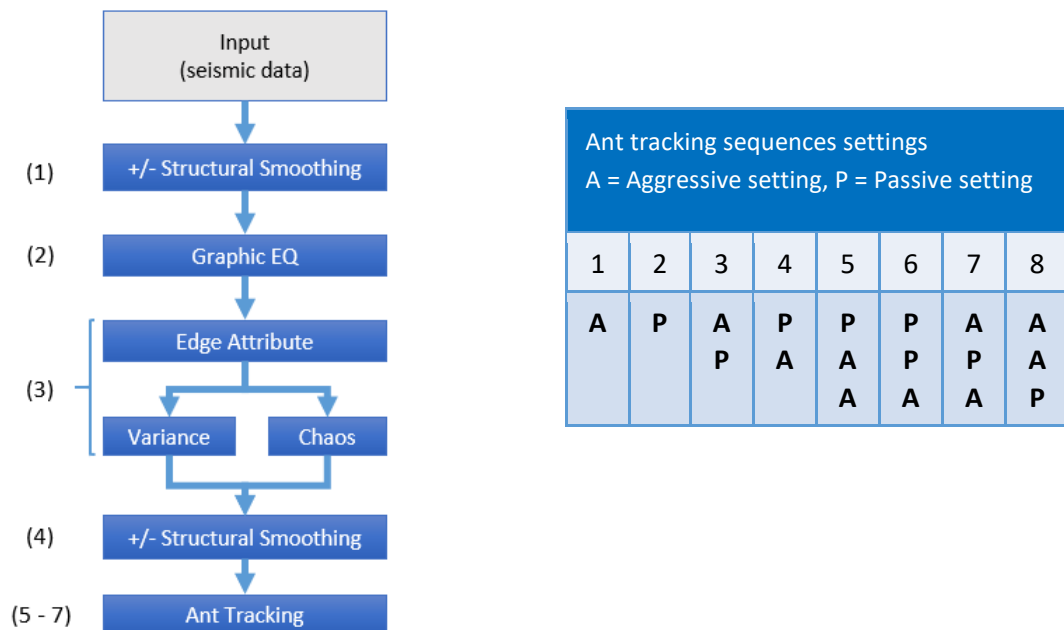


Fig. 13 – Workflow used for ant tracking seismic data. Ant tracking was performed either once, twice or thrice in different orders.

3.8 Quantifying the Minimum Fault Throw Resolution using HIRES MEMA and Ant Tracking

To make a quantitative assessment of the fault throw, different faults or fault sets were selected based on visibility on the surfaces of the DGM v5 and HIRES MEMA, and their visibility in the seismic intersection. The vertical exaggeration, which is function in Petrel to emphasize topographic relief in the surface, is chosen to optimally illustrate the faults on both the DGM v5 surfaces and the HIRES MEMA surfaces with a value most often between 5 and 20. Ideally, a fault is selected that is visible on the DGM v5 surface, the HIRES MEMA surface, and that is also detected by ant tracking. If this is the case, the minimum fault throw at which it is detectable on the DGM v5 surface is measured, as well for the HIRES MEMA surface and the ant tracking. While the same fault is measured, it does not mean the same intersection with the fault is measured (Fig. 14). Most of the faults that have been measured, however, cannot be detected on the DGM v5. For these faults, the minimum fault throw at which they are detectable is measured on a seismic intersection perpendicular to the fault.

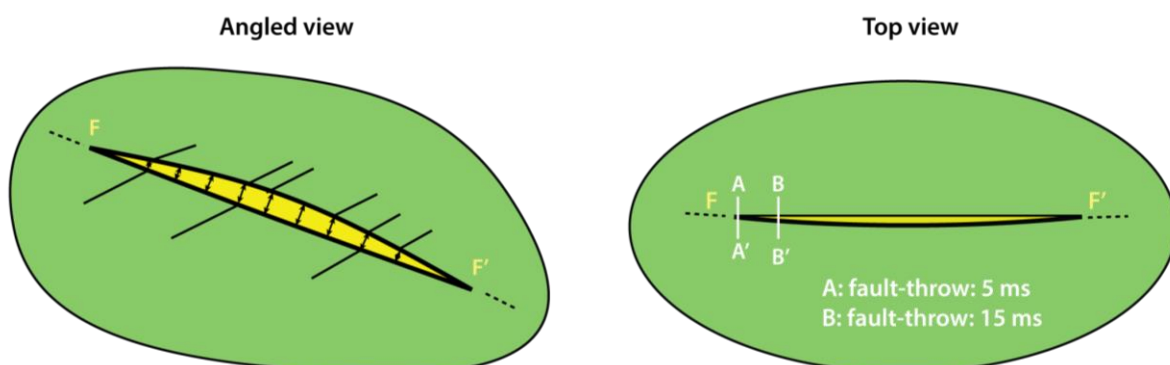


Fig. 14 – Explanation of the fault throw measurement procedure. The same hypothetical fault (F) is displayed from an angled, 3D perspective, to show the difference in fault throw along the plane F-F'. The difference between the HIRES MEMA surface and the DGM v5 horizon lies in the fault throw resolution at which the faults become distinguishable. The same fault will most likely show the minimum fault throw, or ‘edge’ of the fault at cross section B on the DGM v5 surface (15 ms), whereas the same fault can be traced further down to the edge on a HIRES MEMA surface, where the fault throw resolution is three times as high (5 ms). In that case, a seismic cross section is taken here perpendicular to fault F (A-A') after which the fault throw in seismic is measured.

4. Results

4.1 Seismic interpretation

Seismic interpretation is performed for the base NU, NLNM, and CK on four different cubes: Monster, L3NAM, Andel & Waalwijk. These bases are used to determine the differences in fault throw resolution between TNO DGM v5, the HIRES MEMA surface, and the ant tracking results.

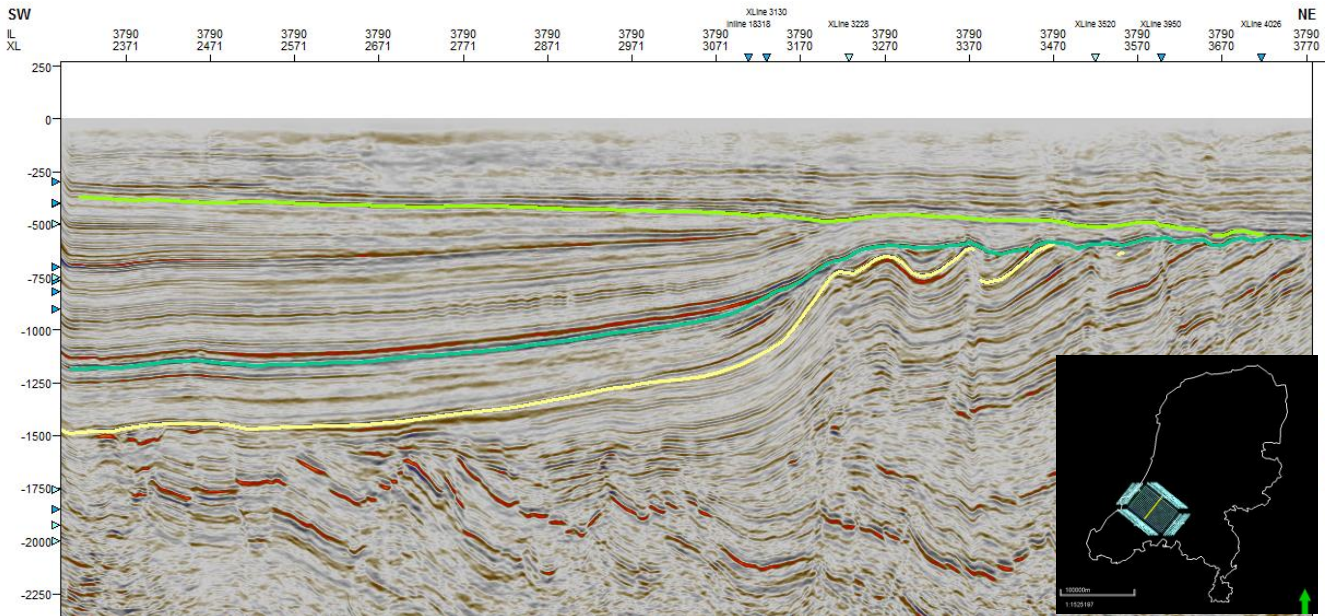


Fig. 15 – Seismic inline in L3NAM running SW – NE through the WNB displaying the interpreted base NU (light green), base NLNM (dark green), and base CK (yellow). The angular unconformities are prominent for both the base NU and the base NLNM. The base CK does not lie unconformable on the Rijnland Group (KN), but does lie unconformable on the Altena Group (AT) in the SW extent of the intersection.

4.1.1 Base Upper North Sea

The base Upper North Sea (B_NU) is found in all of the WNB with a relatively weak amplitude and low angle unconformity, overlying either the Middle or Lower North Sea Group, and increasing in depth towards the north. Combined with the data gaps often encountered in onshore seismic surveys (Fig. 17), this horizon can be difficult to pick, especially when using auto-tracking. The weak amplitude, as well as bad continuity of the loop itself results in a noisy surface (Fig. 16). Due to this signal-to-noise ratio, faults with a small fault throw are less apparent on the resulting surface. These surfaces are often 'smoothed', but often lose fault resolution as result. The unconformity of the base itself is difficult to notice on seismic intersections running NW-SE, and is most easily seen using SW-NE seismic sections (Fig. 15). The base NU becomes shallower towards the SE, reaching up to 321 ms, with a sudden increase in depth in the ESE due to large scale faulting, reaching down to 940 ms.

Faulting in the area is relatively limited, with faulting increasing towards the northeast and southeast. The fault planes are mostly NW-SE oriented, with some of the faults extended through to the base NLNM.

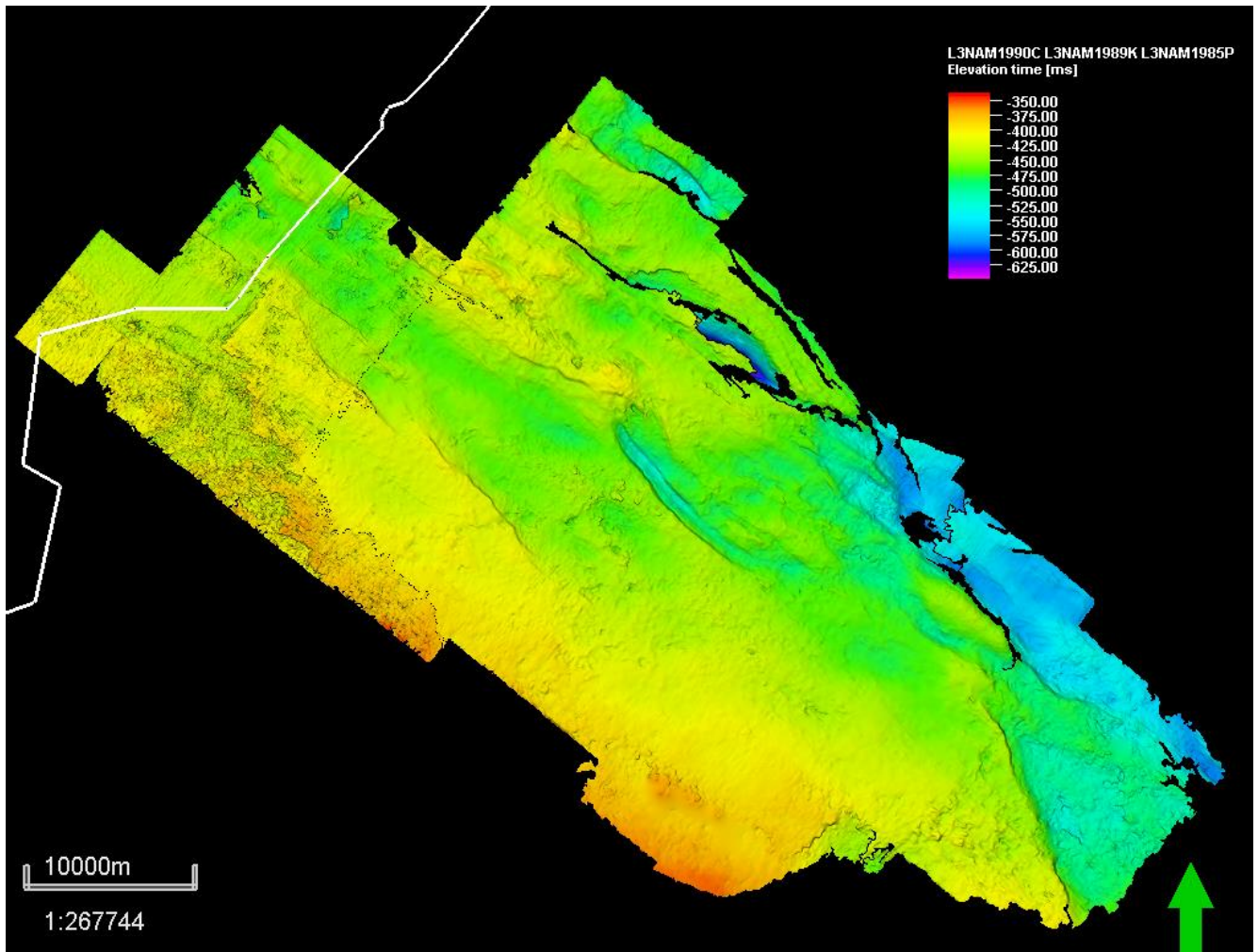


Fig. 16 – HIRES MEMA surface of the base NU for the Monster and L3NAM seismic cubes. Note that this surface has more noise compared to the base NLNM and base CK, most notably in the southwest (see Fig. 17).

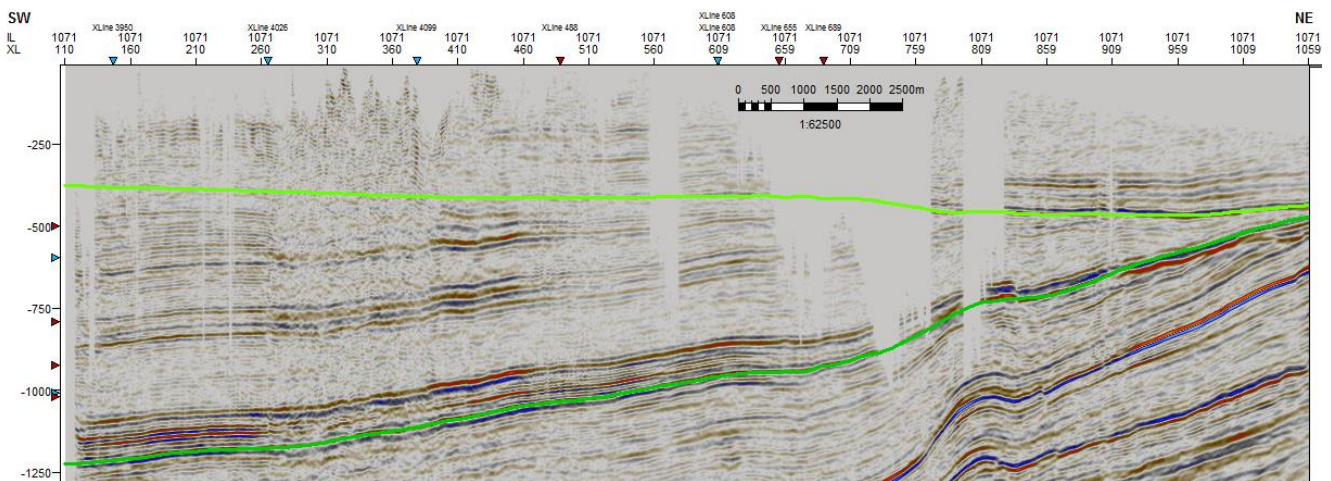


Fig. 17 – Seismic inline of the Monster survey showing the occurrence of large data gaps in the upper section, reaching down to 990 ms in depth and 3 km in width. These data gaps truncate the base NU (light green) most often, and sometimes extend to the base NLNM (dark green), as seen here, making it difficult to interpret this horizon.

4.1.2 Base North Sea Supergroup

The B_NLNM appears as an (angular) unconformity with a strong amplitude in most of the area making it relatively easy to trace. The base was not present everywhere, as it has been eroded in some areas (Fig. 18). In general, the base North Sea

Group is continuous throughout the area and becomes shallower towards the northeast, reaching its maximum depth of 1200 ms in the southwest and 440 ms in the northwest. The only discrepancy in this trend can be found in the Waalwijk survey (southeast), where the B_NLNM appears much deeper in time on the eastern side of the graben structure. In the SW the interpreted loop was deeper than the one used for DGM v5 (Fig. 19). Many of the faults found in the WNB in the B_NLNM can be found in the B_NU as well. Faulting increases in both northeastern and southeastern direction, with the highest density of faults occurring the Andel and Waalwijk seismic cubes (far east). Almost no faulting is observed in the southwestern extent of the B_NLNM in the West Netherlands Basin. Where most faults in the northwestern extent appear to be mostly NW-SE oriented normal faults related to graben-type extension, the orientation of the fault lineations shifts towards N-S in the southeast, with the Waalwijk graben structure as an example (Fig. 20). Furthermore, the high resolution interpretation of the Andel and Waalwijk seismic data reveals a second set of fault lineations running WNW-ESE (Andel) to NW-SE (Waalwijk), which are difficult to impossible to detect on the DGM v5 maps (Fig. 21c & 21d).

Because the seismic signal of the base North Sea Group is strong and continuous, and the signal-to-noise ratio is optimal, faults are easily recognizable on this surface. The base Upper North Sea Group, while in general has less vertical variation, has more noise in the signal, resulting in a chaotic surface that does not allow for small fault throws to be easily detected. For these reasons, the base NLNM surface is deemed most useful for determining the minimum fault throw that can be displayed on a 25x25 m resolution surface.

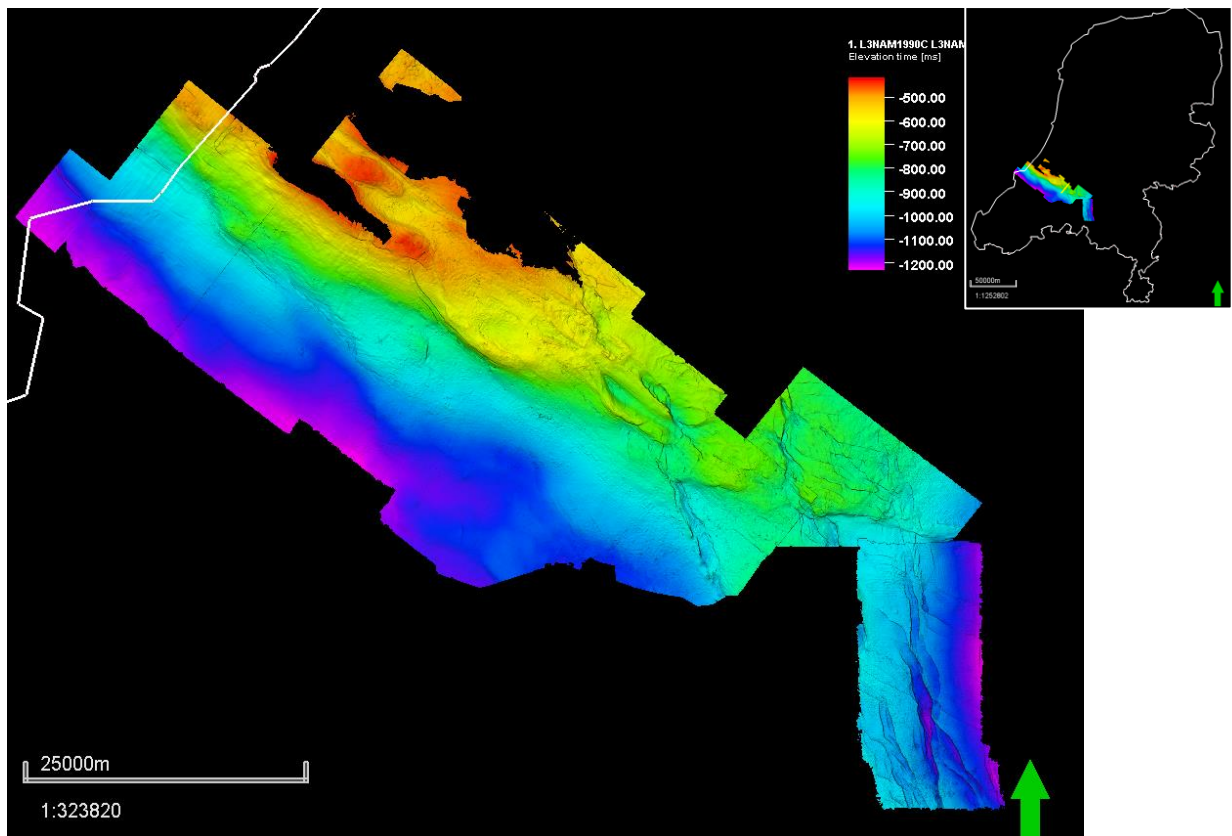


Fig. 18 – High resolution (25 x 25 m) interpretation of the Base North Sea Group (B_NLNM) in the West Netherlands Basin. The edges of the interpretation are either the limits of the seismic data or where the base is not interpreted.

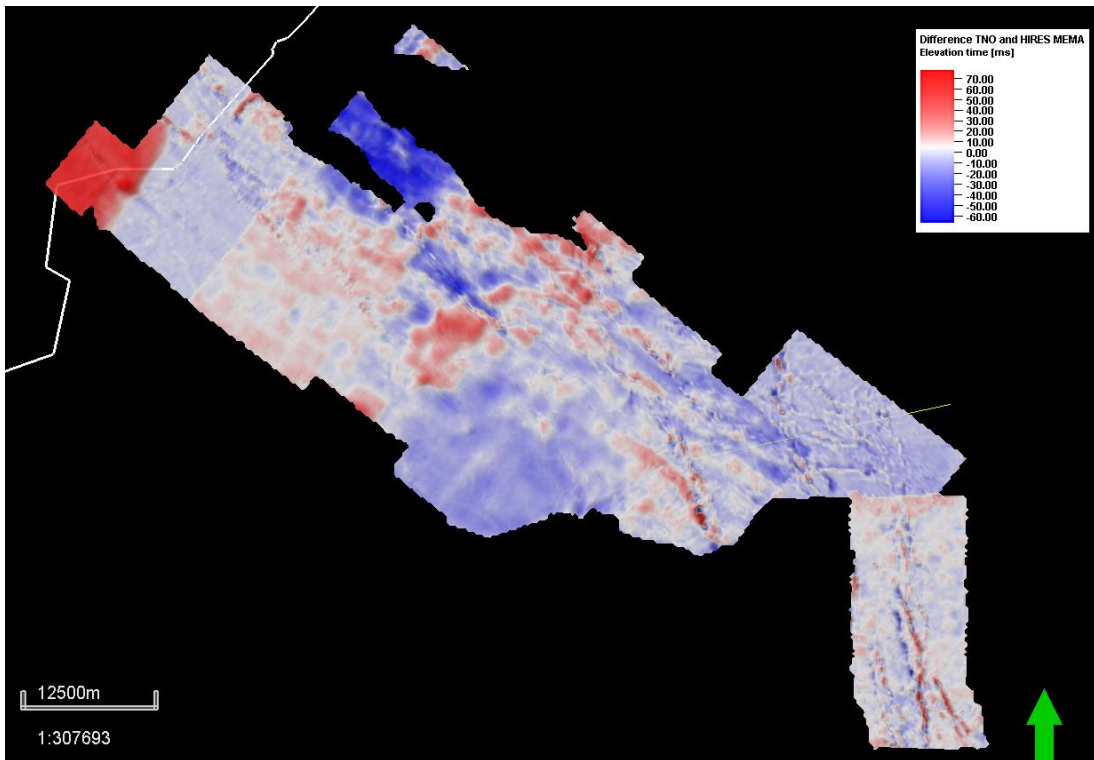


Fig. 19 – Time difference map between the DMG v5 and the HIRES MEMA interpretation for the base NLNM. Note that some areas are generally higher due to picking a different loop in seismic (Monster, NW), and that the fault lineaments are easily seen on the time difference map, as these are the areas of largest topographic relief.

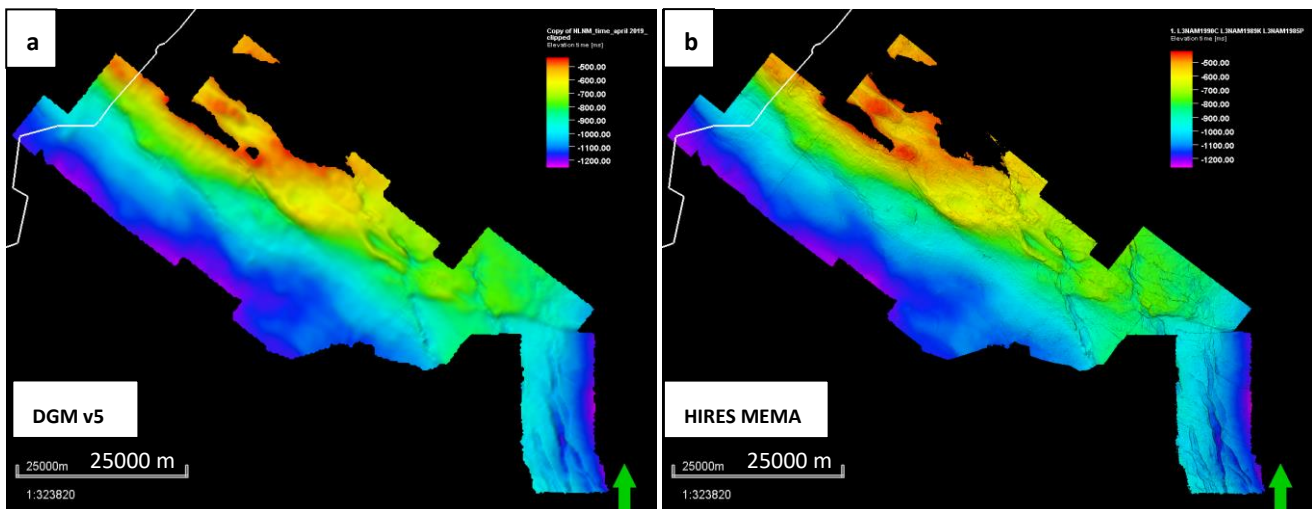
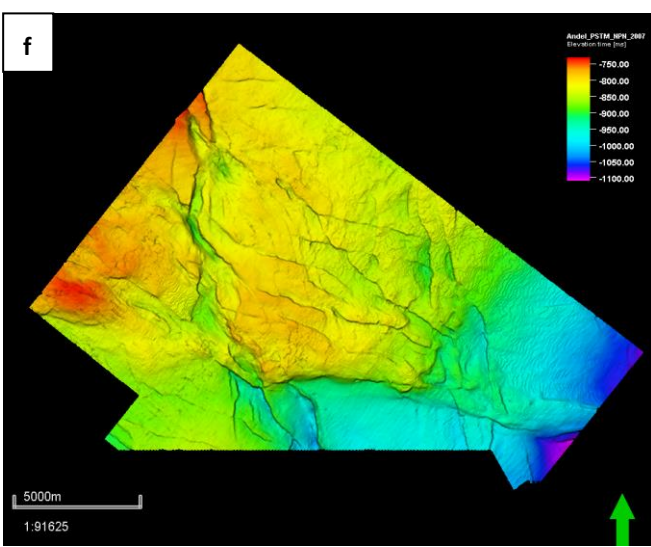
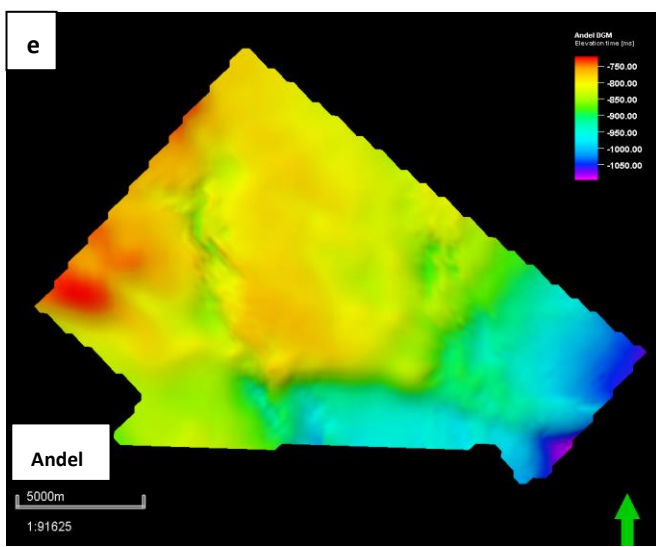
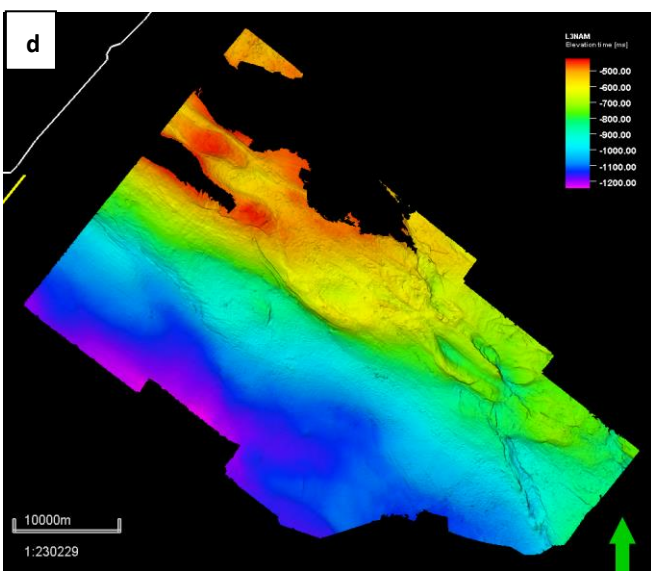
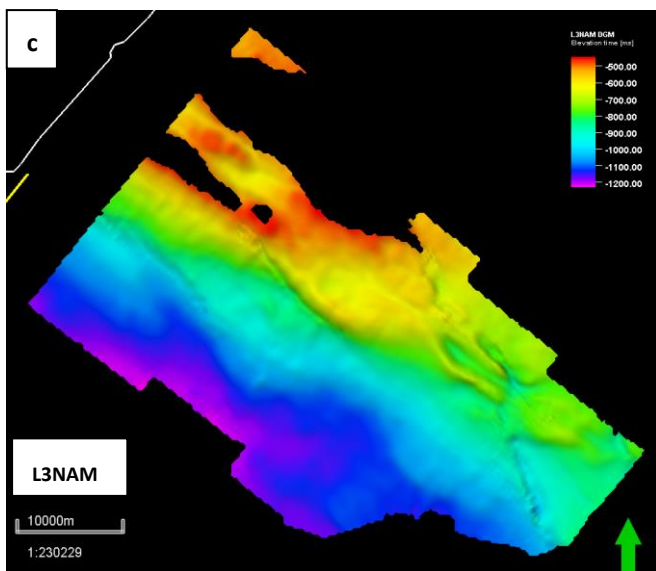
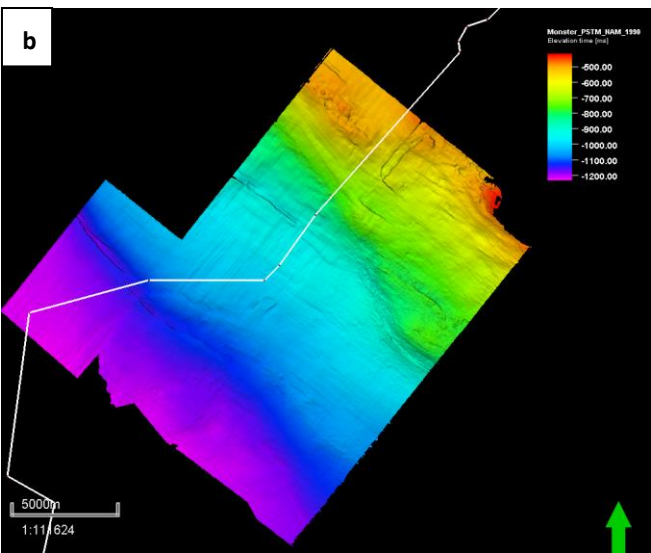
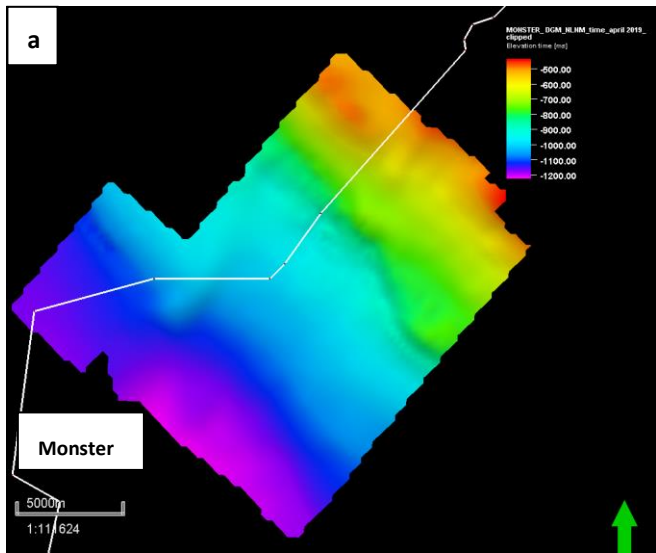


Fig. 20 – Extent and comparison of the base North Sea Group (B_NU) of DGM v5 (a) and HIRES MEMA (b). Note the higher resolution of faulting, specifically in the southeast (Waalwijk area).

TNO DGM v5

HIRES MEMA



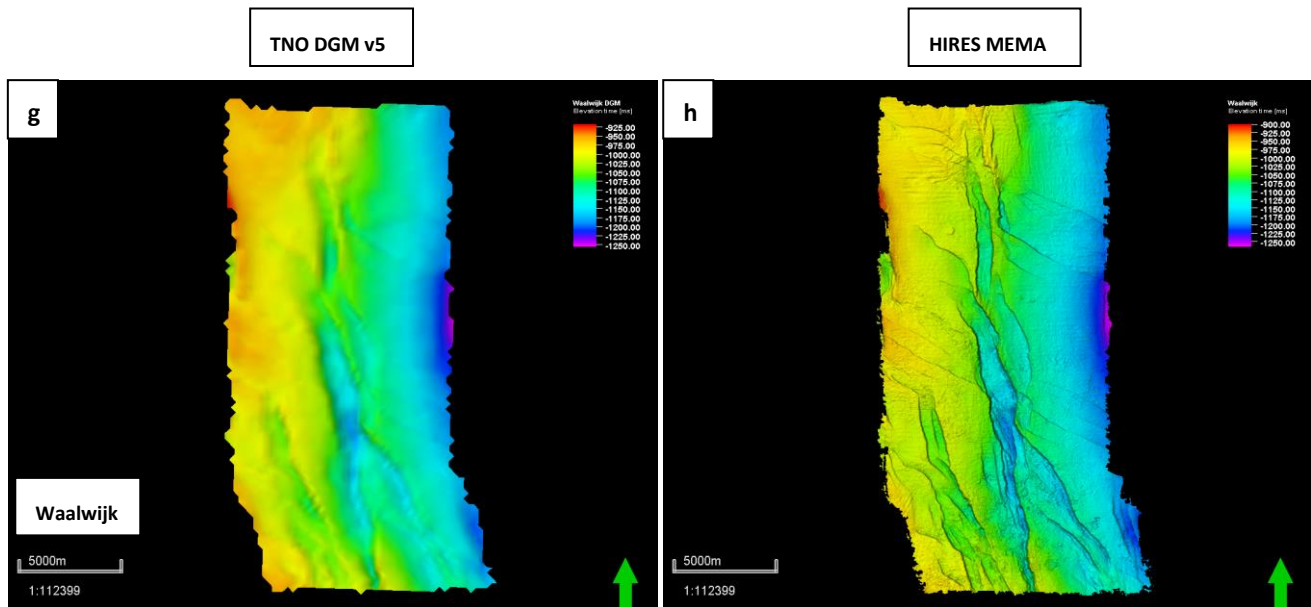


Fig. 21 – Comparison of the DMG v5 and the HIRES MEMA surface of the base North Sea Group for the same seismic surveys. The scale bar is adjusted for each comparison.

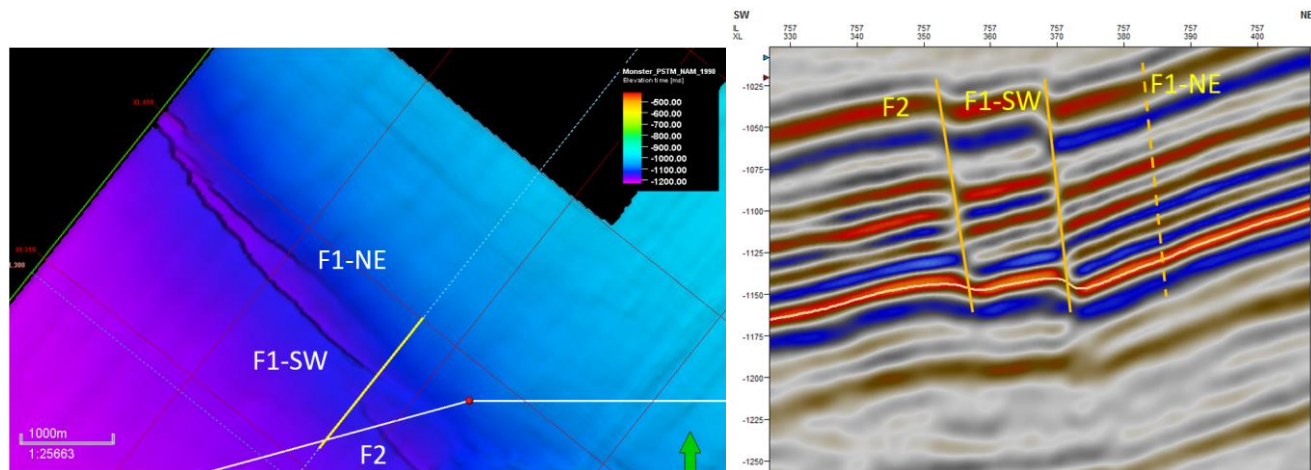


Fig. 22 - Minimum fault throw for the SE extent of the Monster 1 fault. Interestingly, we see the three faults on the map view, and only two clear faults in the seismic section. At this point, the two southern faults display a fault throw of 6 ms, 8 ms, and ~ 1 ms.

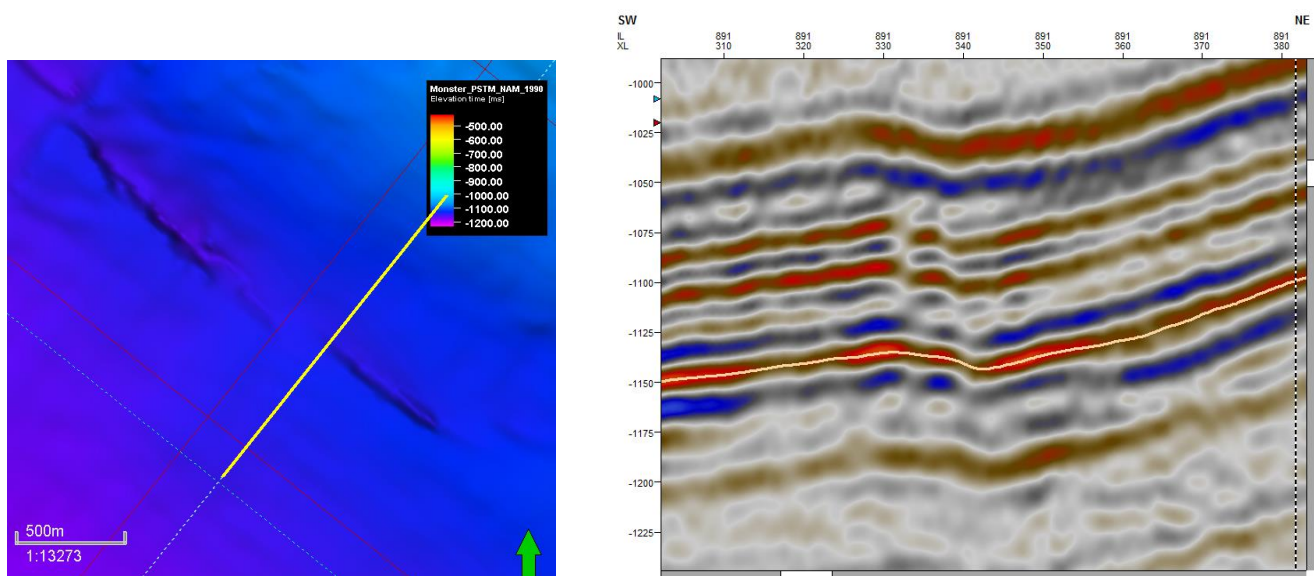


Fig. 23 – Map view indicates initiation of a single fault, with seismic indicating two smaller faults, of which only the northeastern is seen. Fault throw measured at this intersection: 4 ms.

4.1.3 Base Chalk Group

The base Chalk Group (B_CK) is for the most part seen as a strong positive reflector with a good signal-to-noise ratio, which either lies mostly conformable on the lower Cretaceous/Rijnland Group or unconformable on the Altena Group, as well as lower strata (Fig. 15). It is not present everywhere, and is absent in the central part of the Netherlands, which can be seen on the regional-scale maps (Fig. 11). The base Chalk has the highest relief in the area (~ 1200 ms), with its highest structures reaching up to 450 ms in the NW, and the lowest parts in the SE reaching down to 1600 ms. Of the three interpreted surfaces, the base CK displays the least amount of faulting, with most of the faulting occurring in the northeastern half of the area (Fig. 24). Some of the faults that are visible in the base North Sea Group extend into the base CK as well. The base Chalk does show more high angle features that can be confused for fault structures without the help of seismic intersection perpendicular to the structure.

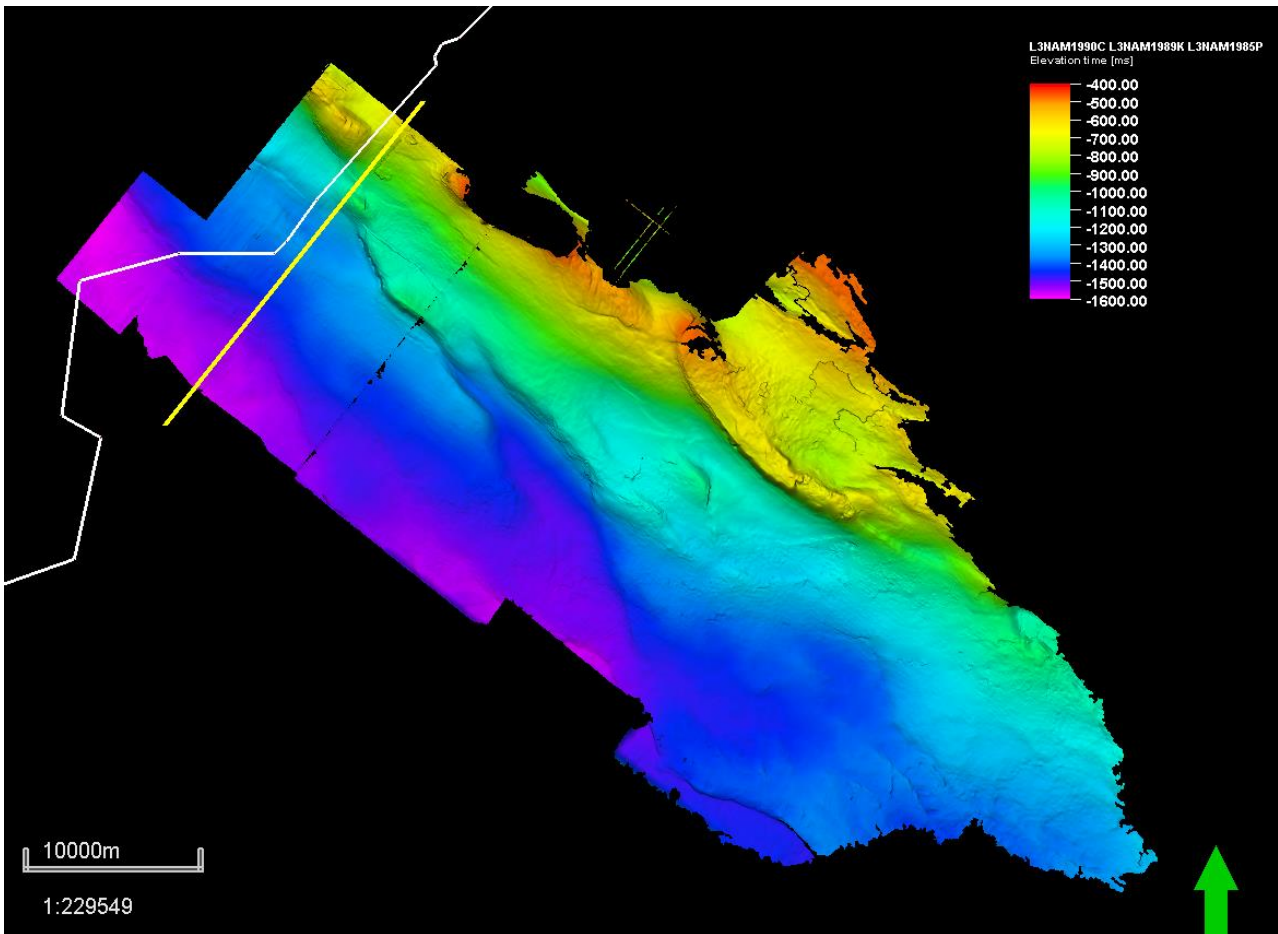


Fig. 24 – Interpreted surface of the base Chalk Group of the Monster and L3NAM surveys. Note the reduced occurrence of high-angle faulting compared to the overlying base North Sea Group.

4.2 Ant Tracking Results

After multiple runs with different set ups, the ant tracking results that most closely followed the fault lineations in the surface were found by computing a Chaos edge cube and then running it at either a custom or passive setting (C or P) and then an aggressive run (A). The custom setting was the CA (custom → aggressive setting) appears to be PA (passive → aggressive setting). In general, seismic data (Fig. Wa) resulted in a Chaos discontinuity cube (Fig. Wb), after which the ant tracing cube was generated (Fig. Wc). Because of the data gaps that occur in the seismic, the stereonet filter was used during ant tracking to filter out results with a ~90 degree dip angle, and parallel to the in- and crosslines.

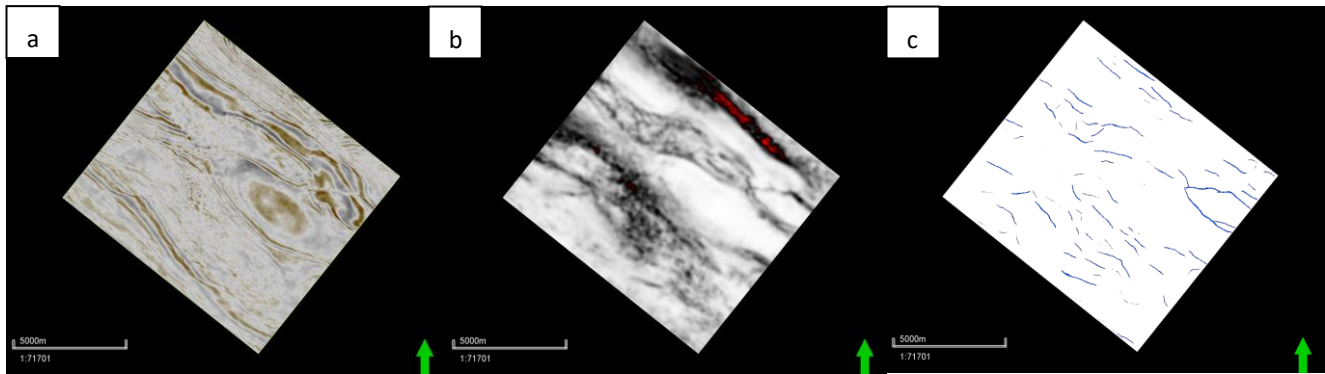


Fig. 25 – Time slice at 1200 ms for a cropped volume of L3NAM. (a) shows the original seismic data, (b) shows the same time slice of the variance cube, and (c) shows the ant tracking resulting from the variance cube.

While the ant tracking results often show more fault lineations than observed on the interpreted surface, they show a strong similarity to the faults visible on the surface, even for heavily faulted areas like the Andel and Waalwijk cubes (Fig. 26). The ant tracking results are used for two purposes in this study: to determine the minimum fault throw at which a fault results in an ant track lineation, and; to extract the ant track results as fault planes, and use the stereonet plot to show the difference in the number of high angle faults between a chaos and a variance cube.

The accuracy of ant tracking correlates best to the quality of the seismic, showing strong similarity in seismic cubes where the seismic data is continuous with very few artifacts and/or noise. If this is not the case, the ant tracking results that represent fault lineations become difficult to distinguish from the ant tracks resulting from seismic noise.

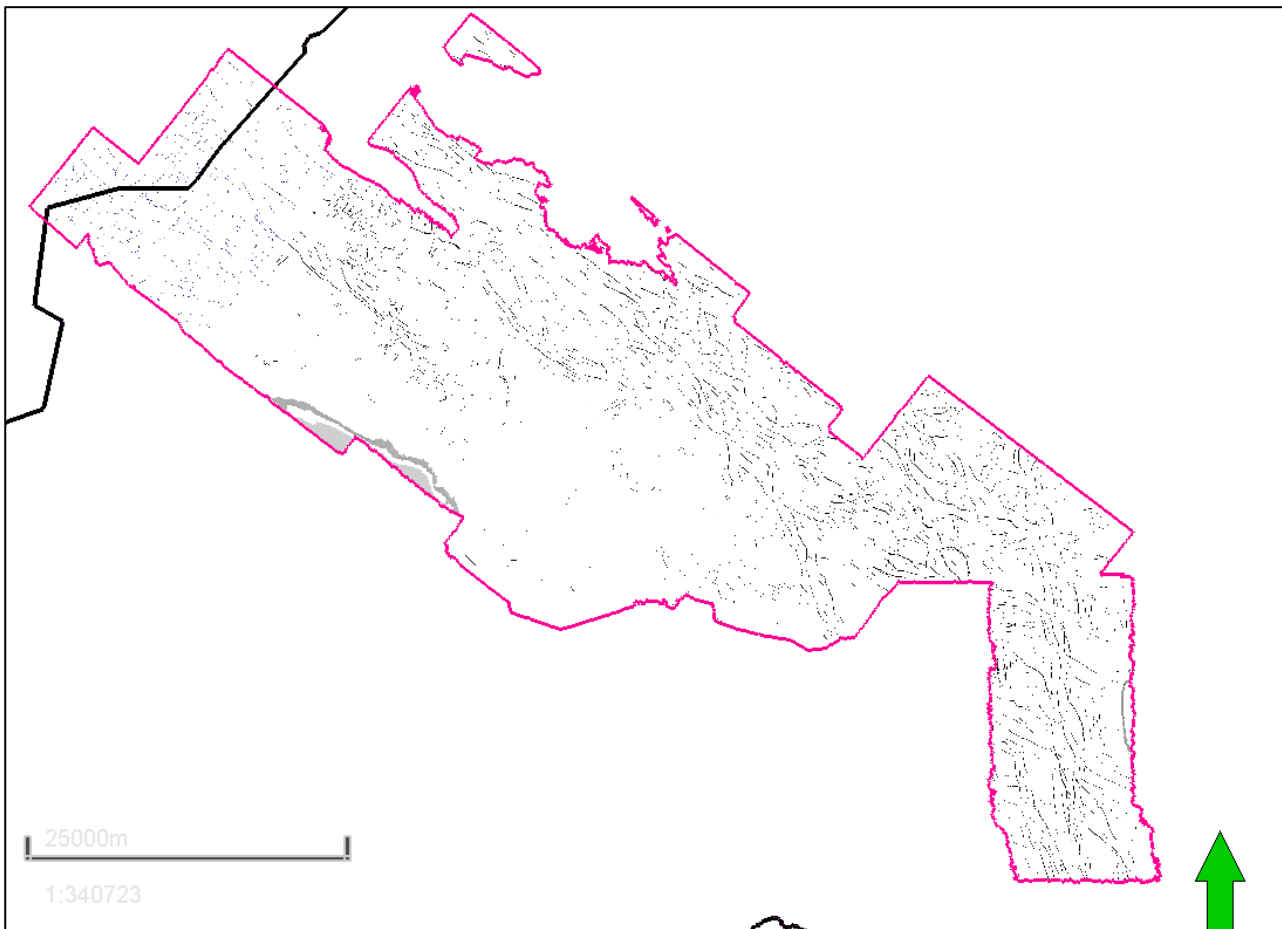
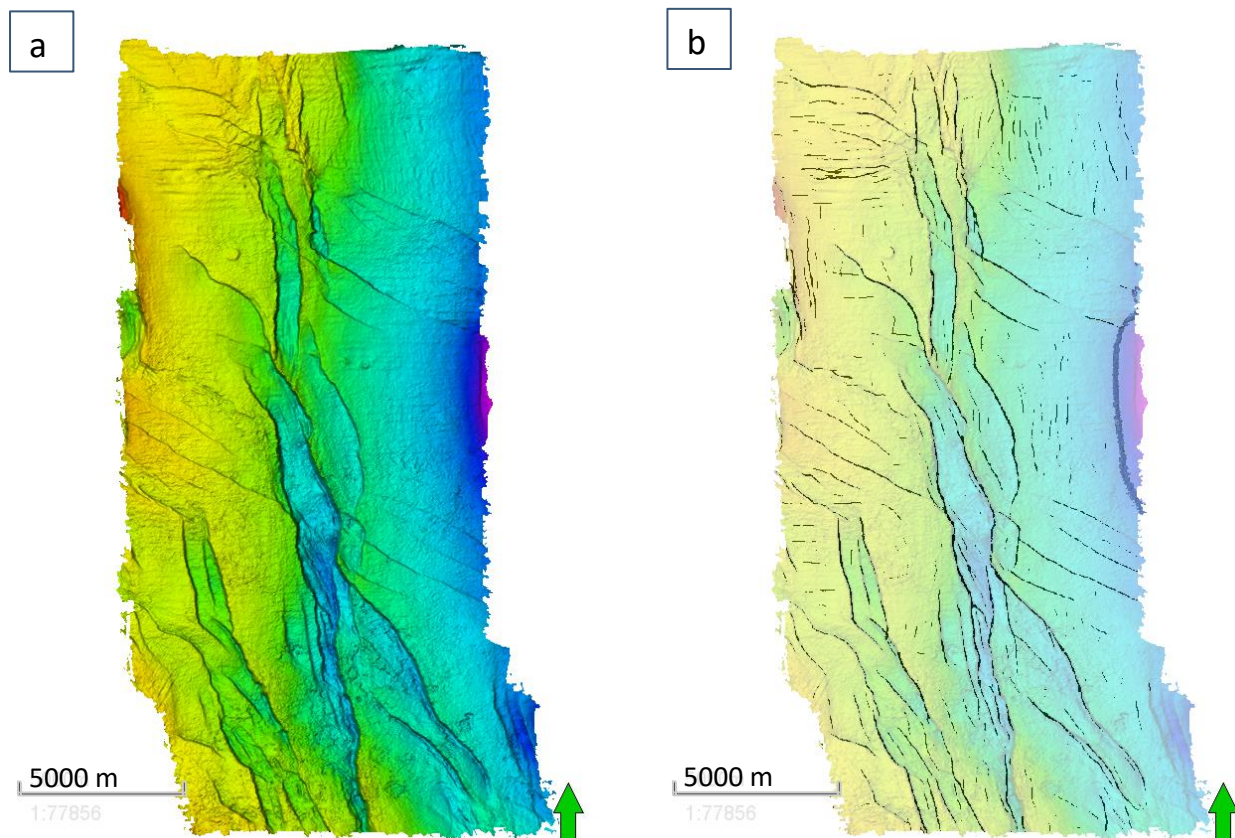


Fig. 26 – Ant tracking results as a surface attribute for the base NLNM over four seismic surveys indicate a fairly accurate representation of the faults in the base North Sea Group. The area in which ant tracking is applied is outlined in pink. It is uncertain what causes the grey area in the southwest of the L3NAM area.

As observed on the HIRES MEMA surface, we see an increase in the number of ant tracks towards the southeast, with the exception of the Monster seismic survey (Fig. 26). As mentioned before, this seismic survey contains many data gaps, resulting in poor processing and very discontinuous data, even at shallow depths. Therefore, the ant track runs return much more noise compared to the adjacent L3NAM cube. As we observed on the HIRES MEMA surface of the base NLNM, we see a decrease in faulting in the southern half of the L3NAM cube, which is reflected in the ant tracking results. Finally, we see, similar to the addition of the HIRES MEMA surface in comparison to the DGM v5 surface, two sets of faulting occur in the Waalwijk area (southeast). Where these faults were difficult to pick up on with the DGM v5, they are shown on both the HIRES MEMA surface (Fig. 27a) and the extracted ant tracking results (Fig. 27b).

The ant tracks can be extracted using the ‘automated fault extraction’ plug-in in Petrel, which is useful to gain an insight into the dipping direction of the fault structures, which cannot be determined based on the lineations alone. The initial results of this fault extraction contain many artifacts that need to be eliminated, such as faults with a 90 degree dip and perpendicular to the cross- and inlines, resulting from seismic acquisition errors. These are eliminated using the ‘dip in seismic’ filtering in settings. Fractures or small, local variations also result in small fault patches, not representative of the fault structures. These are eliminated using the ‘surface area’ filter, with the most representative fault patches remaining (Fig. 27c). When these artifacts are eliminated, the stereonet plot can be used to indicate the azimuth and dip angle of the faults relative to the inline and crossline. Fig. 27d is an example of a stereonet plot for the Waalwijk area that has been rotated 90 degrees to show the fault azimuth relative to true north. It shows three different fault groups: ENE dipping faults (50-110 degrees), the opposing WSW dipping faults (230-280), and a third, SSW dipping fault orientation (190-220). This third fault group represents the faults that cannot be seen on the DGM surface and can be seen on the HIRES MEMA surface.



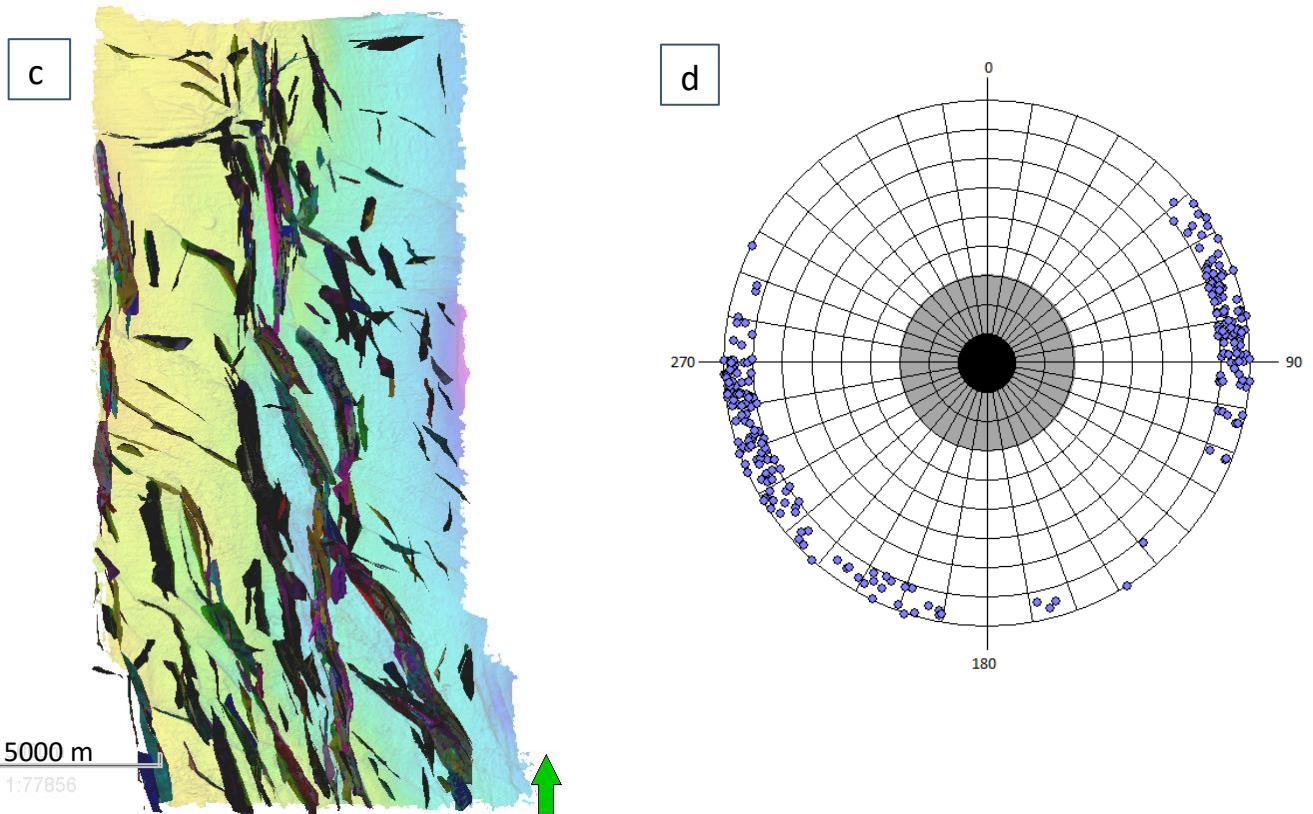


Fig. 27 – The relation between (a) the HIRES MEMA surface for the base NLNM in the Waalwijk survey; (b) ant tracks (in black) resulting from a Chaos cube and two iterations of ant tracking (custom → aggressive) overlaying the surface from (a); (c) the extracted fault surfaces, running from 800-1200 ms, and with the small surfaces removed; (d) the stereonet plot of the filtered fault planes, showing roughly three dipping orientations: WSW, ENE, and SSW.

What makes the fault extraction tool useful, is that the dip azimuth can now be determined without fault interpretation or any other manual work. The dip azimuth appears to be in agreement with the dip in seismic.

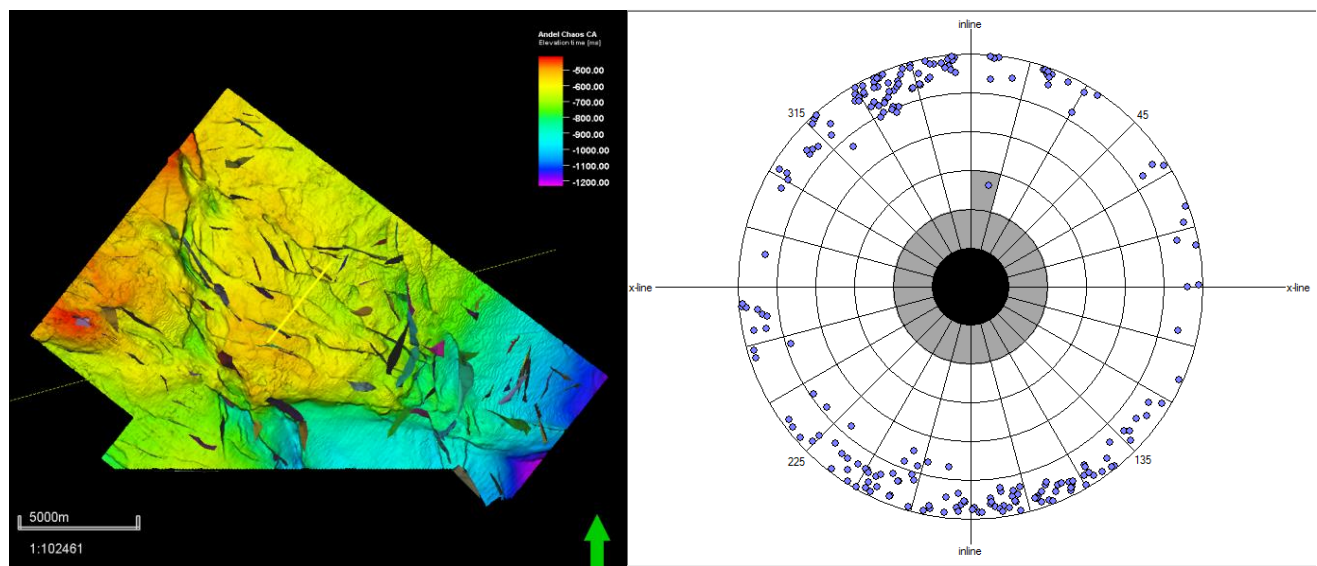


Fig. 28 – Surface of the base NLNM in the Andel seismic cube, with the filtered fault patches. The yellow line represents The corresponding stereonet plot Chaos PA fault extraction, filtered by vertical extent, surface area, dip in seismic, azimuth in seismic.

4.3 Minimum Fault Throw Resolution

To quantify the minimum fault throw resolution, different faults are selected and named for each survey and each base surface (Fig. 29). They are picked based on: visibility on the DGM v5 surface, the visibility on the HIRES MEMA surface, and the minimum fault throw measurable for the respective faults. The results are summarized in Table 3. Of each fault lineations, three images are produced that show the DGM v5 surface, HIRES MEMA surface, and HIRES MEMA surface with the ant tracking attribute, together with a seismic line perpendicular to the faults. Only two of these comparison are shown in this chapter, the other images can be found in Appendix A.

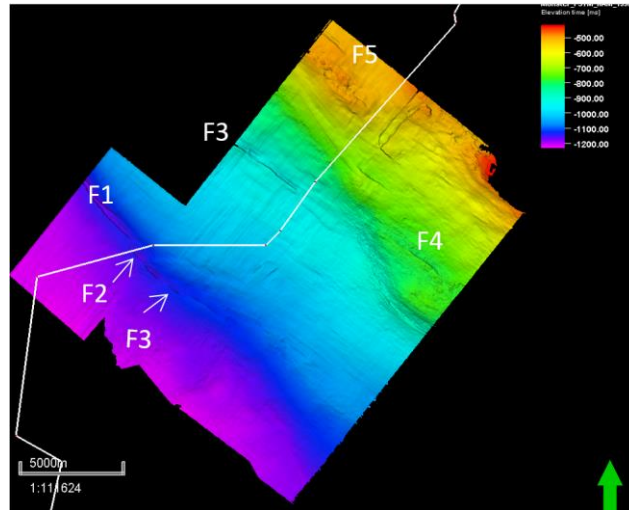


Fig. 29 – Example of the faults that are selected and named on the HIRES MEMA surface in the Monster survey for the base NLNM.

Table 3 – Minimum Fault Throw Measurements							
Base	Seismic Survey	Name	HIRES MEMA > FT (ms)	Visible on TNO DGM v5?	DGM v5 > FT (ms)	Ant tracking > FT (ms)	Factor difference
NLNM	Monster	F1-NE	1	Yes	12	5	12
NLNM	Monster	F1-SW	8	Yes	12	3.5	1.5
NLNM	Monster	F2	6	No	-	5.5	-
NLNM	Monster	F3	4	No	-	5.5	
NLNM	Monster	F4	10	No	-	-	
NLNM	Monster	F5	9	No	-	4	
NLNM	L3NAM	F6	4	Yes	15	4	4
NLNM	L3NAM	F7	5	Yes	13	5	2.5
NLNM	L3NAM	F8	3	No	-	4	
NLNM	L3NAM	F9-A	10	No	-	5	
NLNM	L3NAM	F9-B	-	No	-	6	Only ant track
NLNM	L3NAM	F10-A	8	No	-	8	1
NLNM	L3NAM	F10-B	5	No	-	5	1
NLNM	L3NAM	F11-A	5	No	-	11	2
NLNM	L3NAM	F11-B	6.5	Yes	25	12	4
NLNM	Andel	F12-A	10	No	-	10	
NLNM	Andel	F12-B	14	Yes	14	14	1
NLNM	Andel	F13	3	No	-	7*	Fault ≤ 9ms
NLNM	Andel	F14-A	6.5	No	-	11	
NLNM	Andel	F14-B	6	No	-	6	
NLNM	Andel	F15-A	9	Yes	23	10	2.5

NLNM	Andel	F15-B	4	No	-	4	
NLNM	Andel	F15-C	7	No	-	20	3
NLNM	Andel	F15-D	24*	No	-	-	
NLNM	Andel	F15-E	9	No	-	-	
NLNM	Andel	F15-F	10	No	-	10	
NLNM	Andel	F16 - A	7	Yes	17	13	2.5
NLNM	Andel	F16 - B	9.5	No	-	-	
NLNM	Andel	F16 - C	7.4	No	-	-	
NLNM	Andel	F16 - D	7	No	-	12.5	1.9
NLNM	Andel	F17-A	3	No	-	5.5	1.9
NLNM	Andel	F18-B	5	No	-	-	
NLNM	Waalwijk	F19-A	4.6	Yes	10	3	
NLNM	Waalwijk	F19-B	4	Yes	13	5	
NLNM	Waalwijk	F20	2.8-8.5	No	-	2.8	
NLNM	Waalwijk	F21-A	38	Yes	38	38	Not used
NLNM	Waalwijk	F21-B	6	No	-	3	
NLNM	Waalwijk	F21-C	6	Yes	12	6	
NLNM	Waalwijk	F21-D	7	No	-	1.5	
NLNM	Waalwijk	F21-E	3.5	No	-	4	
NLNM	Waalwijk	F21-F	4	No	-	7.5	
NLNM	Waalwijk	F22-A	4	No	-	5	
NLNM	Waalwijk	F22-B	2.5	No	-	3	
NLNM	Waalwijk	F22-C	3	No	-	3	
NLNM	Waalwijk	F23	4	Yes	10	4	
CK	L3NAM	F24	7	Yes	17	7	
AVERAGE			6.5		14.9	6.7	2.3
STDEV			3.8		4.5	3.9	
MIN			1		10	1.5	

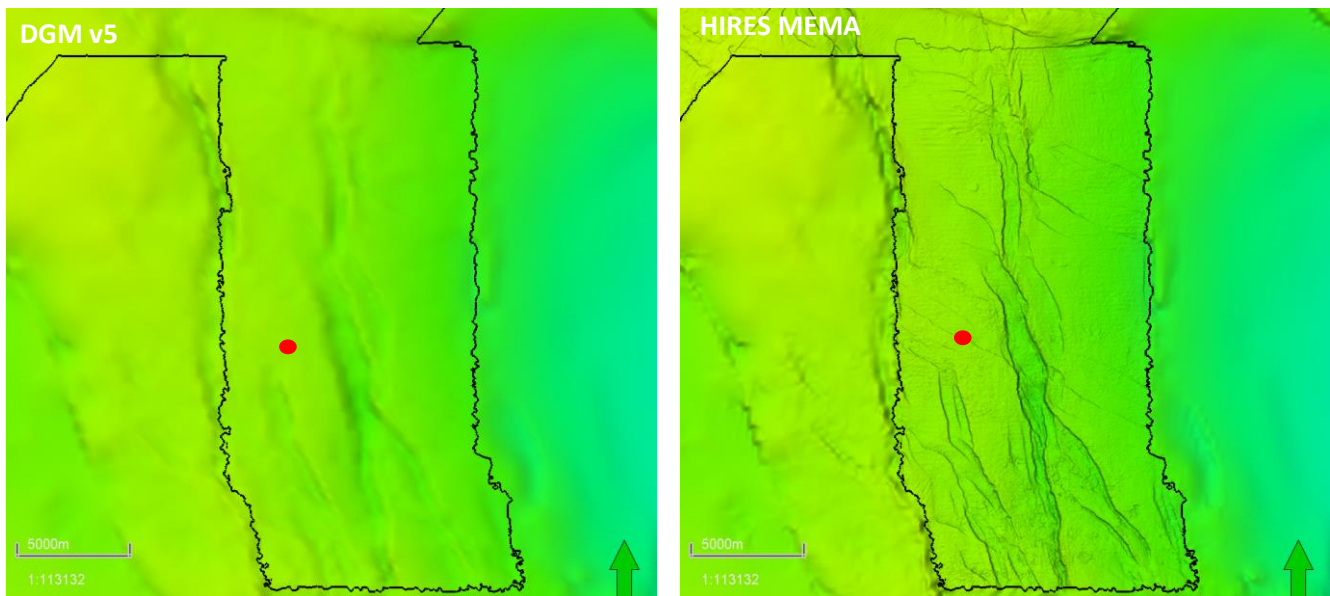


Fig. 30 – Results for the Waalwijk (and Andel) survey for the base North Sea Group, where the black border indicates the extent of the high resolution interpretation. The red dot indicates a hypothetical well placement, which on the DGM v5 surface would appear free of faults, but on the HIRES MEMA is right on a fault.

resolution will most likely affect them relatively more. The assumption here is that an increase with large scale faults with a fault throw > 10 ms, as seen in Fig. 32 relates to an increase in small faults that are <10 ms, as observed with the upper three base horizons in this study (NU, NLNM, and CK).

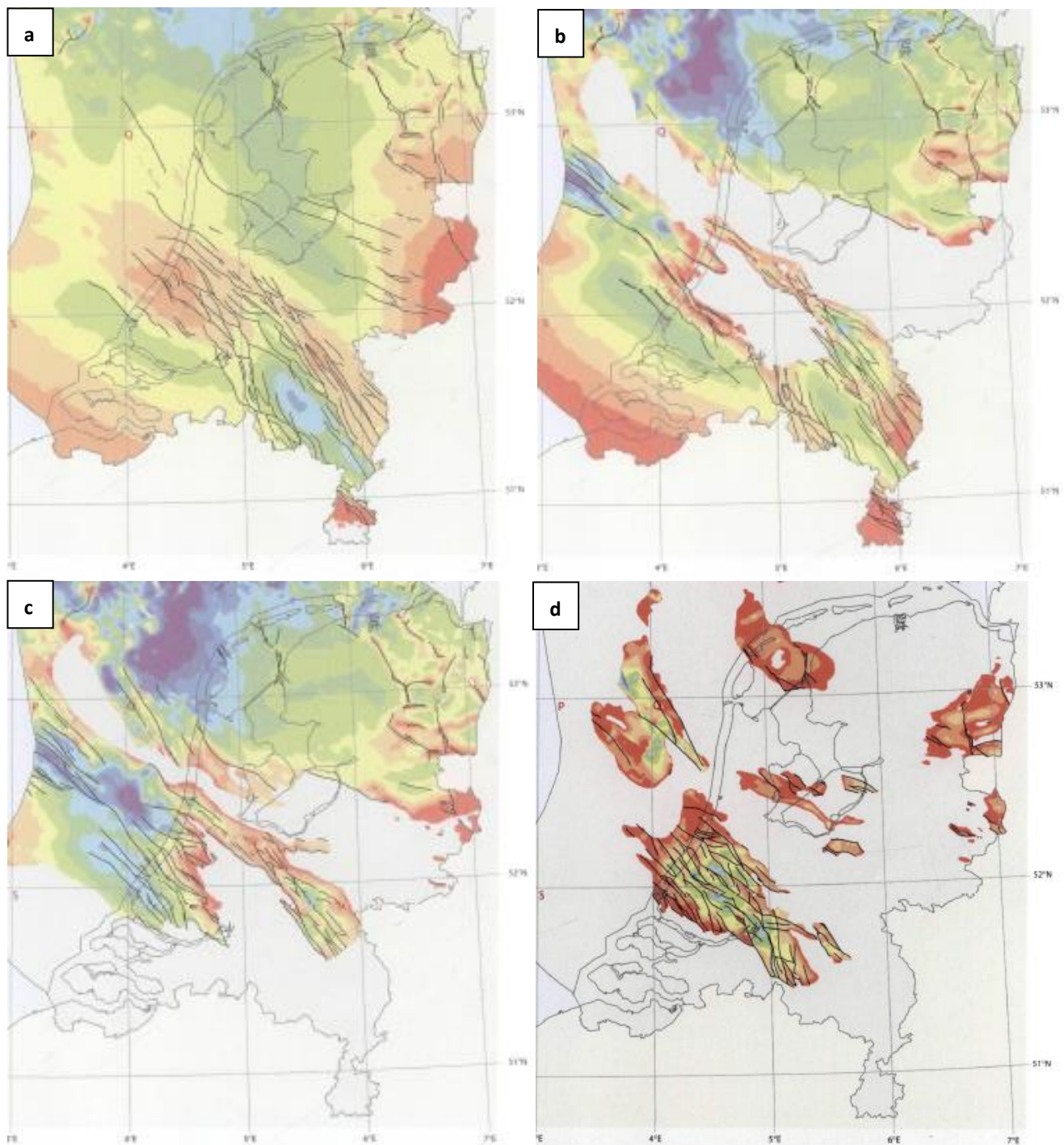


Fig. 32 - Depth and fault maps by Duin et al. (2006) of (a) the base Lower and Middle North Sea Group; (b) the base Chalk Group; (c) the Rijland Group and (d) the base Schieland Group. Note that these structural maps are based on regional mapping by TNO, and may not capture all the structural details. Faulting in the West Netherlands Basin increases with time horizon, most importantly in the base Schieland (d), where the density of faulting is the highest.

5.2 Seismic Interference

Seismic interference and irregularities in the signal have consequences for both the automated fault detection with ant tracking and the observation of fault lineaments on a surface. The continuity of a signal is determined by many factors: the seismic data acquisition, the geological nature of the reflector, and the depth. With onshore seismic surveys, the data acquisition is constrained by the presence of obstacles that are not present in offshore seismic surveys. For offshore seismic surveys, the data is gathered with a marine vessel that is able to completely cover an area, whereas onshore, the presence of e.g. cities, housing, can limit the area where seismic surveys can be performed (Hardage, 1997). This often results in vertical data gaps (see Fig. L, page 17), and a lower quality of the seismic after processing in the shallower parts of the seismic.

In general, the same holds true for larger depths, where the vertical resolution decreases with depth according to $\lambda = v / f$, with v = velocity in m/s, f = dominant frequency in Hz, and λ = dominant wavelength in m. Due to compaction trends with depth, the velocity generally increases with depth, and therefore the dominant wavelength becomes larger (Bouchingour, 2019). Furthermore, processing of data becomes more difficult at large depths (> 2 s) due to reflections from multiple directions (Ebrom *et al.*, 1995). When picking horizons at these depths, the surfaces often reflect this as irregular surfaces. When for instance the high resolution surfaces of the B_NU and the B_NLNM are compared side by side, the differences become quite apparent (Fig. 33). Because of the irregular surfaces, fault lineaments become more difficult to detect, despite having a higher resolution. Smoothing can be applied to decrease the irregularities of a surface, but will come at the expense of detail. For these shallower surfaces that are picked with onshore seismic, the benefit of a high resolution interpretation is therefore relatively less.

As mentioned before, the geology (structure and lithology) also influences the signal from the reflector. The B_CK is found as the boundary between the Chalk Group carbonates and the Rijnland shales, and thereby shows up on seismic data as a strong decrease in velocity with a positive reflection coefficient. This reflector generally has a good SNR with a strong amplitude and picking this horizon leads to a relatively smooth horizon (Fig. 24). The same holds true for the B_NLNM, where, apart from an angular unconformity of the base, the lithology also changes significantly from carbonate to siliciclastic. The boundary that represents the B_NU is mostly structural: an angular unconformity, and not lithological, and therefore has a rather weak and irregular amplitude. For ant tracking this results in a lot more discontinuities, as described in paragraph 5.5. Although deeper horizons, e.g. the Rijnland or Schieland Group, have not been interpreted, their seismic response appears to be relatively strong and continuous. This means that any small lineations/fault throws will be detected more easily compared to the base Upper North Sea Group, which has a lower SNR and is rather irregular in response.

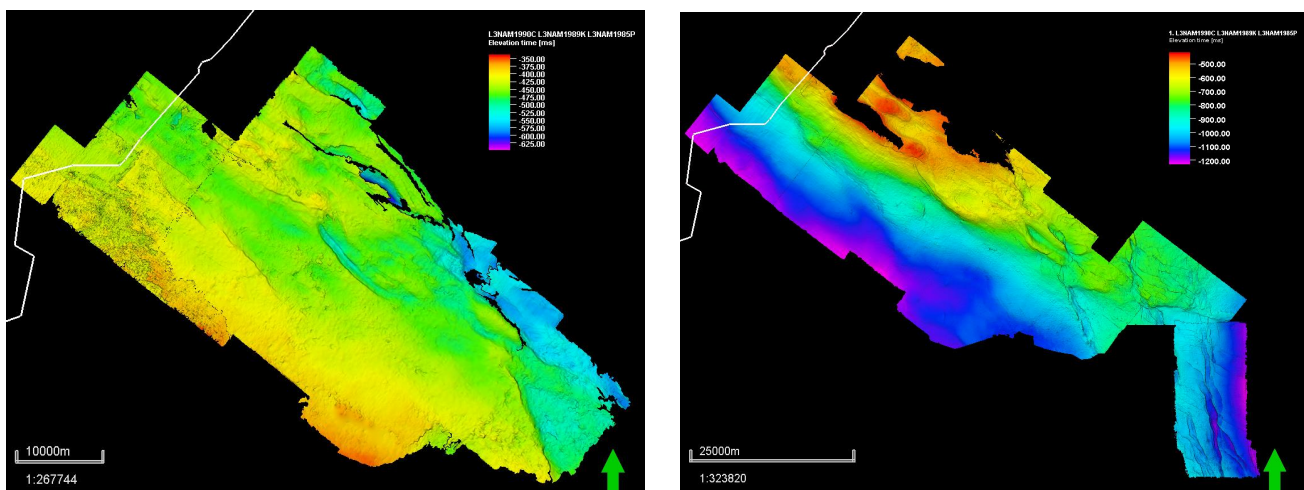


Fig. 33 – Comparison of the B_NU and the B_NLNM surfaces. The difference in continuity of the surfaces is apparent, with a smoother result for the B_NLNM. Note especially in the southwest in the B_NU, where large data gaps exist due to limitations in the seismic survey.

5.3 Angle of the Horizon

When discussing the resolution of a surface in this study, it should be emphasized that it concerns the horizontal resolution only. While the horizontal resolution can be e.g. 25x25 m, the vertical resolution is determined by the angle of the horizon. If the angle of the horizon increases towards vertical, the distance between the seed points increases according to the Pythagorean theorem. For example, when a horizon locally has an angle of 70 degrees and a resolution of 25m, the sampled surface length is 73 m, whereas with a resolution of 250 m, this would be 730 meters. Even if the horizon has an angle of 80 degrees with a horizontal resolution of 25m, the sampling length of the surface is lower (143 m) compared to sampling a horizontal surface at a resolution of 250m. In summary, the relative resolution of the surface decreases with an increasing angle of the surface.

Faults generally occur at 60-90 degrees in the subsurface, and with an increasing surface angle, the angle between the surface and the fault therefore often becomes smaller, making the fault more difficult to detect. With the effect of an increasing sampling distance with an increasing horizon angle it becomes clear that the benefits of a high resolution surface are highest when trying to detect faults on a locally high angle horizon (Fig. 34-2). The same 10 ms fault throw at which a fault could be detected on the DGM surface in the flat areas of the horizon, will now need to be much higher for the steep areas. While this may not be as important for the base Upper North Sea Group, or the base Middle and Lower North Sea Group, as these are relatively flat throughout the Dutch subsurface, the importance increases with surfaces that generally have a high relief, e.g. the base Rijnland Group and base Schieland Group.

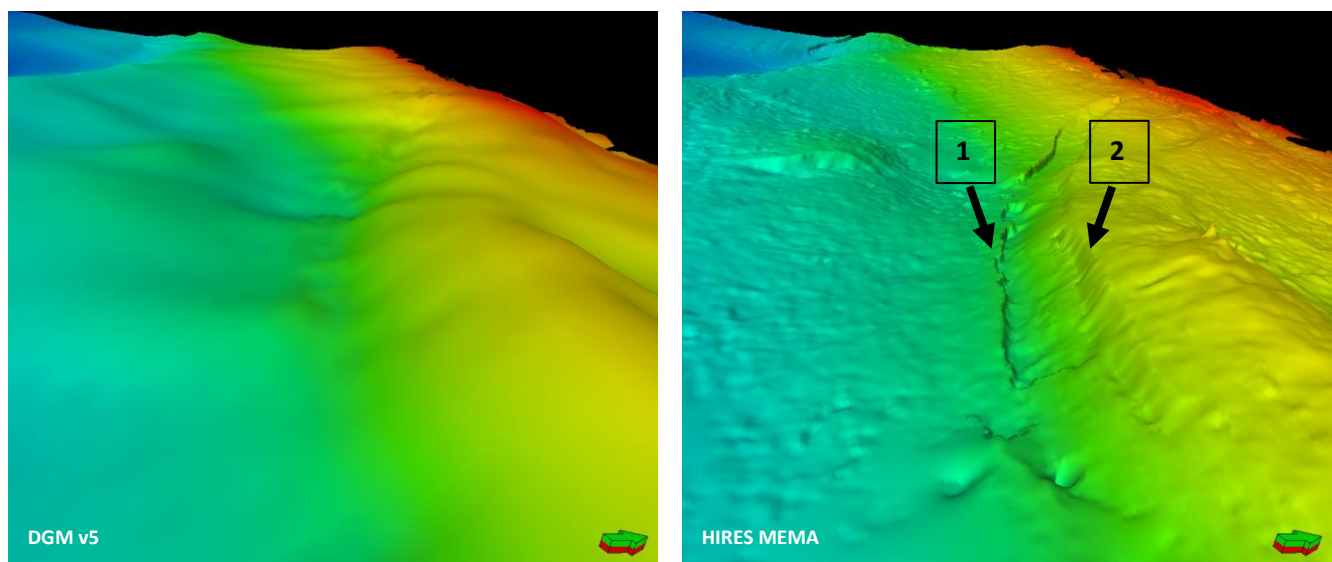


Fig. 34 – Difference in fault imaging between the DGM v5 and HIRES MEMA surface. Notice that fault 1 corresponds to a time difference seen clearly on both surfaces, while fault 2 cannot be detected on the DGM v5, due to the small angle between the fault and the horizon.

5.4 Dip Direction Relative to the Inline and Crossline

Seismic surveys are typically shot in a cross pattern, with receivers spaced 20-25m apart (Ebrom *et al.*, 1997). If there already is existing data or knowledge of an area that is surveyed, the survey is usually set up to enhance the important structures, by making the in- and crosslines perpendicular to these structures. For this reason, the seismic surveys of e.g. the Monster survey are shot perpendicular (and parallel) to the NW-SE fault planes of the normal faults that are characteristic of the West Netherlands Basin (Fig. 33). This way, the sampling distance perpendicular to the structure remains the smallest (20-25m), with the surface interpolated in between. However, similar to the problem described in the previous paragraph, the relative resolution decreases for lineations at an angle with the in- or crossline, with the lowest lateral resolution given at a 45° angle to the in- and crossline. At this specific angle, the distance between seed points that form a perpendicular line to a potential fault is 35.3 m for a 25x25m grid, and 353 m for the 250x250m grid resolution of the DGM v5 horizons (Fig. 35).

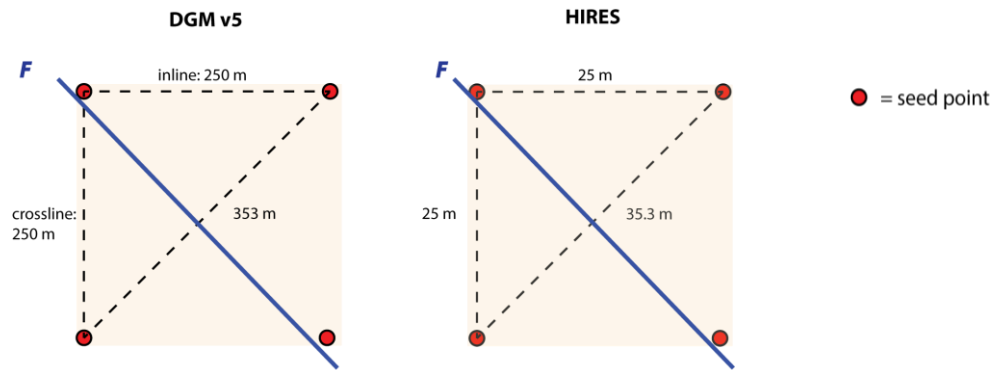


Fig. 35 – Example of a fault lineation (F) on a DGM v5 and HIREs grid resolution horizon that is not perpendicular to the in- or crosslines. In this case, the minimum fault throw may need to be higher to be detected on the surface. For the HIREs surface, this difference will be much smaller than for the DGM v5.

Two problems now occur: 1) Because the relative sampling distance is now larger, the fault throw is imaged over a longer distance, which causes a decrease in the fault dip angle, and 2) a perpendicular cross section to a fault is now at an angle, which alters the apparent dip angle of the fault, according to Table 4. Because mainly the change in angle of the horizon determines whether or not we perceive a fault on a surface, this can cause some faults to not appear as such on a surface when they make an angle with the in- and crosslines.

True Dip α :	If angle between line of section and dip direction Φ is:				
	10°	30°	50°	70°	90°
0	0	0	0	0	0
10	10	9	6	3	0
30	30	27	20	11	0
50	50	46	37	22	0
70	70	67	60	43	0
90	90	90	90	90	-

Table 4 – Apparent dip versus the true dip if there is an angle between the line of section (cross section) and dip direction. These numbers have been calculated based on the Travis apparent dip calculator. The apparent dip (α') decreases if the angle between the line of section and dip direction (Φ) increases. With seismic surveys, which consist of in- and crosslines, the angle between this line of section and dip direction is never larger than 45°.

While the sampling distance increases for both the HIREs MEMA and DGM v5 surfaces, the longest distance between two seed points is only 35.3 m in the HIREs surfaces, which is still an order of 7 lower than the shortest distance between two seed points in the DGM v5 (250m). In other words, faults that are not aligned with the in- or crosslines are presumably detected sooner on a HIREs surface relative to the DGM v5 surface. The fault throw most likely has to become larger to cause enough change in angle of the surface to be detected. Assuming this is a similar percentage for both the HIREs MEMA and the DGM v5 surface, e.g. 40%, this would increase the minimum fault throw for the HIREs MEMA from 1 to a hypothetical 1.4 ms, which is negligible, while for the DGM v5 it would increase from 10 to 14 ms, which is much more significant. Fig. 36 shows the difference between the HIREs MEMA and DGM v5 surface for the Andel survey, where the faults running NNW – SSE (~ 45° relative to the in- and crosslines) are not seen on the DGM v5 surface while appearing clearly on the HIREs MEMA surface.

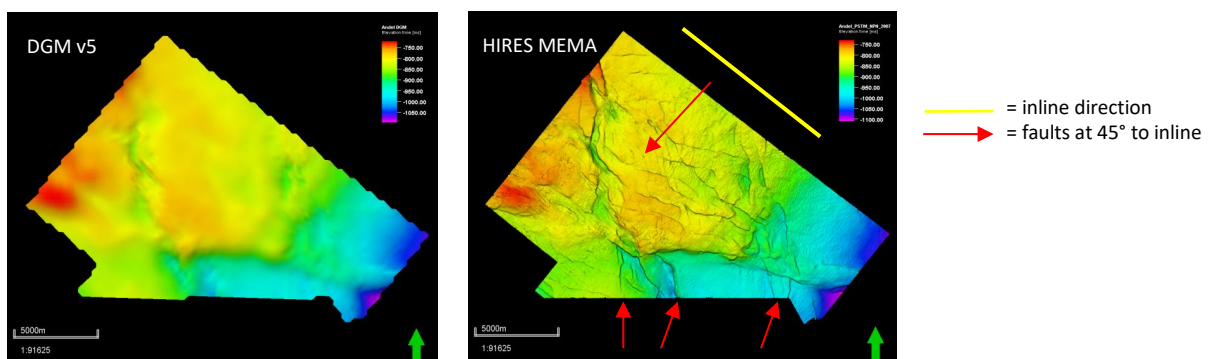


Fig. 36 – Comparison of the DGM v5 and the HIREs MEMA horizon for the base North Sea Group for the Andel survey.

Missing faults therefore becomes more likely when faults are at angle to the in- and crossline, most noticeable with the DGM v5 horizons. However, further research would be required to confirm whether or not a correlation exist between the minimum fault throw at which a fault is detectable and its angle relative to the in- and crossline. For this research, this angle has not been measured.

5.5 Ant Tracking Settings

The final settings chosen for ant tracking are discussed in paragraph 4.2 and shown in more detail in Appendix C. After testing different parameterization for ant tracking, it followed that a Chaos cube into either a passive or custom ant track run followed by an aggressive ant track resulted in the best ratio of the least amount of artifacts and the best representation of the faults seen on the high resolution surface. However, it should be noted that the tracking settings can be adjusted to decrease the minimum throw at which a fault is picked up by ant tracking. As explained in chapter one, the 'aggressive' setting is used to detect fractures or joints, and easily picks up on small discontinuities in the seismic signal, although these are usually smaller in size than the discontinuities found with the passive setting.

It is therefore rather subjective to determine what the 'best' settings are for the ant tracking workflow. While it might be possible to return more discontinuities using more aggressive ant tracking settings, the results show that these are often not related to faults, but rather local seismic noise. Especially when used for the Upper Base North Sea Group, where many data gaps are present due to inconveniences with data acquisition, ant tracking parameters should be set more conservative to prevent too many seismic artifacts. The same can be said of other seismic depths that have a rather noisy signal. The seismic quality always effects what ant tracking parameters are best, and that can vary between seismic surveys. Good examples are the Monster survey in the western extent of the WNB, and the Waalwijk survey in the southeastern extent of the WNB. The Monster survey contains many acquisition related gaps giving a generally more noisy, discontinuous seismic signal (Fig. 33). When ant tracking is applied to this survey, it will return many seismic artifacts, even after applying structural smoothing, which enhances the continuity of the signal in any given direction. In this case, it is almost impossible to return only fault-related discontinuities with ant tracking, and a decision has to be made on the settings for ant tracking to retrieve the most accurate fault-related events. Therefore, a passive setting was chosen for Monster, to restrict the amount of seismic artifacts returned by ant tracking. For 50 % of the faults, ant tracking was able to track a fault to a lower minimum fault throw than was detectable by eye on the surface. With the 'lower' seismic quality, even with the initial passive settings of the ant track run, the ant track results are satisfactory for this specific survey.

The Waalwijk survey exhibits a good continuation of the seismic signal, with very few data gaps, and (therefore) better seismic processing of the data. In this case, a custom ant tracking setting is also possible, which is in between the aggressive and passive setting, allowing for more discontinuities to be picked up, without too many artifacts (Fig. 26). Using the passive setting for ant tracking on this same cube shows a difference in the minimum fault throw at which a fault is detected by ant tracking.

6. Conclusion

With the conclusion of this internship over five months, three products have been delivered to EBN:

- A mapping workflow in Petrel that enables any user to incorporate high resolution (25x25m) interpretations into the larger, lower resolution (250x250m) DGM v5 horizons, see Appendix B;
- High resolution interpretations of the B_NU, B_NLNM and B_CK in the West Netherlands Basin, as well as a part of Drenthe in the east of the Netherlands;
- Analysis of the Hondsrug in Drenthe, East Netherlands.

Based on the available horizons of the DGM v5 by TNO, the self-generated high resolution interpretations, and the automated fault detection and extraction workflow for the WNB, the following conclusions are made in regard to the minimum fault throw at which faults become detectable on surfaces. On average, faults become detectable at a minimum of 1 ms fault throw on the HIRES MEMA surface, 1.5 ms with ant tracking, and 10 ms for the DGM v5 for the base North Sea Group, which is a relatively strong and continuous reflector. When only looking at the average of the 50 analyzed faults, the difference is similar: 8.5 - 9 ms higher for the DGM v5 compared to the ant tracking or HIRES MEMA surfaces. The results of ant tracking closely resemble the results of the high resolution interpretation (Tabel 5).

Tabel 5 – Summary of the Results for the Minimum Fault Throw

	HIRES MEMA (ms)	DGM v5 (ms)	Ant tracking (ms)
AVERAGE	6.5	14.9	6.7
STDEV	3.8	4.5	3.9
MINIMUM	1	10	1.5

As shown most notably with the Waalwijk survey, many faults exist which a fault throw less than 10 ms at the very least, and missing faults can be a real concern when determining the well placement on the DGM horizons. Therefore, it is strongly recommended to use manual interpretation or ant tracking, if possible, when planning a geothermal well onshore, or risk a drilling hazard due to faults that have not been observed.

Acknowledgements

For this internship, I would like to thank first and foremost, my daily supervisor Guido Hoetz. Guido has been supportive, enthusiastic, and with a clear ability to convey his vision of the HIRES MEMA project to actions. I thank you for the time you have invested in me, as well as the other students. Second, I would like to thank Linda Janssen, who has spent the most time with us discussing our progress, and was always willing to help us when we needed help. Third, I would like to thank Martin Ecclestone, who was (to my knowledge) not initially affiliated with the HIRES MEMA project, but became so over the months, as he has joined us in every progress meeting, providing immensely helpful comments to our presentations, and having taught me a lot more about the possibilities that exist within Petrel. I am now also a believer that everything is possible in Petrel, Martin! Furthermore, I would like to thank Mohamed, who has been my reliable coworker, thank you for all the laughs we had and hours spent working on the project together; Marloes Kortekaas, helping me out with ant tracking; Ward Teertstra, for keeping my sharp and focused on my project; Vibhuti Wani, for all the good discussions; Eline van Malderen, for all the coffee/tea breaks and critical thinking; Patrick Reinhard, for all the fruitful discussions about geothermal energy in the Netherlands.

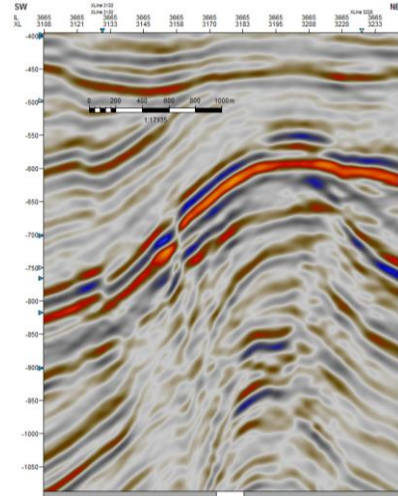
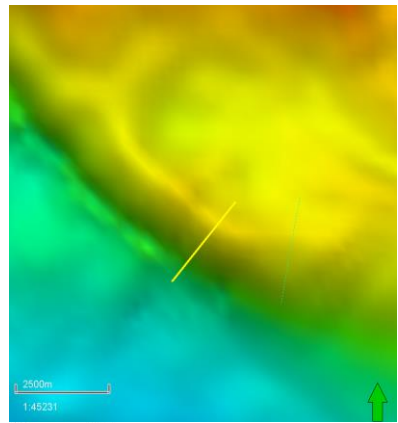
References

- Bahorevich, M. & Farmer, S. 1995. The coherence cube. *The Leading Edge*, 1053-1058
- Bouchingour, M. 2019. High Resolution Mega Mapping the North Sea and Chalk Group Base Horizons – Towards an Improved Petrel workflow for Multi-Resolution Grid Merges and a Velocity Model for the Dutch Northern Offshore. MSc Thesis for Earth Sciences, Geology & Geochemistry, Vrije Universiteit Amsterdam
- Ebrom, D., Li, X. & McDonald, J. 1995. Bin Spacing in Land 3-D Seismic Surveys and Horizontal Resolution in Time Slices. *The Leading Edge*, 14, 37-41. Doi: 10.1190/1.1437061
- Hardage, B. A. 1997. Principles of Onshore 3-D Seismic Design. *Geological Circular*, 97 -5, Austin Texas: Bureau of Economic Geology, University of Texas
- Herngreen, G. F. W. & Wong, Th. E. 2007. Cretaceous. In: Wong, Th. E., Batjes, D.A.J. & De Jager, J. (eds): Geology of the Netherlands. *Royal Netherlands Academy of Arts and Sciences (Amsterdam)*, 127-150.
- Masterplan Aardwarmte 2018: <https://kennisbank.ebn.nl/het-masterplan-aardwarmte-nederland/>
→ <https://kennisbank.ebn.nl/wp-content/uploads/2018/08/20180529-Masterplan-Aardwarmte-in-Nederland.pdf>
- Lokhorst, A. & Wong, Th. E. 2007. Geothermal energy. In: Wong, Th. E., Batjes, D.A.J. & De Jager, J. (eds): Geology of the Netherlands. *Royal Netherlands Academy of Arts and Sciences (Amsterdam)*, 341-346
- De Jager, J. 2007. Geological development. In: Wong, Th. E., Batjes, D.A.J. & De Jager, J. (eds): Geology of the Netherlands. *Royal Netherlands Academy of Arts and Sciences (Amsterdam)*, 5-26
- Den Hartog Jager, D.G. 1996. Fluvio-marine sequences in the Lower Cretaceous of the West Netherlands Basin: correlation and seismic expression. *Geology of gas and oil under the Netherlands*, 229-241. BSN: 9789400901216
- Donselaar, M. E., Groenenberg, R., Gilding, D. 2015. Reservoir Geology and Geothermal Potential for the Delft Sandstone Member in the West Netherlands Basin. *Proceedings World Geothermal Congress 2015*
- Duin, E. J. T., Doornebal, J. C., Rijkers, R. H. B., Verbeek, J. W. & Wong, Th. E. 2006. Subsurface structure of the Netherlands – results of recent onshore and offshore mapping. *Netherlands Journal of Geosciences*, 85-4, 245-276
- Kortekaas, M. & Jaarsma, B. 2017. Improved definition of faults in the Groningen field using seismic attributes. *Netherlands Journal of Geosciences*, 96-5, 71-85
- Lima, F. 2005. Automatic Fault Extraction Using Ant-Tracking Algorithm in the Marlim South Field, Campos Basin. *SEG Technical Program Expanded Abstracts (2005)*. Doi: 10.1190/1.2148294
- Randen, T., Pedersen, S., Sønneland, L. 2001, Automatic extraction of fault surfaces from three-dimensional seismic data: 72nd Annual International Meeting, *SEG, Expanded Abstracts*, 551–554
- Stichting Platform Geothermie Oude Delft 37 - 2611BB Delft - info@geothermie.nl

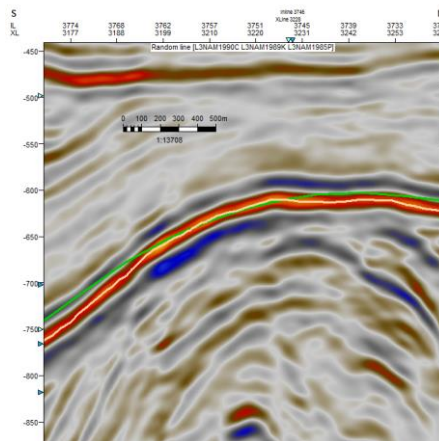
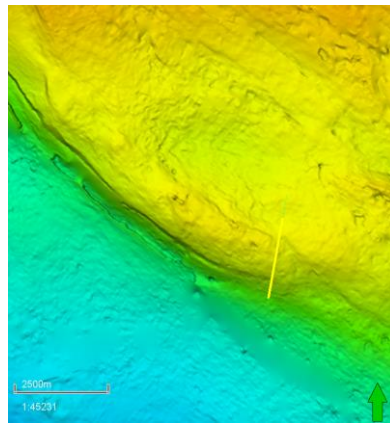
- Van Adrichem Boogaert, H.A. & Kouwe, W.F.P. (eds), 1993. Stratigraphic nomenclature of the Netherlands, revision and update by RGD and NOGEP. *Mededelingen Rijks Geologische Dienst 50, Section A, General*, 25
- Wong, Th. E. 2007. Jurassic. *In: Wong, Th. E., Batjes, D.A.J. & De Jager, J. (eds): Geology of the Netherlands. Royal Netherlands Academy of Arts and Sciences (Amsterdam)*, 107-125
- Wong, Th. E., de Lugt, I. R., Kuhlmann, G. & Overeem, I. 2007. Tertiary. *In: Wong, Th. E., Batjes, D.A.J. & De Jager, J. (eds): Geology of the Netherlands. Royal Netherlands Academy of Arts and Sciences (Amsterdam)*, 151-171
- Worum, G. & Van Wees, J.D. 2017. High-resolution quantitative reconstruction of Late Cretaceous-Tertiary erosion in the West Netherlands Basin using multi-formation compaction trends and seismic data: implications for geothermal exploration. *Acta Geod Geophysics (2017)*, 52, 243 – 268. Doi: 10.1007/s40328-017-0196-6
- Yonez-Banda, M., Ruzhnikov, A., Kasimin, A., Husien, M., Malagon, C. & Al-Wahedi, K. 2017. Working together for Successful Drilling through a Fault: Risk Management, Planning and Execution. *Abu Dhabi International Petroleum Exhibition & Conference*, 13-16
- Ziegler, P. A. 1988. Evolution of the Arctic-North Atlantic and the western Tethys. *American Association of Petroleum Geologists, Memoir 43*, 198, 30 plates

Appendix A - Fault Measurement Images

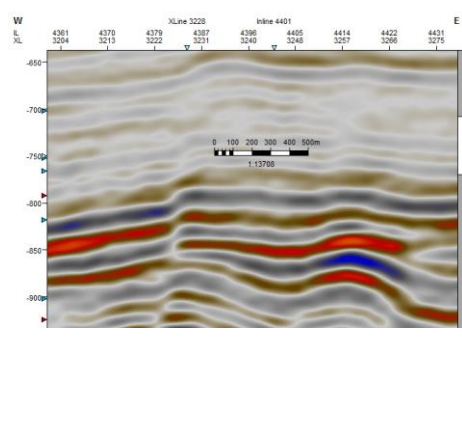
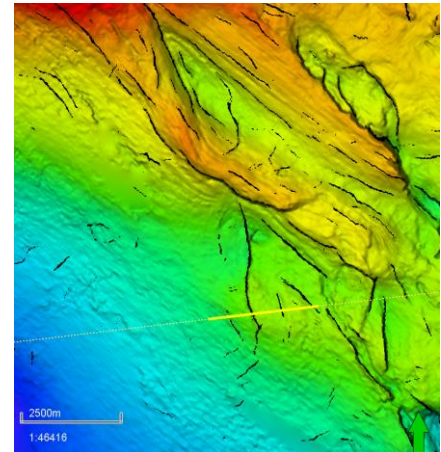
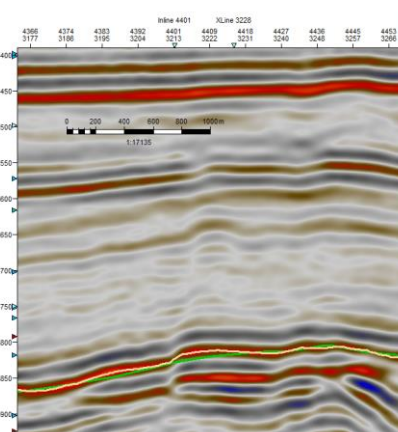
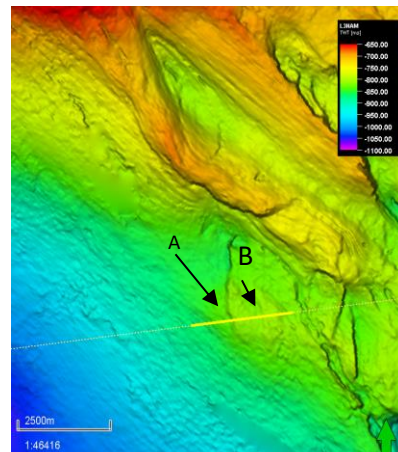
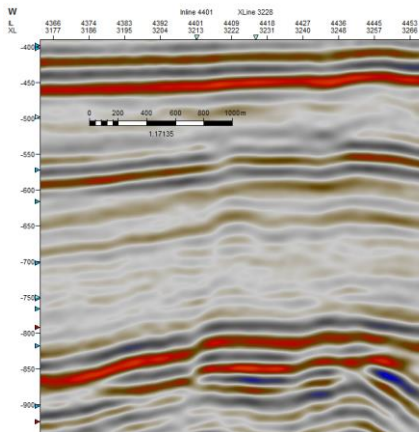
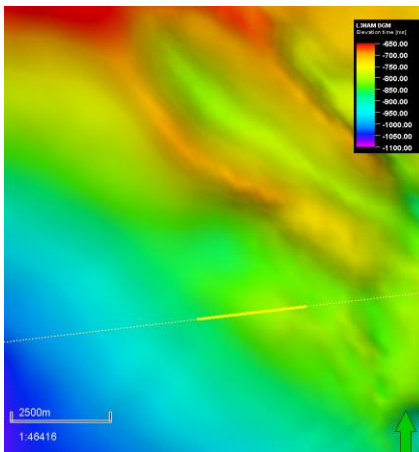
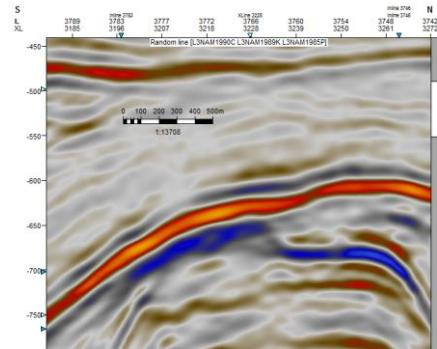
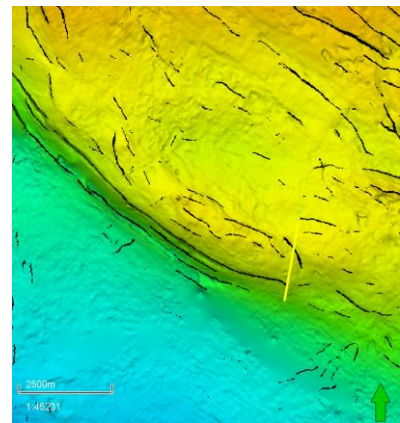
DGM v5

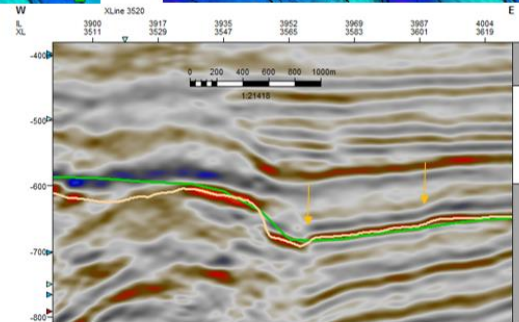
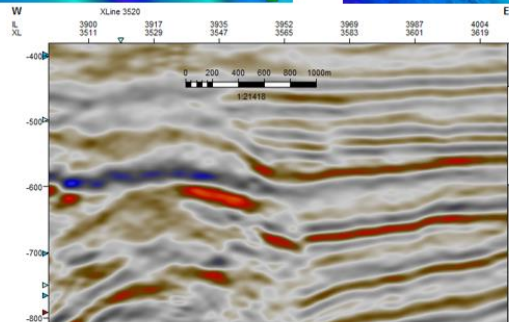
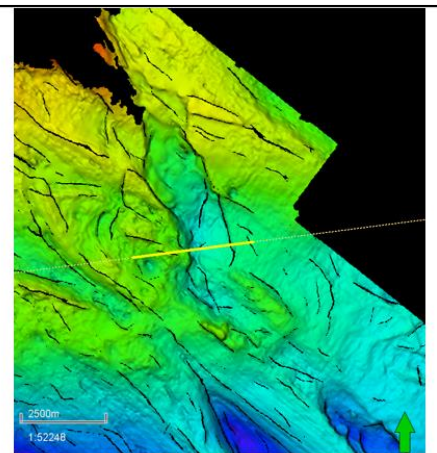
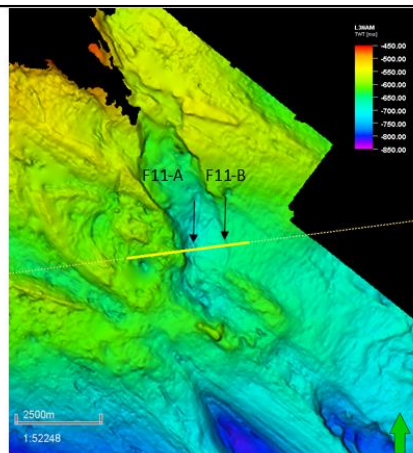
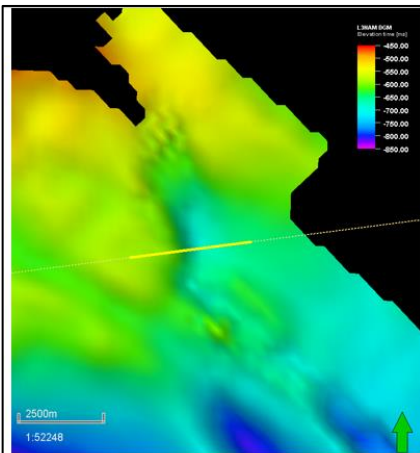
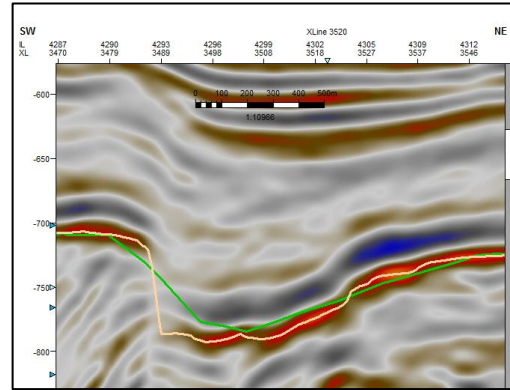
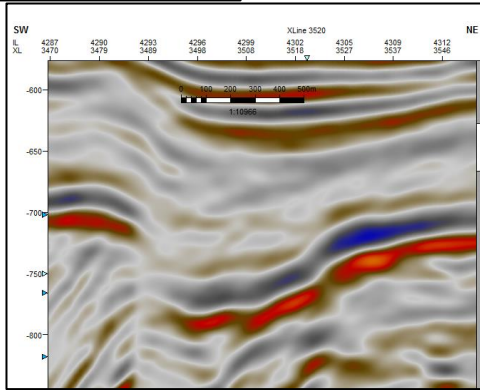
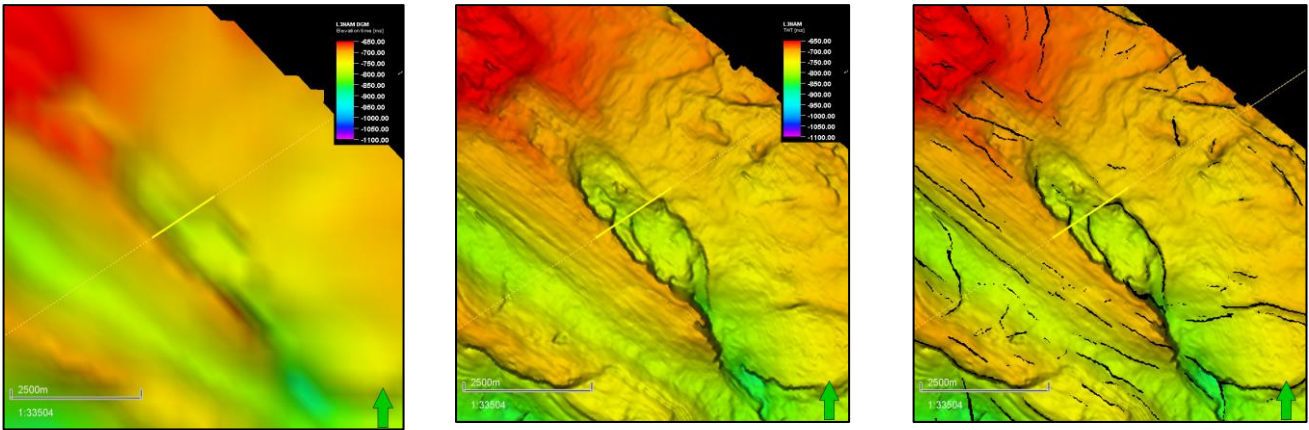


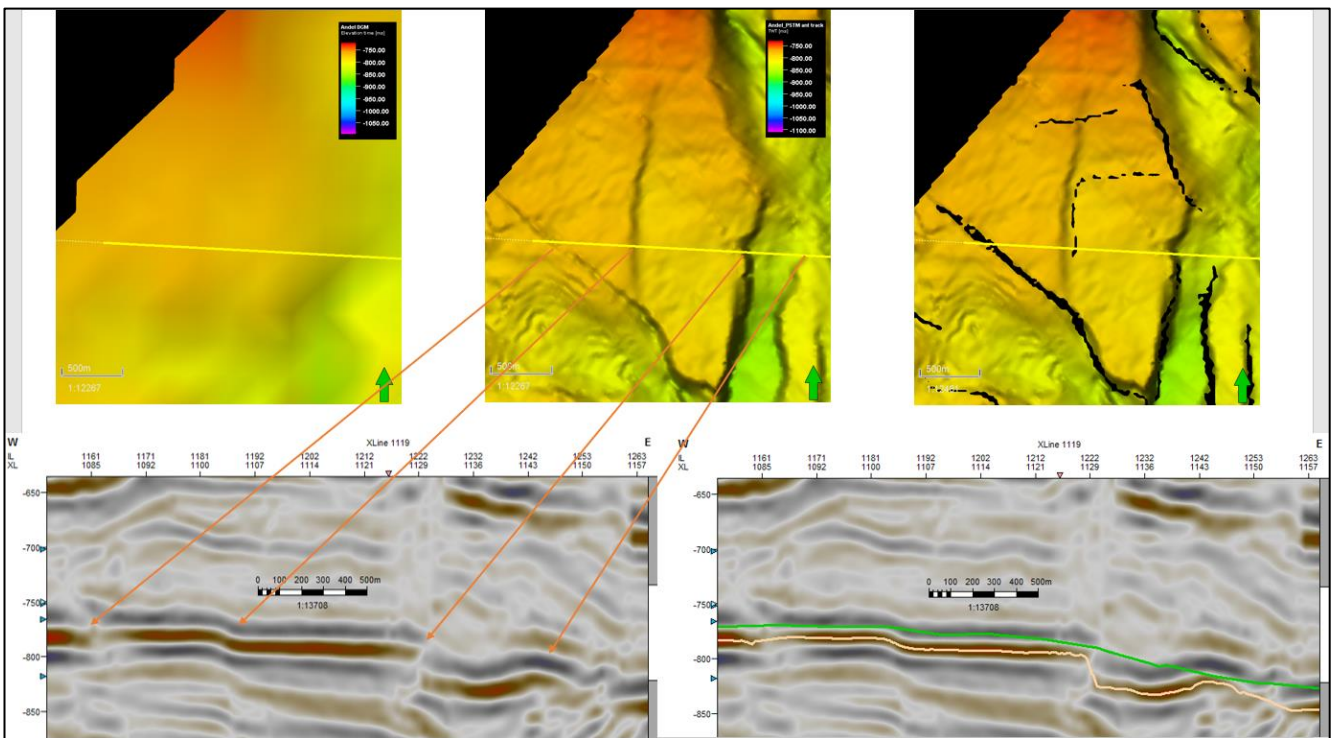
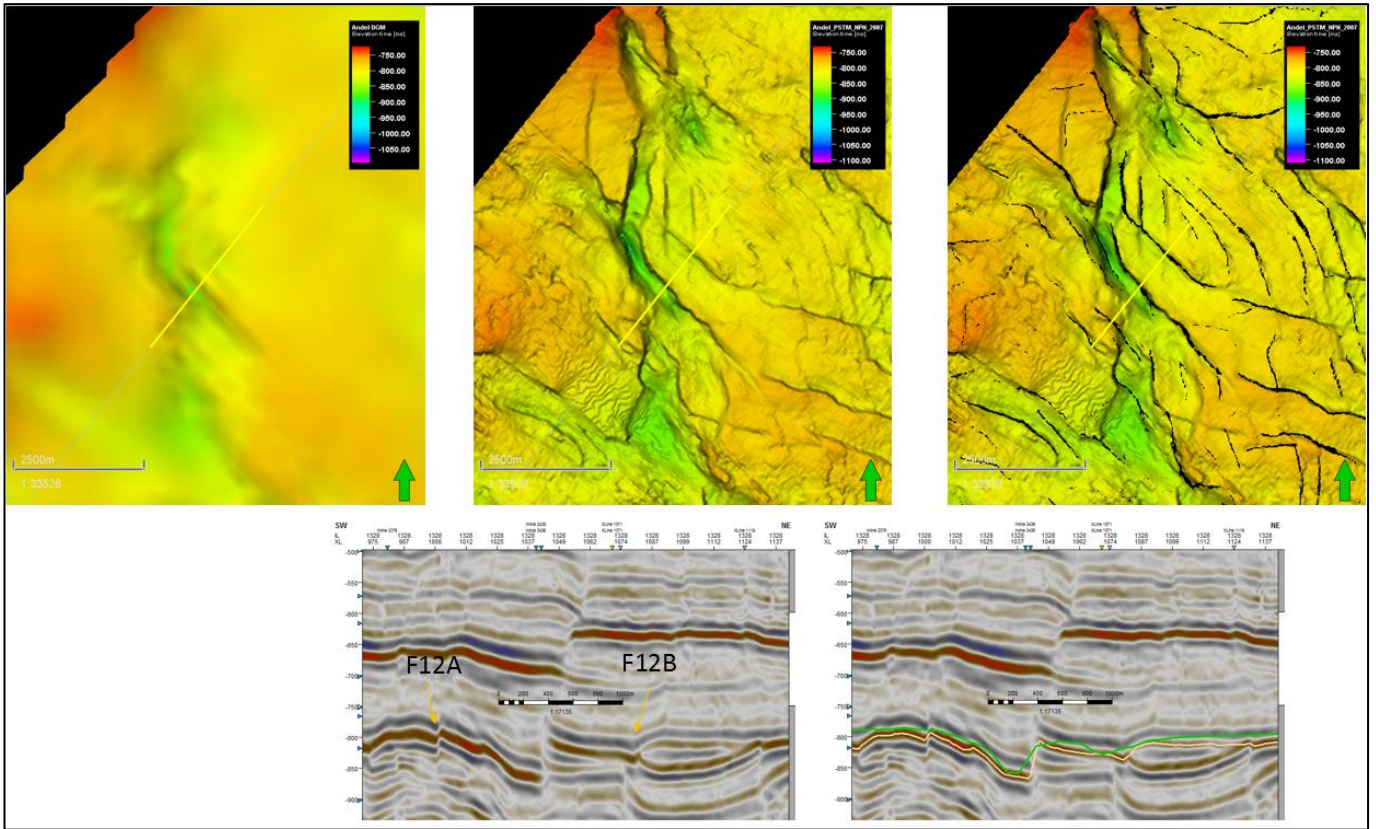
HIRES MEMA

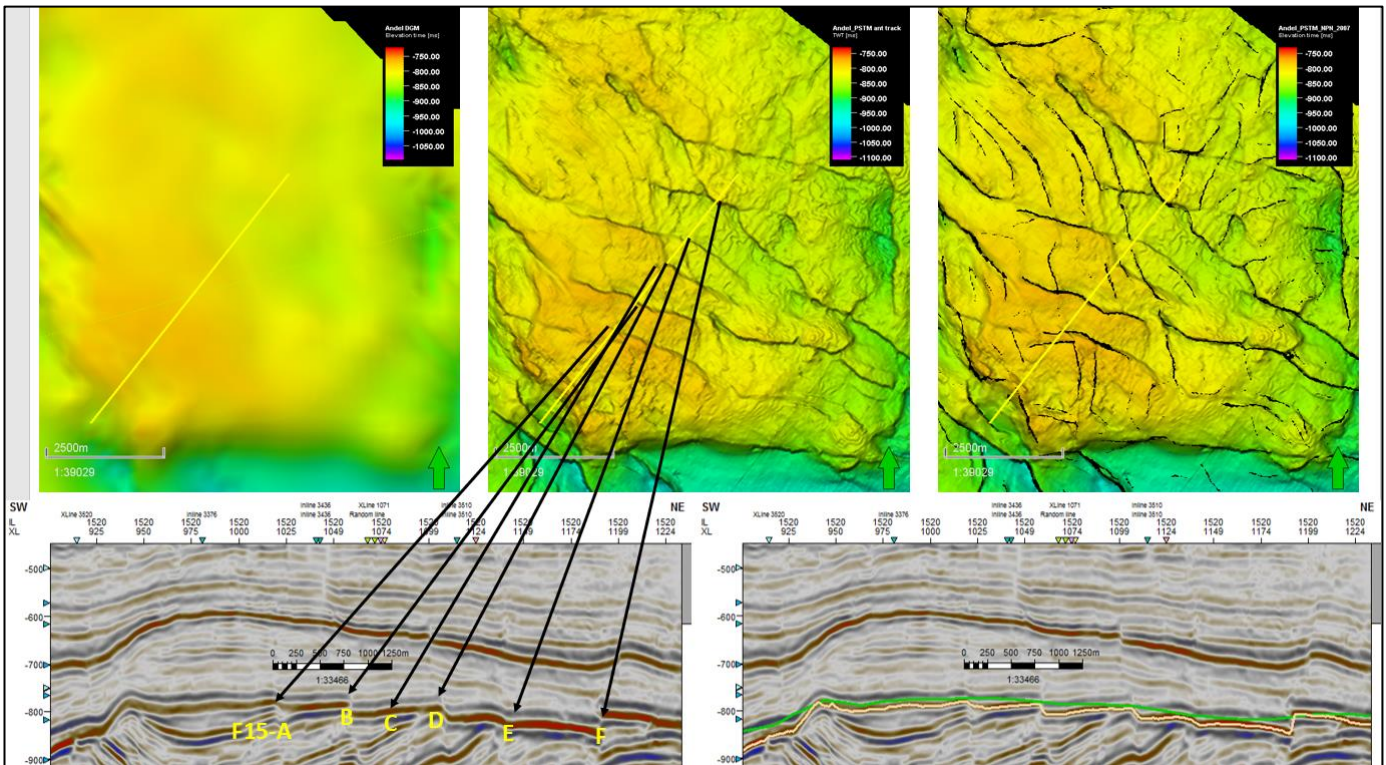
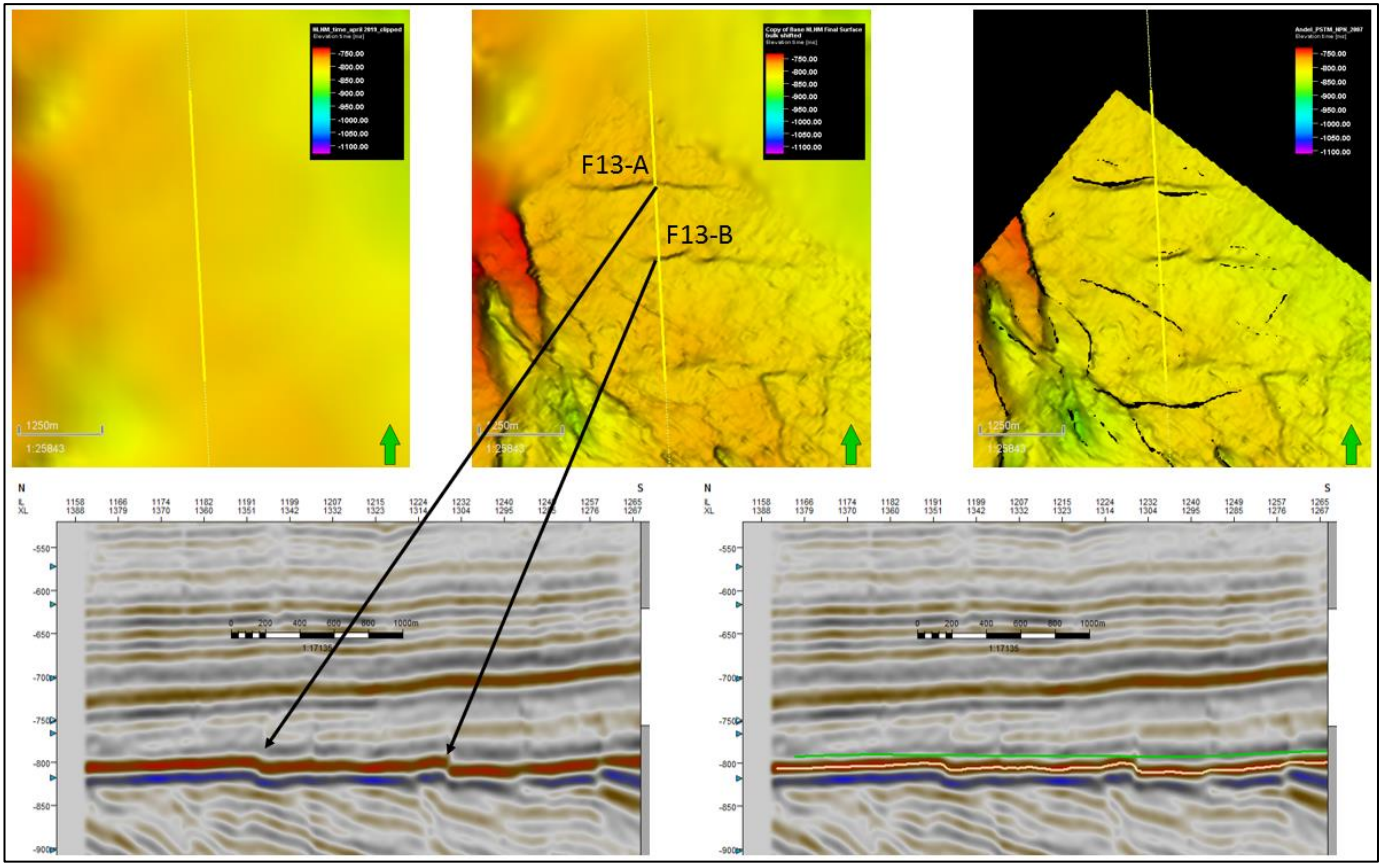


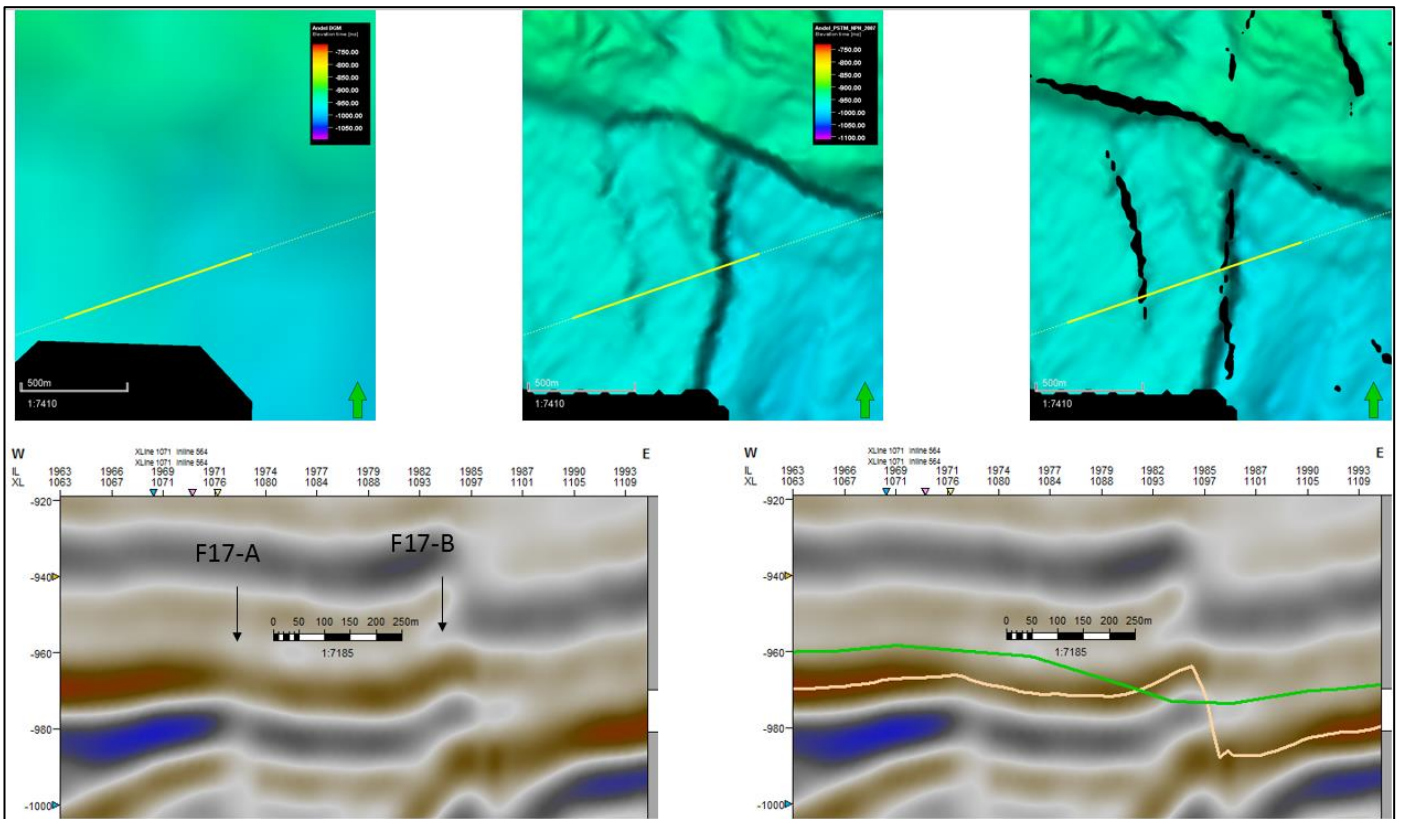
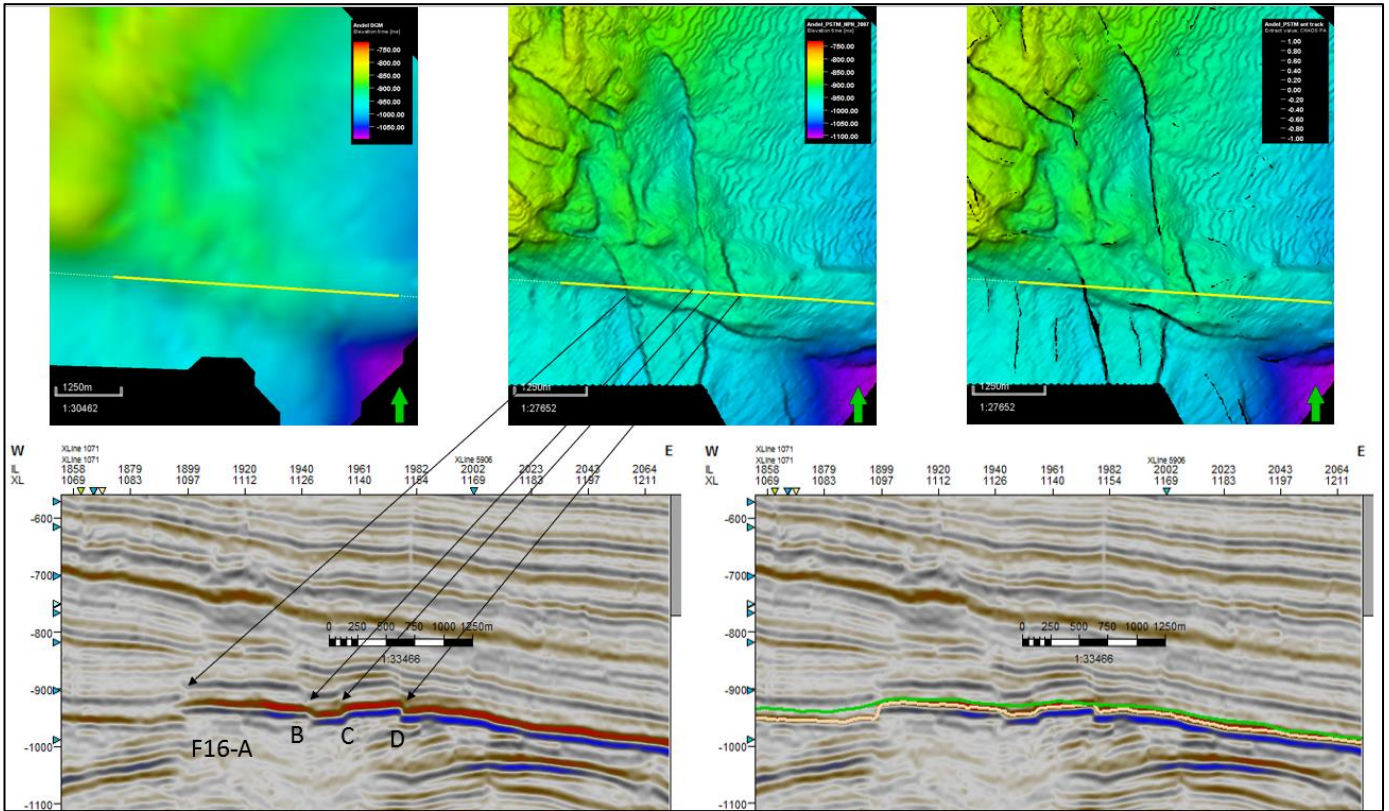
HIRES MEMA + ant track overlay

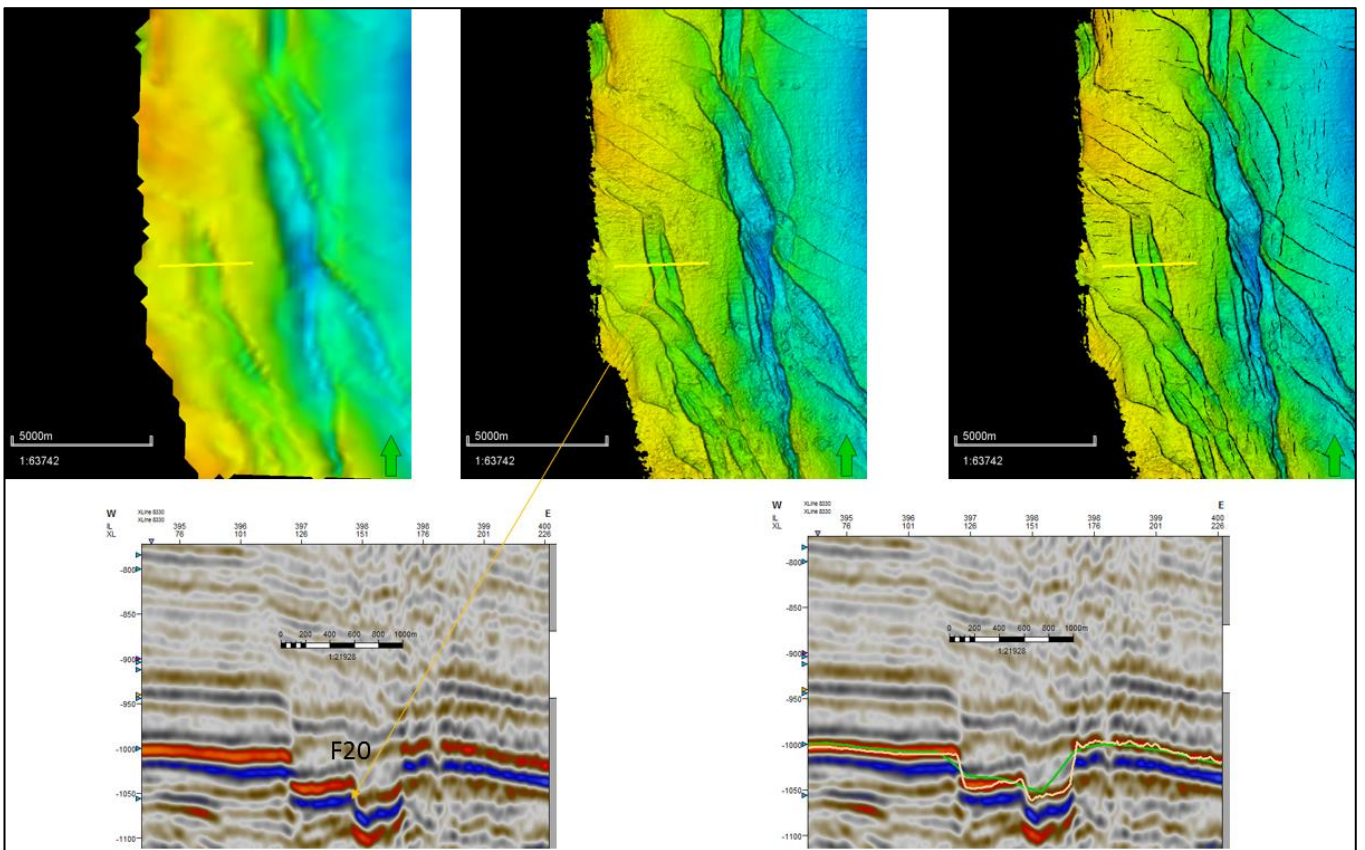
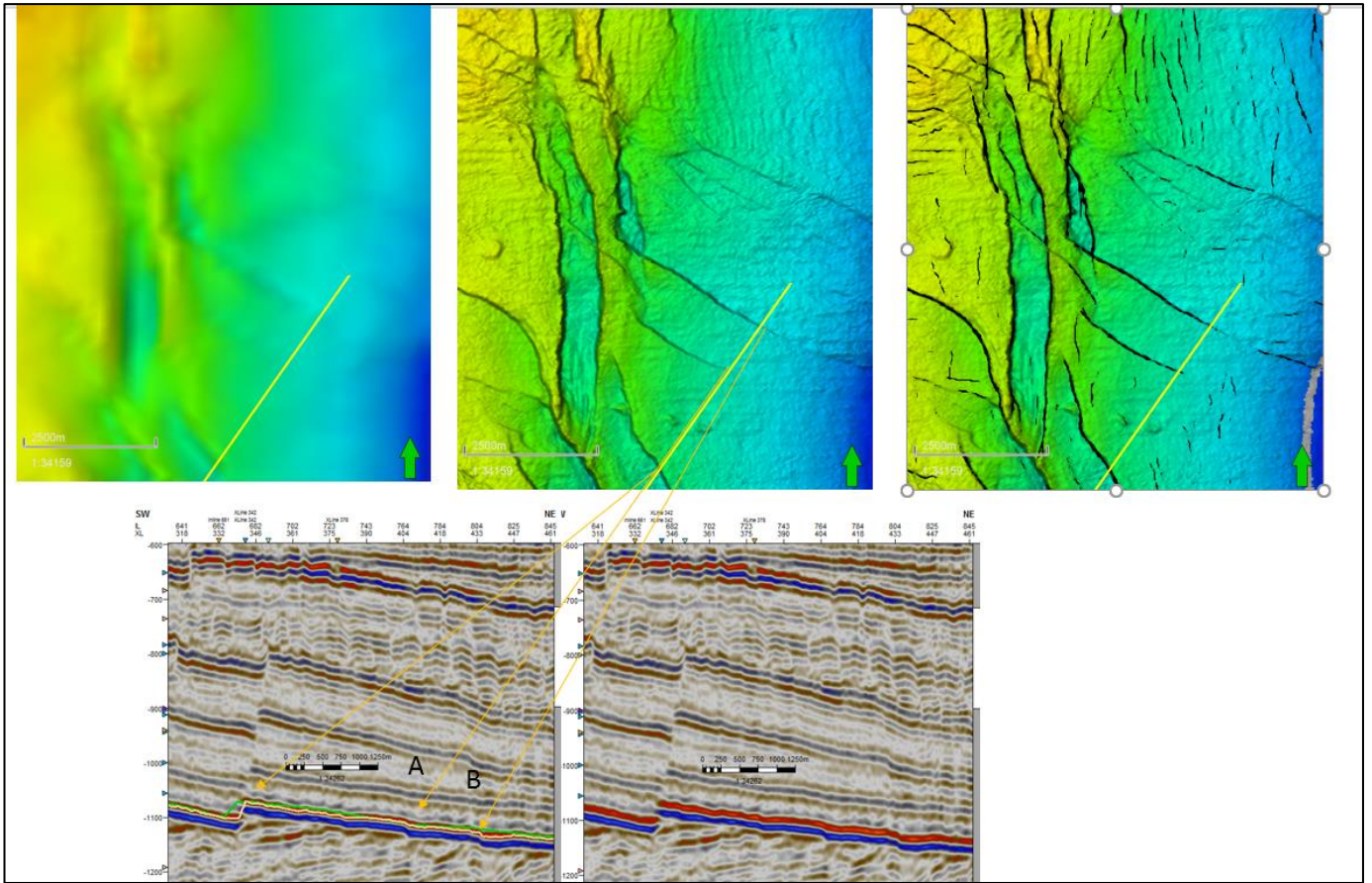


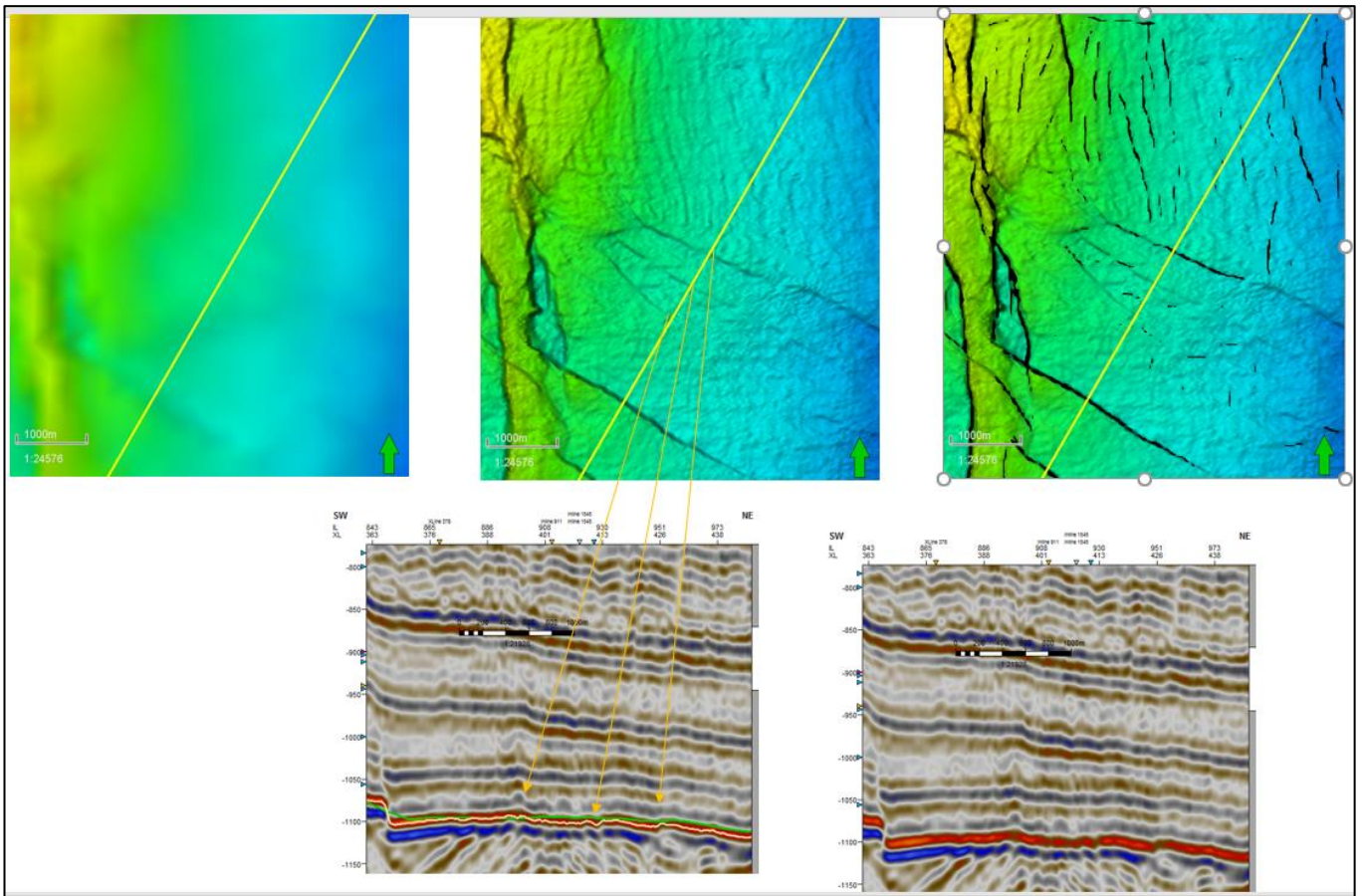
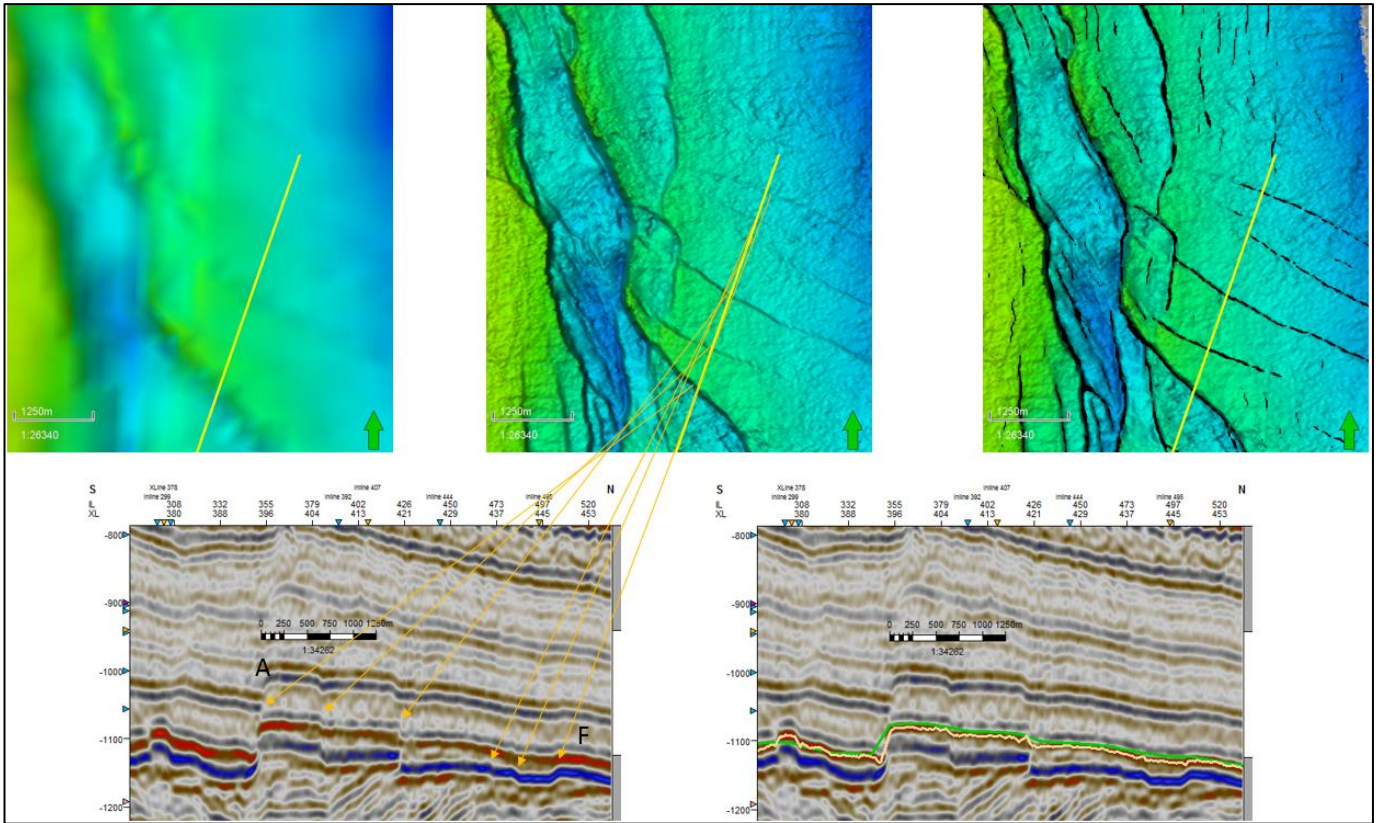












Appendix B - Mapping Workflow

The workflow used to create the new, final surfaces will only briefly be discussed in this thesis. The surfaces are made using a Petrel workflow that replaces the DGM v5 horizon where the high resolution interpreted horizon is available. A series of different workflows are linked to create one 'master' workflow which uses the next processes:

1. Convert the 3D hires interpretations to point files;
2. Remove the overlapping area from the TNO surface and convert the resulting surface to points;
3. Append (merge) both point files to create one complete point file;
4. Convert the final point file to a surface of 25x25 m

A schematic overview of the process can be seen in Fig. B1.

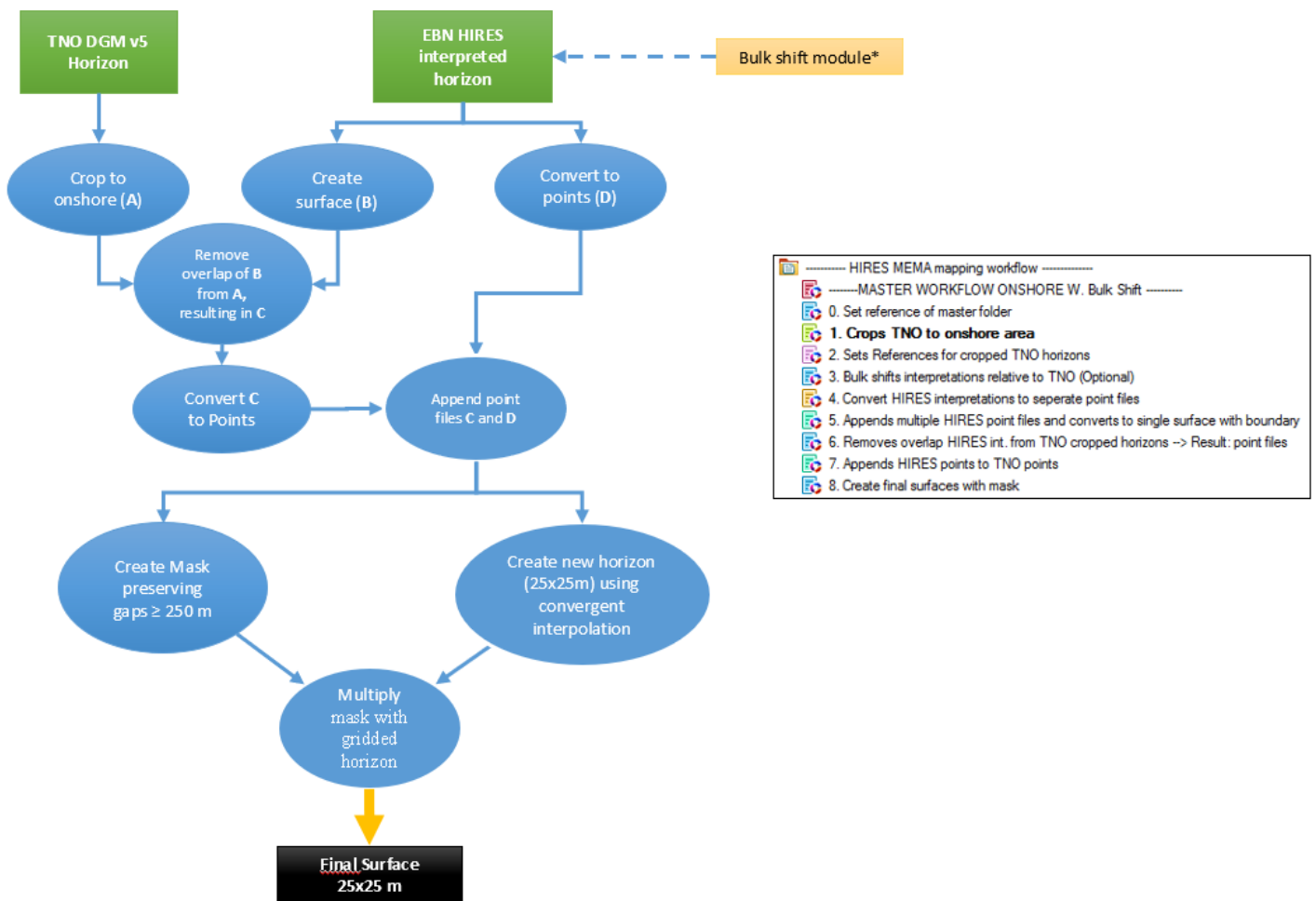


Fig. B1 - Summary of the mapping workflow in Petrel.

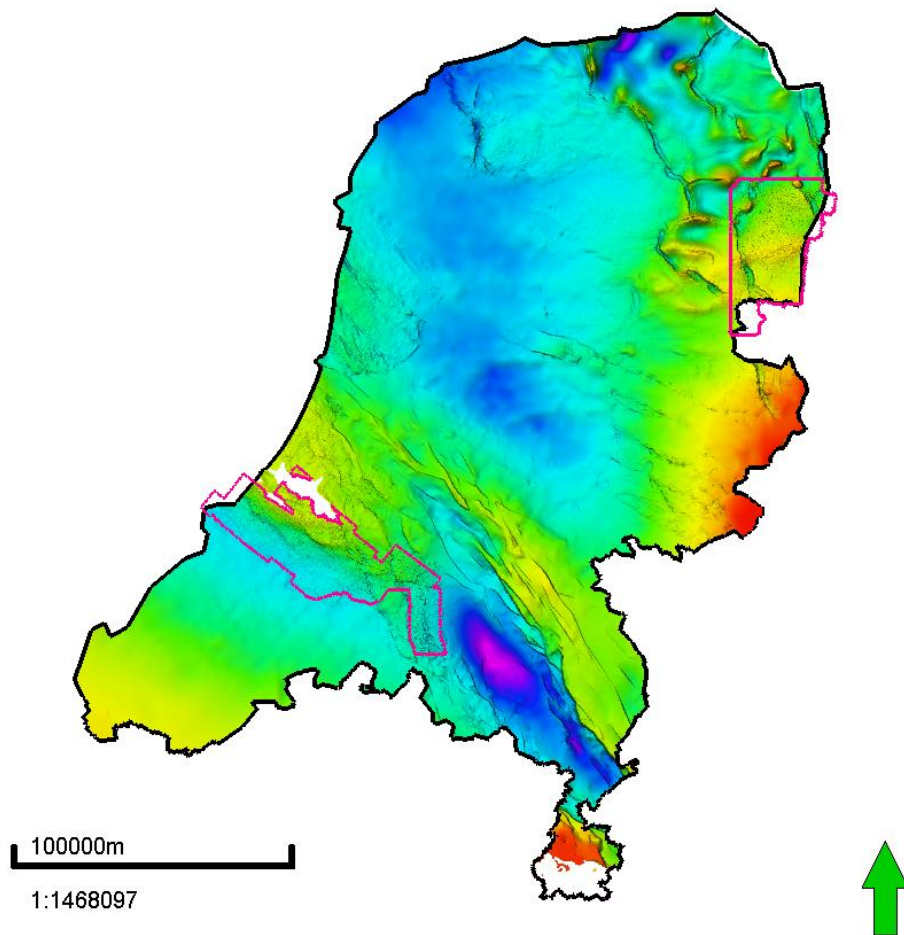


Fig. B2 – Result of the mapping workflow for the onshore area of the Base North Sea Group. The added interpretations of 25x25m are automatically outlined in pink.

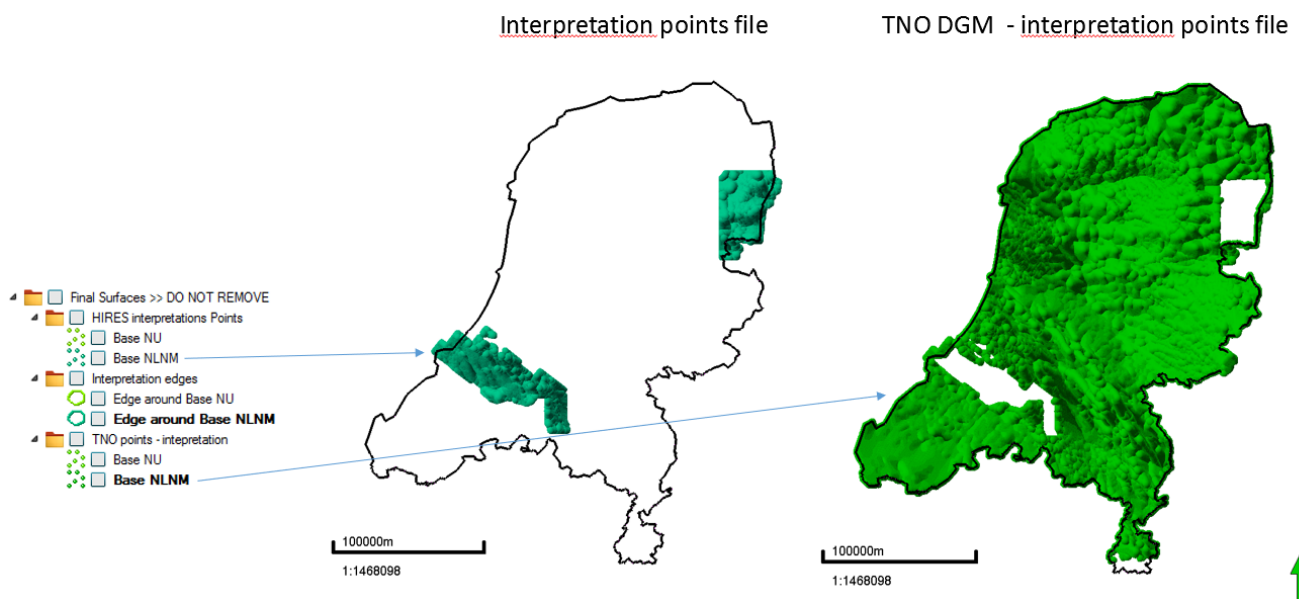


Fig. B3 – Left: the hires (25x25m) interpretations for the B_NLNM after conversion to point files, right: point file of the DGM's B_NLNM horizon (250x250m) minus the areas of the high resolution interpretations.

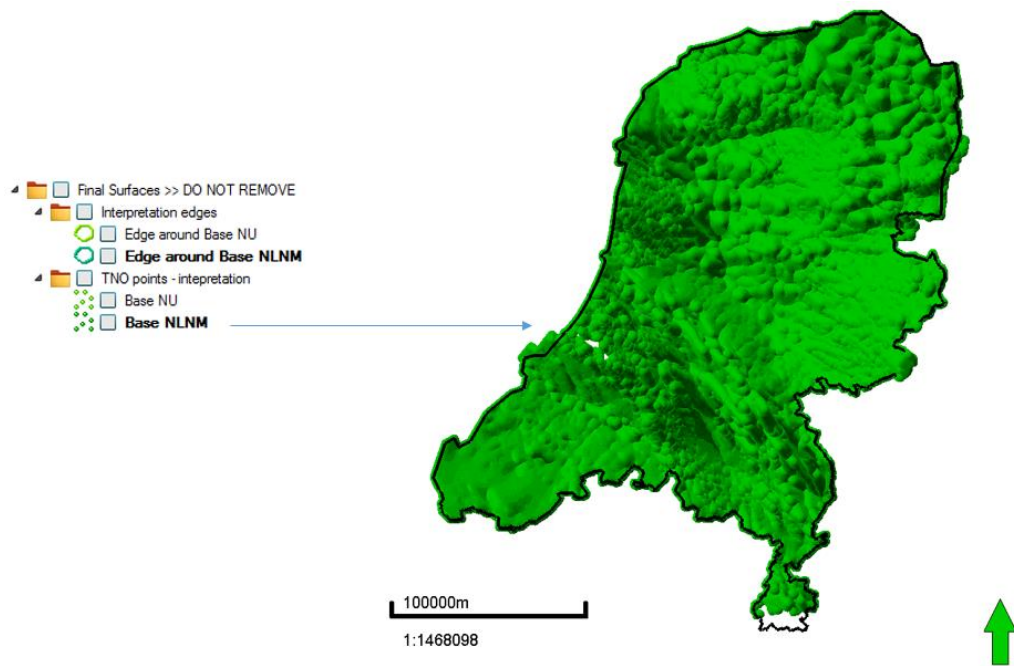


Fig. B4 – The DGM v5 points file appended to the high resolution points files, forming one points file with a different gridding resolution. From this points file, two surfaces are produced. One that is gridded everywhere with a resolution of 25x25m, and another that is used as a mask, preserving gaps in the appended point file (as seen in the WNB and the southern tip of the Netherlands for the base NLNM). These are then multiplied, resulting in the final surface with a resolution of 25x25m with gaps preserved (Fig. B1).

Bulk Shift Module

Due to time shifts between the seismic surveys, a module was included in the workflow to automatically correct the time shift between the smaller, local interpretation and the TNO horizon. The module takes any local (hires) interpretation grid, and calculates the mean time difference between the interpretation and overlapping TNO horizon. Because the mode cannot be extracted directly from Petrel, the outliers of the data are removed to more closely approximate the mode with the mean. A limit of plus and minus 20 milliseconds was used to remove the outliers (Fig. B5) The mean time shift is then recalculated and subtracted from the interpretation. Through this process, the probability of a time shifts between the separate, smaller interpretation grids and the larger TNO horizon are reduced, although not eliminated. This module is not working without problems yet, and the approach is only one of multiple options one as to remove time differences between the individual seismic surveys.

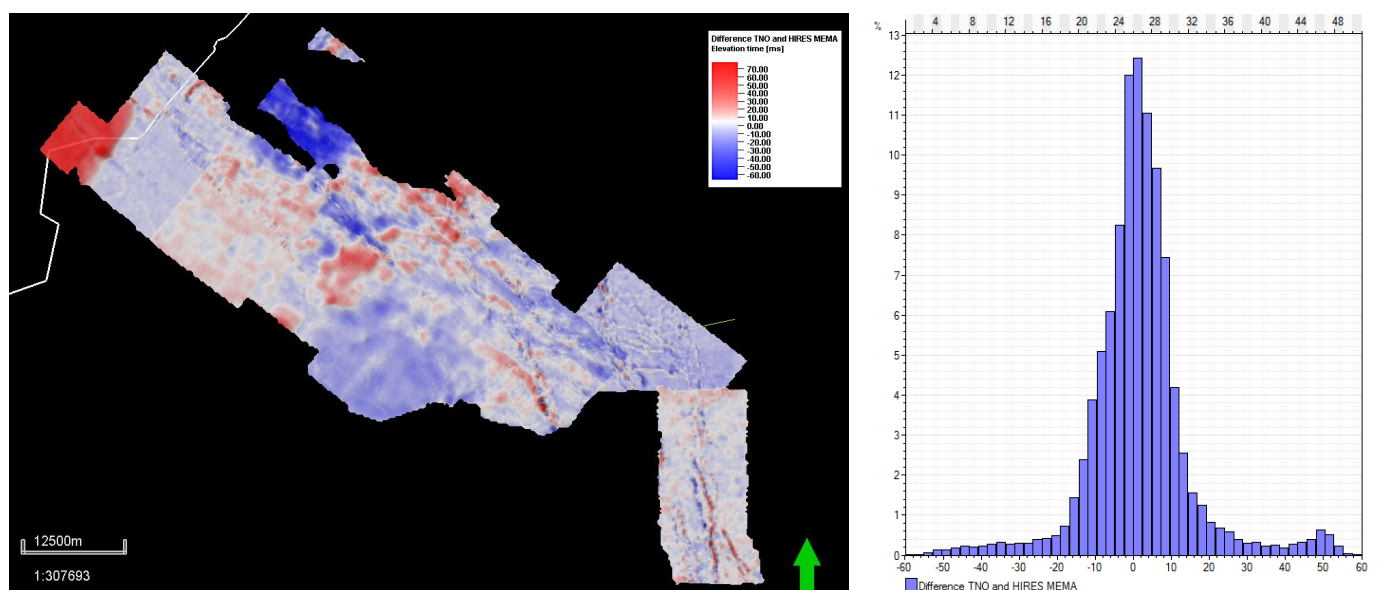


Fig. B5– Left: time difference map for the base North Sea Group between the DGM and the high resolution interpretation. Right: histogram of the time difference (x-axis) and the percentage (y-axis) of the left image.

Appendix C – Ant Tracking Workflow

The input parameters for the ant track workflow are given below. The stereonet plot is used to filter out ant tracks that are steeper than 88° in general, as well as events that are higher than 84° parallel or perpendicular to the seismic inlines. With this workflow, the most realistic results were found with ant tracking, with the best ratio between faults seismic artifacts. Given below is the ant track workflow with the Custom → Aggressive ant track iteration. The Passive → Aggressive ant track iteration is found on the next page.

